2015

WARWICK SUB

ISR Design Report

Team Members

Verity Armstrong

Rupert Barnard

Sam Clifton

Jack Fairweather

Richard Freeman

Theo Saville

Matt Shanahan

Stuart Snow

SUMMARY

This report documents the progress of the third iteration of the Warwick Human Powered Submarine project in the design, manufacture and test of a new submersible to enter into the 13th International Submarine Races in 2015.

The race, based in Washington DC, requires entrants to design and build a flooded-hull, underwater vehicle powered exclusively by a human occupant. The central aim of the competition is to achieve the maximum possible speed on a 100 metre straight line race course, with additional awards recognising holistic design goals such as 'Innovation' and 'Overall Performance'. The previous iteration of the project, *HPS Shakespeare*, competed in the 2014 European International Submarine Races and saw unprecedented success, placing fourth in the world and second in the UK. The authors hope to improve on this performance in the 2015 race.

The project emulates a situation commonly encountered by a multidisciplinary team of professional engineers: designing to a complex specification, in a fixed timeframe, with finite resources. The challenges presented by this project exemplify the Systems Engineering process, whereby a number of self-contained elements are required to interface and interact with one another in order to bring about the desired end goal.

The new submarine, *HPS Godiva*, is designed with three principle themes: efficiency, practicality and innovation; and represents a step change in multi-objective optimisation and manufacturing technologies, whilst taking a unique approach to the additional challenge of competing internationally.

DECLARATION

We, the authors, declare that the content of this document related to the University of Warwick Human Powered Submarine project is exclusively our own work.

Miss V. Armstrong 1101192		Mr R. Freeman 1006395	
Mr R. Barnard 1113187		Mr T. Saville 1109055	
Mr S. Clifton 1003484		Mr M. Shanahan 1111737	
Mr J. Fairweather 1110214		Mr S. Snow 1120699	

TABLE OF CONTENTS

LIST OF FIGURES

LIST OF TABLES

ACKNOWLEDGEMENTS

Warwick Sub would like to take this opportunity to thank everyone who has helped and contributed to this project this year.

Dr Ian Tuersley for his continued support, engagement and contribution to the successes of Warwick Submarine, without whom the initiative would not have been able to flourish.

Mr Nigel Denton for his expertise, time and patience in enabling the team to become competent divers and presenters.

Professor John Flowers for providing valuable direction at the project outset and encouragement throughout.

The School of Engineering workshop staff for their support in the design and manufacture of the submarine.

Dr Kerry Kirwan of WMG for his financial support contributing to the team's efforts to compete at the ISR.

Dr Nick Mallinson of WMG Catapult for his financial support allowing *HPS Godiva* to explore novel technologies.

Mrs Margaret Lowe for her organisational skills and pivotal role in helping realise one of the team's key aims in outreach engagement.

Dr Gregory Gibbons of WMG for his provision of 3D printing support and for organising the manufacture of our propellers.

Dr Neil Reynolds of WMG for sharing his time and composites expertise.

Dr Tony Price and the School of Engineering for their provision of funding toward entrance to the ISR.

Mr Roland Cherry, Mr Mick Bradley and Ms Burnadette White of Concept Group International for their knowledge, expertise and generous provision of resources to enable the laying up, finishing and painting of the hull.

Mr Jamie Fairbairn, Mr Shane Wickramasuriya and the 2013-14 *HPS Shakespeare* team for their support and laying strong foundations on which *HPS Godiva* hopes to build.

Mr David Radley of Davall Gears for his interest in the project and valuable sponsorship contribution to the powertrain.

Mr Stuart Reid and Mr Rob Stevens of GrabCAD for the provision of their Workbench PDM software.

Ms Swetlana Mieth, Ms Nadja Knittel and Mr Dennis Kronimus of Stratasys GmbH for provision of 3D printing materials.

Richard Wooldridge of Ford Motors for the manufacture of our propellers.

Mr Kris Harrison of Selex ES for financial support of the team's electronics package.

Mr Pierluigi Ferri of Entropy Resins for sharing expertise and providing sponsorship for the composite matrix.

Mr cYrille Boinay and Mr. Reto Aebischer of Bcomp for sharing expertise and providing sponsorship for the flax fibre.

Mr Phil Holyome of WDS Component Parts for his advice and sponsorship contribution to the fixings and furniture of the hull.

Ms Emma Hockley of Big Bear Plastic Products Ltd for her advice, patience and sponsorship of the nose-cone.

Ms Eilidh Webster of Bosch Rexroth AG for her financial support.

Ms Trish Banks of Subsea UK for her early support of the project and providing the team with a platform at the annual Subsea Expo.

Mr Ben Higgins of Société Générale for financial support of the team.

Mr David Watts of Axiom Propellers for sharing his expertise in propeller design.

The founders of the Arthur Shercliff Travel Sponsorship for financial support and believing in the merit of this project.

Mr Jo Engebrigtsen of Navisafe for the kind provision of strobe lights to ensure the safety of the submarine.

Mr Robin Corder of Velotech Services Ltd for the kind provision of bicycle componentry.

Mr Gordon Freeman of Augustus Martin for the provision of all sponsorship and promotional material.

SPONSOR LOGOS

CONCEPT GROUP INTERNATIONAL

GROUP OF COMPANIES

CATAPULT

High Value Manufacturing

WMG

Innovative Solutions

THE UNIVERSITY OF WARWICK

School of Engineering


3M
Rexroth
Bosch Group
Big Bear
PLASTIC PRODUCTS LIMITED
Stratasys®
DAVALL
GEARS
UNDERWATER
WORLD
Stoney
Cove
GRABCAD


SOCIETE
GENERALE


SUBSEA
UK


NAVISAFE


Bcomp


entropy
RESINS


Selex ES


ROTOR
BIKE · COMPONENTS


WDS
www.wdsltd.co.uk


AXIOM PROPELLERS LTD.

NOMENCLATURE

A_f	Frontal area [m^2]
A_s	Side area projection [m^2]
b	Beam [m]
$\dot{b}$	Angular acceleration [ms^{-2}]
C_d	Drag coefficient [-]
C_l	Lift coefficient [-]
c	Chord length [m]
D	Rotor diameter [m]
d	Displacement from centre of pressure [m]
E	Young's modulus [GPa]
F_b	Buoyancy force [N]
F_{cent}	Centripetal force [N]
F_d	Drag force [N]
F_l	Lift force [N]
F_r	Rudder force [N]
g	Acceleration due to gravity [ms^{-2}]
I	Moment of inertia [kgm^2]
K	Correction factor [-]
l	Characteristic length [m]
M	Moment [Nm]
m	Mass [kg]

n	Number of blades [-]
P	Power [W]
R	Radius of turn [m]
r	Propeller radius [m]
Re	Reynold's number [-]
T	Torque [Nm]
V_{ad}	Advance velocity [ms^{-1}]
V_f	Volume fraction [-]
V_∞	Velocity (free stream) [ms^{-1}]
V_{tip}	Blade tip velocity [ms^{-1}]
v	Volume [m^3]
v_b	Volume of buoy [m^3]
α	Angle of attack [rad]
ε	Strain [-]
η	Efficiency [-]
μ	Kinematic viscosity [m^2s^{-1}]
ρ	Density [kgm^{-3}]
σ	Stress [Pa]
τ	Time [s]
ω	Angular velocity [$rads^{-1}$]
ARA	Aircraft Research Association
A-Surface	Exterior hull surface
Advance Velocity	Forward velocity of the craft

Beam	Maximum vessel width
CAD	Computer Aided Design
Cadence	Pedalling RPM
CFD	Computational Fluid Dynamics
COTS	Commercial Off-The-Shelf
CPU	Central Processing Unit
eISR	European International Submarine Races
FEA	Finite Element Analysis
FMEA	Failure Modes and Effects Analysis
HPS	Human Powered Submarine
IC	Integrated Circuit
ISR	International Submarine Races
MCU	Microcontroller Unit
NACA	National Advisory Committee for Aeronautics
PDM	Product Data Management
PWM	Pulse Width Modulation
RANS	Reynolds Averaged Navier-Stokes
RPM	Revolutions Per Minute
SCUBA	Self Contained Underwater Breathing Apparatus
Servo	Servomotor

PROJECT AIMS AND OBJECTIVES

The University of Warwick Human Powered Submarine project consists of the following high level aims, which have been distilled into a number of concise objectives:

- To compete at the 13th International Submarine Races in Washington DC
    - Finish manufacture and testing by 21st May 2015 for timely shipment
    - Achieve a speed target of 6 knots
    - Design for packaging to reduce transportation costs
- To design with three key themes
    - Efficiency – optimise the design using computer simulation packages
    - Practicality – modular design ethos for ease of assembly
    - Innovation – use of novel technology to enhance performance
- To raise the profile of Warwick Sub
- To promote STEM disciplines in schools and the wider community

Figure 1 – *HPS Godiva*

1.0 INTRODUCTION

June 2015 marks the 13th biennial International Submarine Race (ISR), held at the David Taylor Basin, Naval Surface Warfare Centre, situated in Washington DC. Participating teams are tasked with the challenge of the design, manufacture and test of a human powered flooded submersible to be raced on a straight line course, with the principle design goal of obtaining the greatest absolute speed. The competition is intended to 'foster advances in subsea vehicle hydrodynamic, propulsion and life support systems' [1] and provide an excellent opportunity to translate theoretical knowledge into reality.

The previous iteration of the Warwick Human Powered Submarine project was entered into the 2014 European International Submarine Race, and saw unprecedented success. The competition, held over three days, saw *HPS Shakespeare* and the team win the third day of racing and place fourth in the overall rankings. This iteration of the project, *HPS Godiva*, aims to build upon *HPS Shakespeare*'s performance from the dual perspectives of: modularity as the overriding design ethos, permitting simple and fast repair and overhaul operations; and improved hydrodynamic efficiency to increase the absolute speed of the submersible.

Design and manufacture of a safe, fast craft within the horizon the project requires a concurrent engineering approach which naturally lends itself to the dissemination of tasks to eight constituent sub-functions which represent major design challenges. These are:

- Hull
- Chassis
- Powertrain
- Steering
- Propulsion
- Electronics
- Safety
- Composites

This report documents the process of design and manufacture of *HPS Godiva* within each of the declared sub-functions, which are brought together in the most sophisticated submarine design produced by the University to date.

Find a detailed Cost-Benefit Analysis appended at the end of this report.

1.1 MODULARISATION ETHOS

The hardest part of building a system is deciding precisely what to build. [2]

The success of previous submarine iteration *HPS Shakespeare* is attributable to robustness in design from an excessive factor of safety and use of fundamentally simple mechanisms. The 2015 iteration of submarine design holds true to the principle of robustness, but instead from the perspective of modularity and a Systems Approach Framework (SAF) [3]. The SAF utilises system concepts such as goals, objectives, modules and integration; while formally acknowledging the interdependency of project elements. By consideration of the: objectives and performance of the whole system, resources available, individual modules and module interaction; adopting a Systems Engineering approach facilitates a structured means to coherently develop an improved design.

With a vision to compete at the ISR, where access to resources allowing repair and overhaul to the submarine are constrained, the SAF has emphasised the importance of building in subsystem modularity from the conceptual stages of design. The Fozberg and Mooz 'V-Model' shown in Figure 2 specifies an iterative cycle of 1) top down analysis of details or decomposition of high level objectives, and 2) bottom up synthesis confirming the stakeholder's objectives are met [3]. This naturally lends itself as a framework with which to base development, construction and testing of *HPS Godiva*.

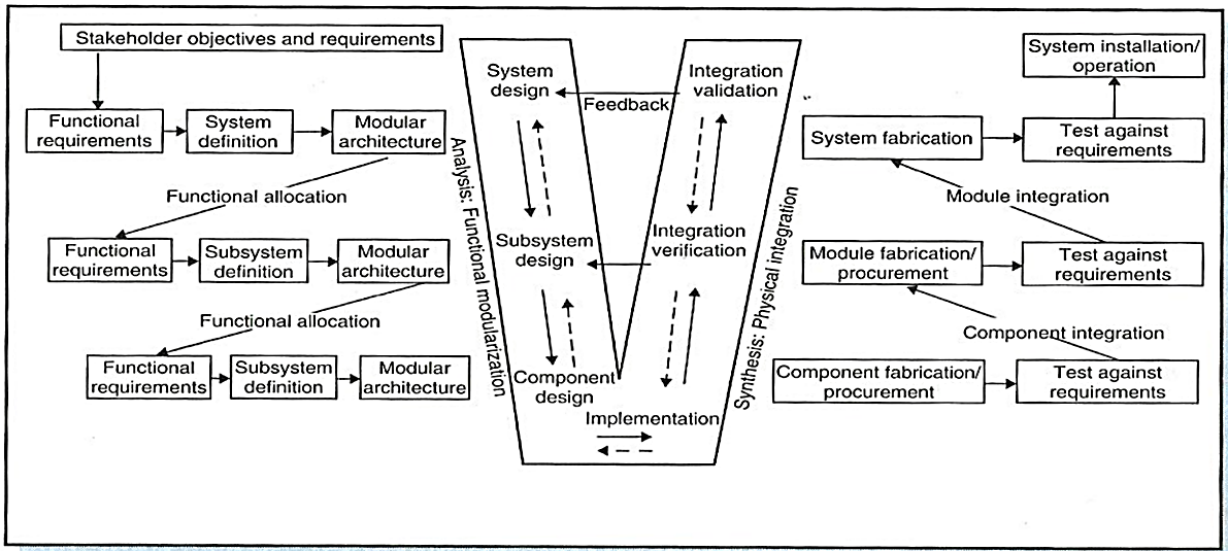

Figure 2 – Fozberg and Mooz 'V-Model' Schematic [3]

1.2 INTERNATIONAL SUBMARINE RACE 2015

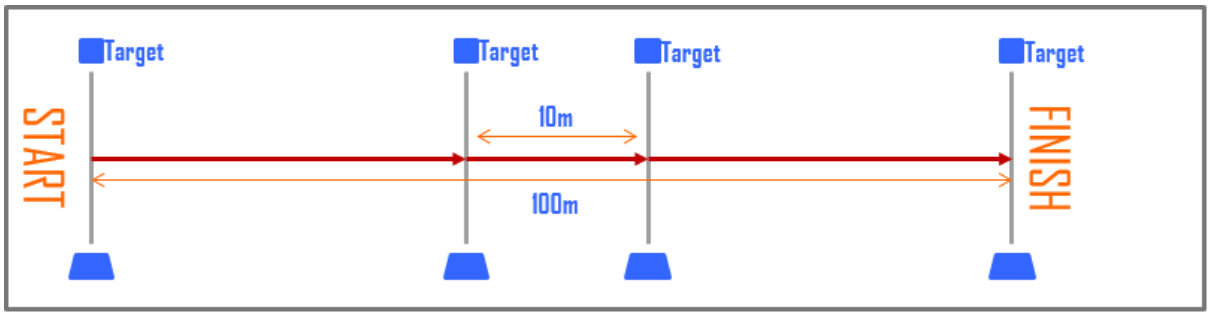

Figure 3 – 2015 ISR race course schematic [1]

1.2.1 ISR RACE COURSE

The 2015 racecourse layout schematic is given in Figure 3 above, and is designed to test singularly the absolute speed of the submarine. The course consists of the following stages:

1. A 30.5 metre acceleration zone leading to the start gate at 0 metres
2. First timing gate activated. 45 metres to next gate
3. Second timing gate activated. 10 metres to next gate
4. Third timing gate activated. 45 metres to finish line
5. Fourth timing gate activated. Race complete

The competition speed is assessed for the distances of 100 metres and 10 metres, which will define the winner of the Absolute Speed award.

1.2.2 THE AWARDS

The ISR define a number of criteria against which the merit of a submarine team design is judged. The following awards are presented when the competition is complete:

- Absolute Speed
- Innovation
- Best Use of Composites
- Best Design Outline
- Overall Performance
- Best Spirit of the Races

The team have matched design efforts to the awards through the use of a uniquely packaged hull, natural fibre composite materials and a design ethos centred on modularity and robustness. By doing so, the team hope to be in with an exceptional chance to win at least one award at the 2015 ISR.

1.3 HPS GODIVA

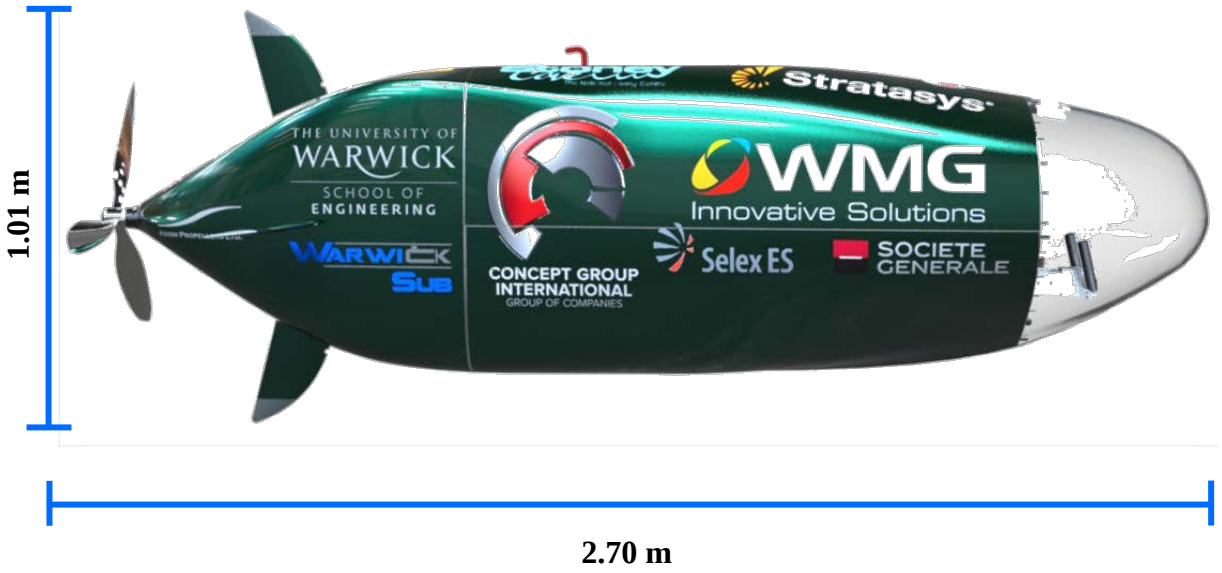

2.70 m

0.65 m

0.98 m

Figure 4 – *HPS Godiva* general dimensions

2.0 DESIGN

The following sections detail the design process of multi-objective optimisation of a human powered submarine which adheres to the guidelines specified by the ISR. Each of the sub-sections as defined in Section 2.0 follow a similar structure to communicate the design journey to a completed assembly. The structure is given by:

- **Introduction** including a summary of the main design aims.
- **Technology Summary** to give a high level summary of the academic literature which has driven the initial design decisions.
- **Concept Selection Pugh Matrix** which explores and constrains the sub-function design space to converge on an optimal solution.
- **Design Evolution and Validation** which describes the process of finalising the design based on more comprehensive theory and validation techniques. This section will detail specific case studies where theory has been applied to draw a specific and noteworthy conclusion.

2.1 HULL

2.1.1 INTRODUCTION

The hull structure is a key component of the submarine. Although not strictly necessary for submersible travel, the ISR Design Guidelines submarine is:

*"[…] a free flooding (liquid-filled) vehicle that **fully encapsulates the occupant**(s), and operates entirely beneath the surface of the water. The submarine must fully encapsulate the occupants for the entire race."* [4]

Therefore the hull structure is not a pressure vessel, as would be normal when considering submersible vehicles. Consequently reduced emphasis is placed on structural integrity and more of the design effort can be afforded to shape optimisation for hydrodynamic efficiency, whilst working within the ISR Guidelines. Hydrodynamic optimisation of the hull has required a substantial investment of both time and computational resources, which is expected to pay dividends in competition and yield significant improvement over the previous submarine iteration.

2.1.1.1 SUMMARY OF MAIN DESIGN AIMS

- To ensure pilot safety, focusing on ingress/egress, visibility and dynamic stability.
- To offer a hydrodynamic body solution, packaging for pilot, chassis and powertrain.
- To align with the project modularity ethos by the ability to be disassembled for ease of transport.

2.1.2 TECHNOLOGY SUMMARY

2.1.2.1 HYDRODYNAMIC DESIGN OF SUBMARINES

When submerged, resistance to movement for a traditional submarine can be attributed to two forms of parasitic drag – pressure and skin-friction [5].

Pressure acts normal to the surface of a submerged body at every point, and therefore varies under hydrodynamic loading. This variation results in pressure gradients that the flow must overcome to prevent separation from the hull surface and the formation of a low pressure wake. Both areas of high and low pressure act to exert a parasitic force on the hull that resists the limited thrust provided by a pilot-driven propeller, as such the reduced separation of flow reduces form drag on the hull. Burcher and Rydil verify that form drag can be minimised by varying the hull shape to reduce negative pressure gradients. However sharp shape changes are to be avoided - edges and chines act as trips for flow separation and wake generation [6].

Skin friction drag occurs due to the frictional shear force between the wetted hull surface and the surrounding flow field. As skin friction is the integral of shear stress over the hull surface, any increase in surface area should be considered as a skin friction increase [7].

For a streamlined body, it is given that the overall drag force is split between pressure and skin-friction drag such that their individual contributions are of comparable magnitude. Joubert states that by increasing the length of the hull, a more slender shape is attained and so the form drag is reduced. However the same action increases the wetted area of the hull, leading to a proportional increase in the skin-friction [5]. Therefore there is a natural trade-off between drag origins and so an optimum point exists at which the length-to-beam ratio should give a minimum overall drag. The variation of drag types with increasing length-to-beam ratio is given in Figure 5.

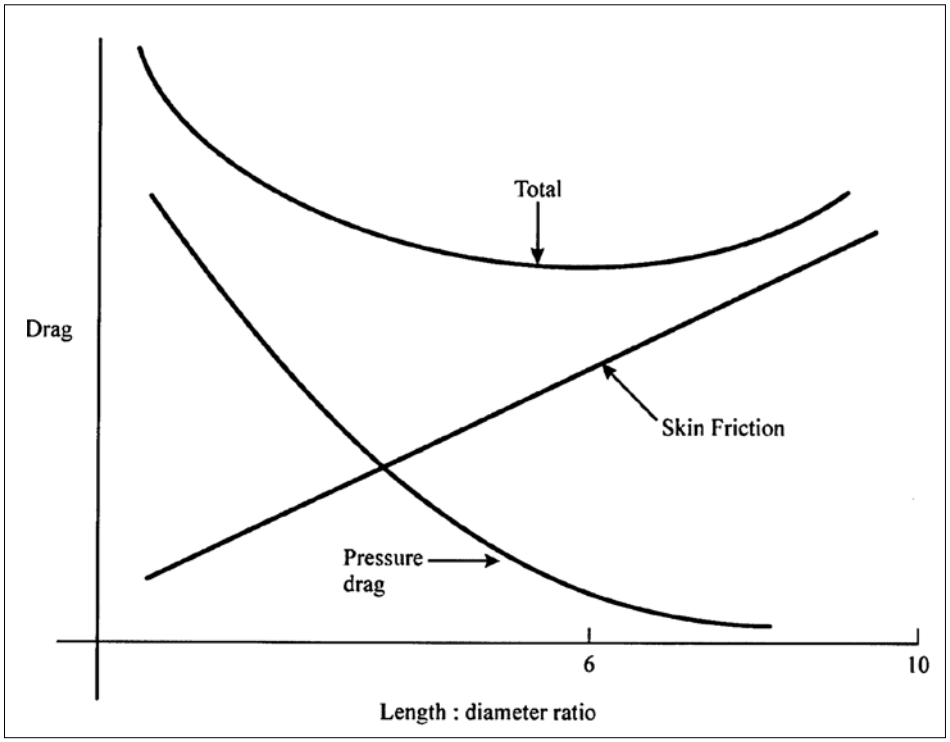

Figure 5 – The effect of length/diameter ratio on drag [6]

Increasing the length-to-beam ratio above that for minimum drag is shown to have a greater immediate impact than reducing it, and so therefore the argument of using a reduced length-to-beam ratio to minimise internal volume is justified.

2.1.2.2 PACKAGE VOLUME MINIMISATION

Minimisation of the internal volume of the submarine would, in a pressure vessel design, reduce the displacement of the vessel. However in a flooded hull, internal volume reduction is directly linked to reducing the submarine's inertia. For a human powered vehicle, this is advantageous; if the energy expended on overcoming inertia is reduced, the saving can then be utilised as increased thrust.

The shape of the hull envelope is the critical starting point for a submarine. Hervey states that a *"well streamlined outer shell which has a shape optimised for high underwater speed, low length to beam ratio (less than 8:1), bulbous bow, maximum width at about a quarter length from the bow and then tapering almost to a point at the stern"* is the ideal [8]. Joubert corroborates, promoting the continuous change of hull 'diameter' and citing an ellipsoidal bow and parabolic stern as the ideal profile shape (see Figure 6). The bow shape especially is key in defining the flow conditions over the hull surface. Hervey and Joubert's shape definitions for an 'ideal' hull profile align with the dimensions and package volume of a prone human pilot, who is naturally widest at the shoulders.

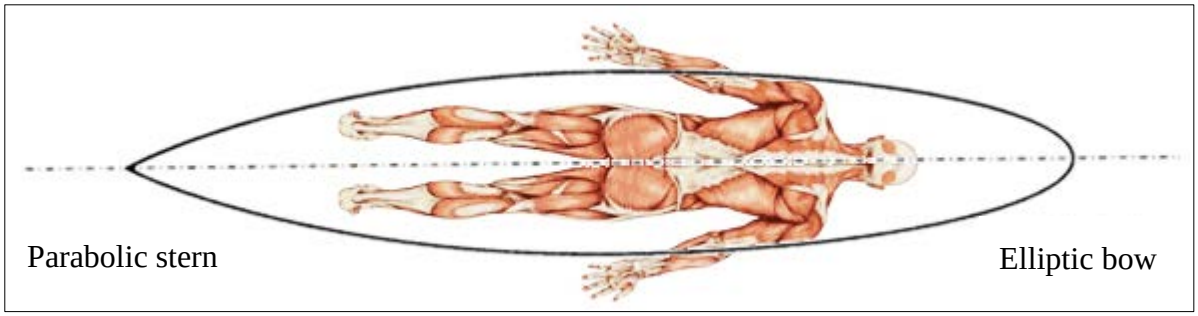

Figure 6 – Plan view overlay of Joubert's 'ideal' hull profile onto the human male in a prone position [6] [9]

Such a profile would need to accommodate the full range of movement seen in a prone cycling position, as discussed in Section 2.2. In order to minimise volume, a relatively short aerofoil shape with a large thickness is required to allow packaging of the pilot and Submarine systems. The Griffith aerofoil offers such a profile.

2.1.2.3 GRIFFITH AEROFOIL

The Griffith aerofoil is designed such that it provides a favourable pressure gradient at all points along the profile, apart from at a single instance where a pressure discontinuity occurs. Thus there is a need for suction at the point of discontinuity to prevent separation. Goldschmied states that at a low Reynolds Numbers and with a smooth surface, it is possible to retain a laminar boundary layer throughout the aerofoil's length, regardless of thickness [10]. Such a property is highly advantageous as the profile allows a large interior volume, whilst providing a low-drag solution.

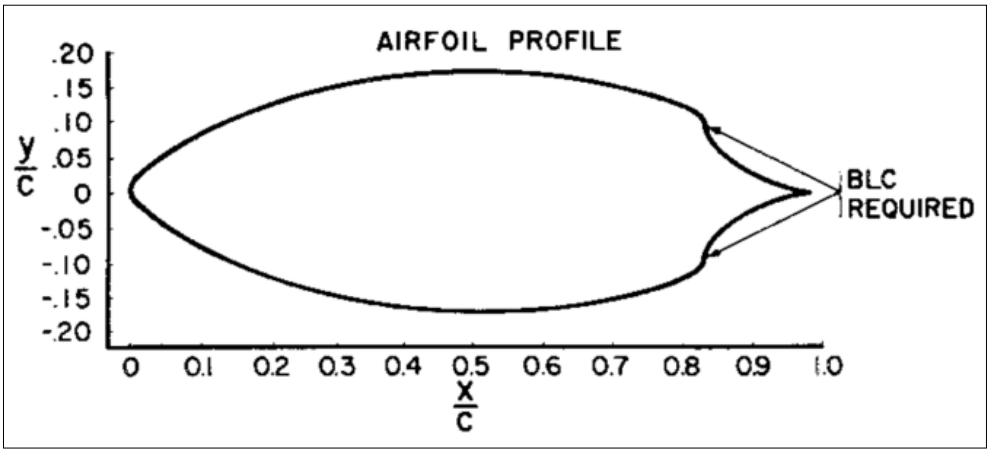

Figure 7 – Griffith aerofoil profile [8]

Although boundary layer control is required to retain a laminar boundary layer throughout, the pressure drag caused by the separation of flow at the point of discontinuity may be mitigated if contained within the diameter of the propeller. Therefore the need for suction to

be applied at the discontinuity could possibly be neglected. Joubert is of the opinion that *"It is very difficult if not impossible to maintain laminar flow on large objects moving through fluids"* as it is known that laminar boundary layer separation occurs more easily than separation in turbulent flow [11]. Though the Griffith design requires a very narrow stern, there is also a case for the profile to allow a fuller stern when considering buoyancy and overall trim of the submarine [5].

2.1.3 CONCEPT SELECTION PUGH MATRIX

A number of concepts were conceived to explore packaging the prone pilot in a hydrodynamic manner. Resulting CAD models generated from the initial sketches are given in the appendix, Section 7.1.3. In order to evaluate concepts 1-4, a number of judging criteria were selected and weighted according to their perceived importance. A summary of the weighted selection criteria in order of significance with justifications is given in the appendix, Section 7.1.4.

Using the weighted criteria, concepts were compared against *HPS Shakespeare* via a Pugh matrix to find the best design. Table 1 shows the results, highlighting Concept 4 as the most applicable starting point for the detail design.

Table 1 – Hull concept Pugh matrix

Body Shape Concepts – Pugh Matrix Decision Sheet						
Attribute	***Weighting***	***Shakespeare*** 	***Concept 1*** 	***Concept 2*** 	***Concept 3*** 	***Concept 4*** 
Robustness	13	3	0	-1	1	2
Minimised $C_D \times A_f$	12	3	4	6	5	2
Neutral C_L	11	3	7	6	4	5
Simplicity	10	3	2	-1	0	1
Minimised C_D	9	3	4	7	5	6
Minimised Internal Volume	8	3	4	7	6	5
Innovative Shape	7	3	2	6	5	4
Best Design Practice	6	3	6	4	5	7
Cost	5	3	4	5	6	7
Minimised Frontal Area	4	3	5	6	4	6
Engineering Judgement	3	3	4	2	5	6
Ease of Manufacture	2	3	4	2	5	6
Ease of Assembly	1	3	4	2	5	6

Total	273	327	361	351	374
Optimum Choice					

2.1.4 DESIGN EVOLUTION AND VALIDATION

2.1.4.1 PILOT ENVELOPE

To design a hull which packaged the pilot and his associated SCUBA equipment, the pedalling position and worst case package volume were defined. Figure 8 (left) shows the volume envelope for the pilot's assumed cycling position around which the Hull was sketched as shown in Figure 8 (right). An Ergo Link 95th percentile mannequin was used for an accurate pilot package volume, while 20 mm of clear space around each volume was defined.

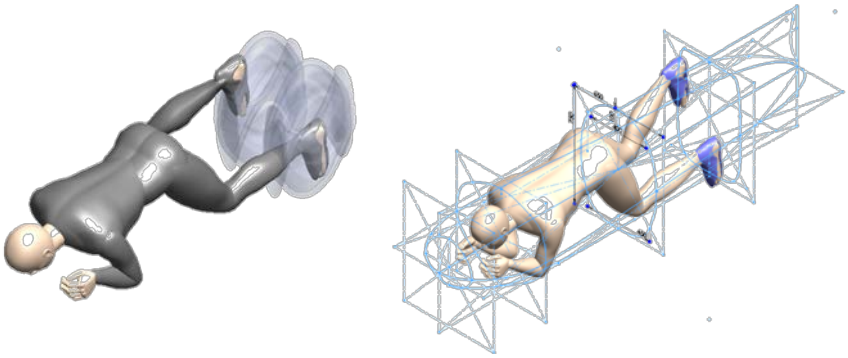

Figure 8 – Pilot's pedalling volume (left), sketched hull profiles around the pilot volume (right)

2.1.4.2 HULL PROFILE

The design of the hull took the form of a number of planar profiles – a plan and side elevation with four profiles in the front elevation were used to guide the hulls shape along its length. These profiles are shown to fit around the pilot in Figure 8 (right), and are discussed in detail in the appendix.

The resultant hull shape is presented in Figure 9 .Once this initial shape had been generated, hydrodynamic optimisation was initiated using commercial CFD software to minimise the drag and lift of the design.

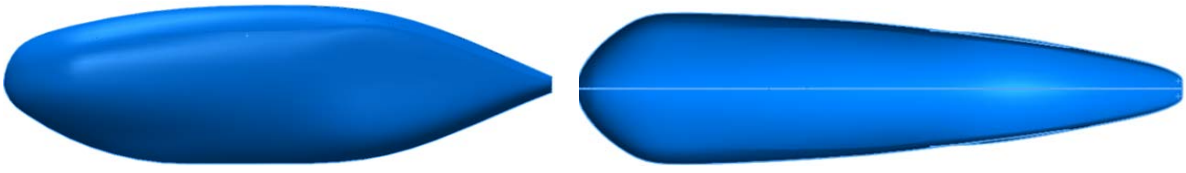

Figure 9 – Hull surface: (left) side elevation, (right) plan elevation

2.1.4.3 CFD OPTIMISATION

A commercially-available computational fluid dynamics solver was employed to assess the flow around the submarine. Star-CCM+ allowed high quality CAD representations of the hull to be assessed, with the software solving a simplified set of Navier-Stokes equations. To facilitate the iterative design process, the steady-state RANS method was used to achieve a fast turn-around time, with the K-Epsilon model to approximate the main effects of turbulence.

Mesh refinement was used to further decrease case turn-around time, as it reduces computational cost by focusing on areas of interest with smaller cells, and using a larger mesh in areas that are far away from the hull surface.

The hull analysis was initiated with the setup of a standard CFD case into which successive hull design iterations would be inserted. This was achieved using ellipsoid shapes, resulting in a case setup that could be validated using established data. White gives data for 3D ellipsoids for a range of length-to-beam ratios that was used as a comparison to the case results [7]. The mesh refinement and case validation results are presented in the appendix, Section 7.1.6. As the results were comparable to White's data and CFD was used for design iteration comparisons rather than providing absolute values, the case setup was found to be appropriate for the needs of the project.

Both quantitative and qualitative analyses were used to optimise the hull. The primary measurable was the Drag Coefficient (C_d) monitor. Based on given reference values and pressures acting over the frontal area of the hull, C_d was calculated via:

$$C_d = \frac{F_d}{\frac{1}{2}\rho A_f {V_\infty}^2} \qquad [2.1.1]$$

Similarly the Lift Coefficient (C_l) was also monitored, and was calculated by Star-CMM+ using reference values and pressures acting over the lift area of the hull. C_l was calculated via:

$$C_l = \frac{F_l}{\frac{1}{2}\rho A_l {V_\infty}^2} \qquad [2.1.2]$$

Both values were recorded for each design iteration, so that the benefits and drawbacks of each design change could be quantified. These delta values, or 'counts' gained enabled a walk-down to the final design, which ultimately was a compromise between hydrodynamic efficiency and packaging needs. Figure 10 shows the iterative development of the hull design.

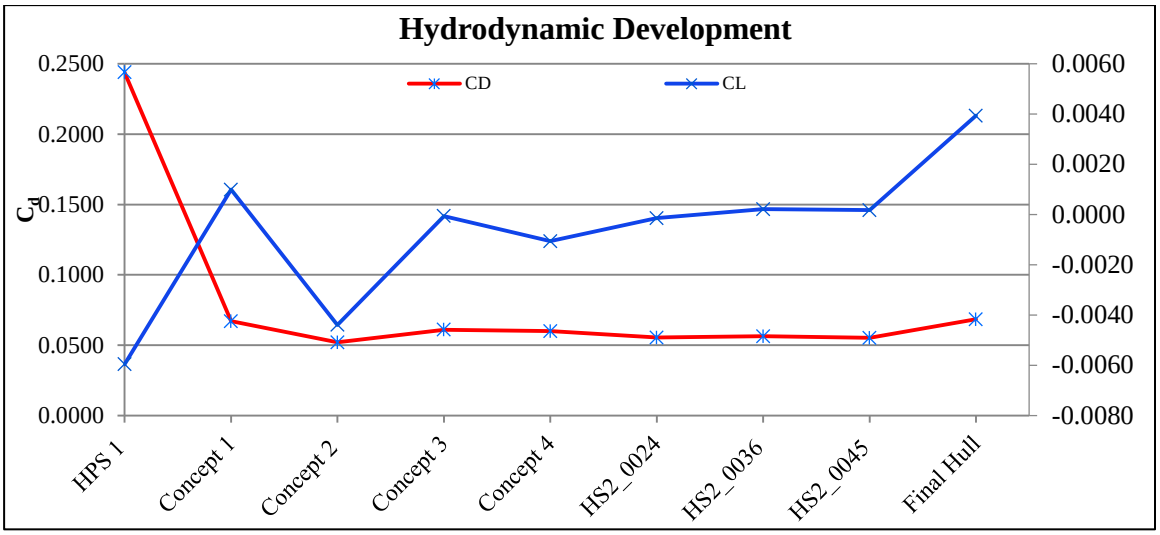

Figure 10 – Hydrodynamic development of the hull shape

Qualitative analysis was performed by interrogation of velocity, pressure and vorticity plots along with overlays of the pressure distribution onto the hull. The initial and final design plots are presented in Figure 11 for comparison.

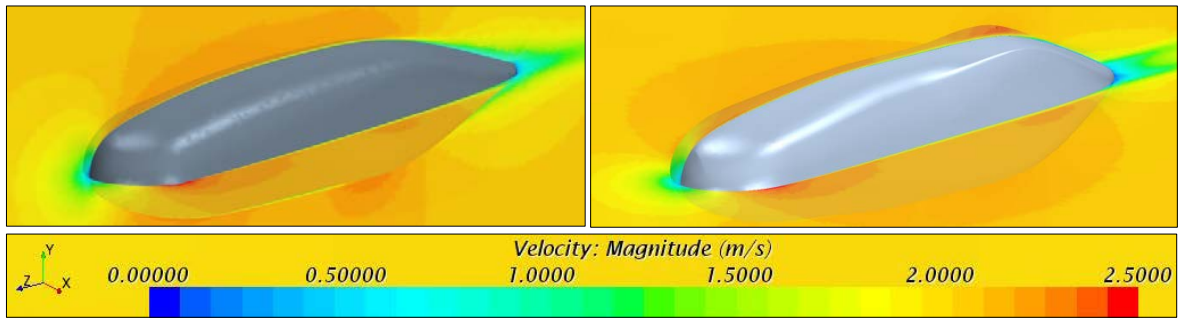

(a)

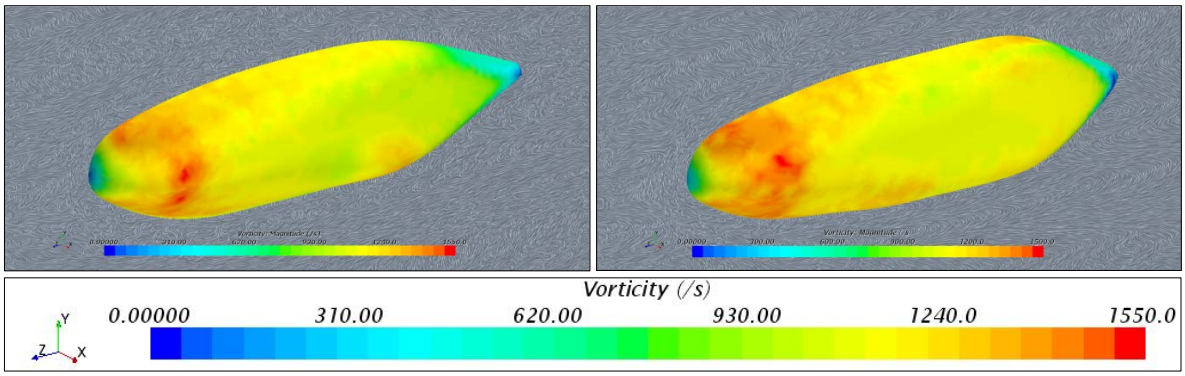

(b)

Figure 11 – comparisons of (a) side and plan elevation velocity centreline plots and (b) surface vorticity distributions and centreline flow vorticity for the initial and final hull shapes respectively

The development of overall shape from initial designs can be seen to have increased the wake size. Figure 11 (a) shows that the sharper tail with increased width (for packaging purposes)

leads to a shallow but wider wake profile. Though wider at the stern, comparison of the initial and final designs showed that the final profile retained the flow to a point further aft than the initial one. This is confirmed when consulting Figure 11 (b) which shows the side elevation vorticity centreline plots. By comparison, the final hull flow profile was shown to exhibit reduced flow disturbances forward of the tail, whilst a pair of vortices were seen to form as the tail converges onto the prop shaft. However it is expected that the effect of the propeller causing a low pressure area ahead of it will result in the reduction in tail-section turbulence and so hull drag may be further reduced.

Though concessions to hydrodynamics had to be made to facilitate packaging needs, the analysis of CAD and CFD data shows that in all relevant measurable areas of the hull design, improvements have been made (as shown in Table 2).

Table 2 – Estimated hull design measureable improvements of Godiva over *HPS Shakespeare*

Parameter	**Shakespeare**	**Godiva**	***Percentage Reduction***	***Verification***
Drag Coefficient (C_d)	0.2439	0.06839	72%	Physical Testing
Lift Coefficient (C_l)	-5.96 E-03	3.93 E-03	34%	Physical Testing
Frontal Area (m^2)	0.046061	0.03575	22%	CAD
Plan-form Area (m^2)	1.668351	1.301035	22%	CAD
Volume (m^3)	0.928021	0.677649	27%	CAD

2.1.4.4 HULL SPLITTING AND INTERFACE

To satisfy the requirements given in Table 3 there was a need to split the hull down into 4 sections.

Table 3 – Requirements for hull splitting

Requirement	***Justification***
Safety considerations	Having a large escape hatch as a single panel allows easier access to the pilot in case of an emergency
Assembly	Having a split hull facilitates easier and therefore safer assembly of the submarine
Modular design	Following the submarine's modular design philosophy, the use of a split hull allows inter-changeability of parts, such that future development can be achieved in a Kaizen manner
Transportation	To reduce transport costs, splitting the submarine down into sections

	that stack would allow the volume of the submarine to be reduced, such that the packing crate required would be smaller

The Hull splits (nosecone, escape hatch, keel and tail) can be seen in Figure 12 (left), while Figure 12 (right) shows the packaged hull.

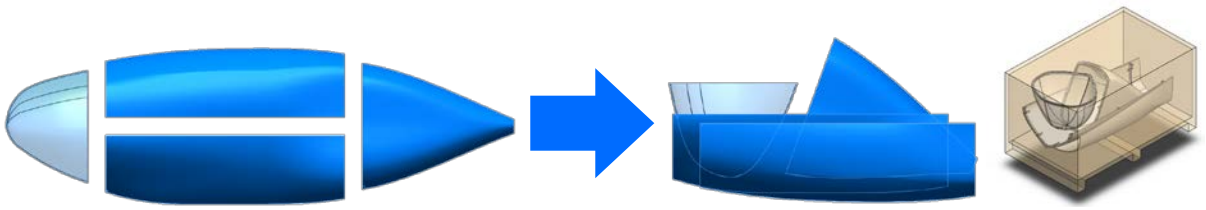

Figure 12 – Packaging of the split hull

With the described split there was a need to structurally reinforce the hull for durability and rigidity. A flange and edging system was designed to both support the individual hull sections and provide mating faces for assembly as shown in

Figure 13, integral to the flanges and edging are Grub-screws which were threaded into the parts to give a strong keying surface for the composite shell.

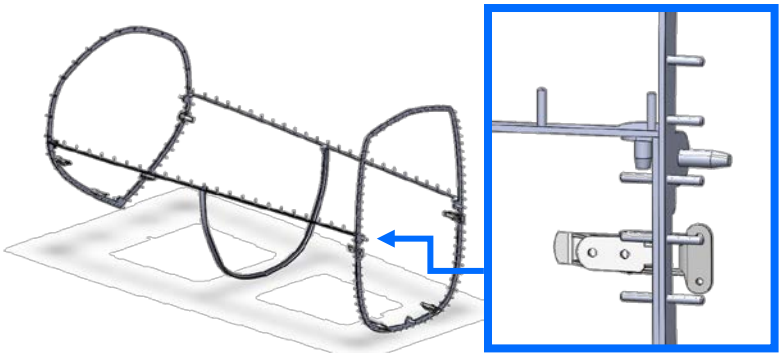

Figure 13 – Support flange and edging system

To preserve the interior volume for packaging, the flanges and edges have been designed to protrude as little as possible into the submarine interior, which also facilitates efficient stacking. The Escape Hatch mounts using the keel flanges for locating pin support, while the escape hatch release system uses the Nose and Tail Flanges as retaining surfaces. The hull also has to accommodate the requirements of a number of sub-systems as outlined in Table 4.

Table 4 – Hull interfaces and resulting features

Interface	***Accommodating Hull Feature***
Chassis	To allow connection between the chassis and the support trolley-pins which to fit into the chassis reliefs
Powertrain	Bushed hole in the tail section for the prop-shaft as per the powertrain needs
Safety	The tail section includes a profile that has been removed to allow the buoy to sit flush with the A-surface
Steering	Bushed holes in the tail section for the hydroplanes and rudder shafts as

	required
Electronics	Bushed hole in keel section to facilitate the fitment of a removable pitot-tube

2.2 CHASSIS

2.2.1 INTRODUCTION

As discussed earlier in this report, *HPS Godiva* is a free-flooding vehicle and thus does not have the same structural requirements as that of a pressure vessel-type submarine. Instead, the loading experienced by the submarine is from several sources: the forces exerted by the water on the hull of the submarine, the human powertrain and the weight of critical components, such as the SCUBA diving equipment. In addition to these load bearing capabilities, the submarine must support its essential systems such as the steering and safety mechanisms.

To understand the design problem and the challenges faced with the submarine's chassis construction, research was undertaken on existing designs, including a comparison of ladder frame and monocoque designs, an examination of recumbent and prone bicycle frames and an analysis of frame material options. Also investigated was the effect of the ISR competition rules on the design of a chassis, and a brief analysis of previous competitors' designs; these studies can be found in the appendix, Section 7.2.2 Chassis Appendix.

2.2.1.1 SUMMARY OF MAIN DESIGN AIMS

- Rigidly support the submarine hull and powertrain in a lightweight package.
- Versatility and flexibility in assembly, both of the chassis and component attachment.
- Ease of manufacture, using standardised components to allow for a simple modular assembly.

2.2.2 TECHNOLOGY SUMMARY

2.2.2.1 LADDER & MONOCOQUE CHASSIS

As the fully-flooded submarine has no requirement to withstand pressure, its hull and chassis can be constructed using more traditional techniques.

A ladder chassis has two longitudinal rails connected by lateral cross braces. The longitudinal members provide compression and bending stiffness, while the lateral members grant torsional stiffness. The advantage of this type, such as the Land Rover Defender chassis in Figure 14, is its durability and rigidity, as well as versatility in its particular shape or

configuration, however the need for a chassis and an outer body shell leads to a heavy design [12].

Monocoque chassis are single-shell structures that use the external 'skin' to distribute the load, rather than an internal frame. These structures are light and stiff, but they are not as durable as the ladder design, and any attachment must be somehow adhered onto the shell itself, as can be seen on the Volkswagen XL1 monocoque chassis in Figure 14 [13].

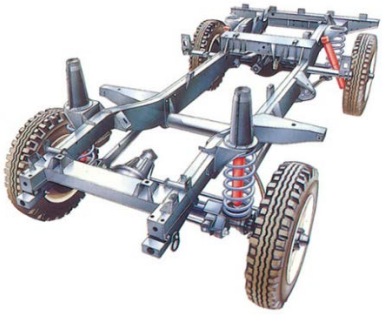

Figure 14 – Land Rover Defender ladder chassis [49]

Figure 15 – Volkswagen XL1 monocoque chassis [50]

Using a combination these two designs, an optimal submarine structure was developed. The hull acts as a monocoque chassis, distributing the pressure loading from the water throughout the hull, and transferring it to the internal chassis to which it is mounted. This internal chassis is a variant of the ladder chassis, and is designed to receive the loading from the hull, and to support the operating loads from the human powertrain and component loads, such as the SCUBA equipment. This chassis meets the modular design ethos by being designed for ease of assembly and transportation, and it is versatile and flexible in its mounting of components.

2.2.2.2 RECUMBENT & PRONE BICYCLES

Due to the similarity in loading conditions of the frame, research into bicycle frame design was undertaken to further inform the chassis design. There are two classes of bicycle that are particularly relevant to this design problem: recumbent and prone bicycles. A comparison of these bicycles with specific regard to the submarine can be found in Table 5.

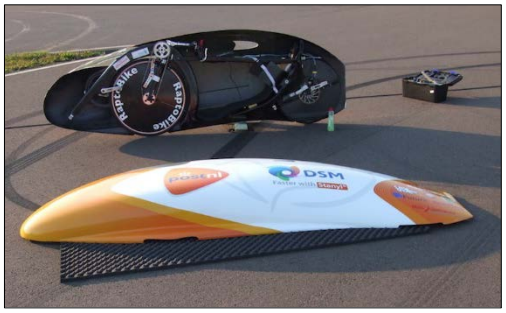

Figure 16 – University of Delft/Amsterdam's Recumbent VeloX

Figure 17 – Graham Obree's prone 'Beastie' [52]

Table 5 – Comparison of recumbent and prone bicycles for a human powered submarine

	Recumbent	Prone
Advantages	Optimal Power Output HPV record held by VeloX 3, a developed VeloX 1, see Figure 16. Natural pilot stance optimal for physical exertion.	Reduced packaging space, and thus better hydrodynamics, see Figure 17. Better pilot visibility. Space below pilot for SCUBA equipment.
Disadvantages	Chains and control cables must be routed extensively to the rear of the vehicle. Poor visibility, thus safety concern. Limited gearbox space at rear for propeller driven vehicle due to pilot.	Lower maximum power and thus lower top speed, which are high priority for the ISR Unnatural pedalling stance relative to conventional or recumbent cycling.

2.2.2.3 FRAME MATERIALS

Having learnt from the previous Warwick Sub team that their welded aluminium box-section chassis had been a time-consuming part of the total build, choosing a material that would be easy to manufacture was imperative.

Due to environmental conditions, ferrous materials were discounted for the chassis, leaving two leading options: stainless steel and aluminium. Stainless steel is both difficult to process and expensive, whereas aluminium comes in a variety of beam types, is lightweight, easy to work, cheap and will not corrode underwater. Thus, the chassis is aluminium.

The next stage was the selection of a type of aluminium. One particular beam used in the manufacture of multi-purpose frames is the Bosch Rexroth Aluminium Extrusion Series, henceforth known as 'Aluset'. This beam comes in a variety of beam profiles suitable for light and heavy duties, and is designed to work in a modular system as it can be easily bolted to another beam due to its 'X'-like cross sectional profile. This modular ability was key, as it

eliminated time-consuming manufacturing processes in favour of simply assembling cut-to-length beams with the propriety connectors, see Figure 18.

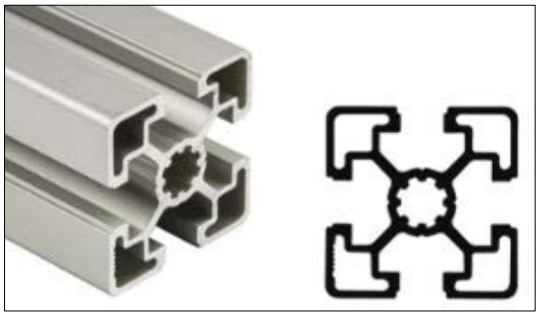

Figure 18 – Bosch Rexroth 'Aluset' 45x45mm cross-section [14]

2.2.2.4 FURTHER DESIGN ANALYSIS

Further analyses of the effects of the ISR rules on the chassis design and the ISR past competitor analysis can be found in Section 7.2 Chassis Appendix.

2.2.3 CONCEPT SELECTION PUGH MATRIX

2.2.3.1 COMPARISON OF CONCEPTS

Table 6 – Chassis concept comparison

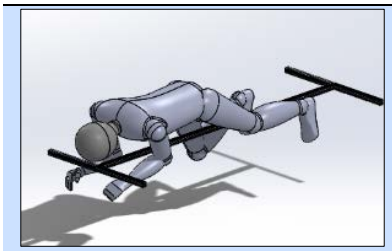 **I-Bar Concept**	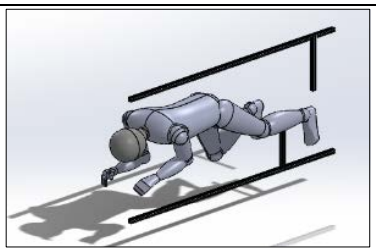 **Vertical Concept**	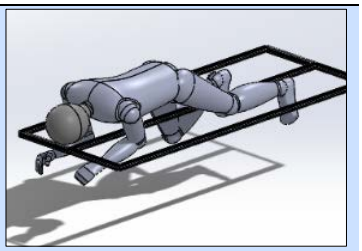 **Frame Concept**
Hull connects to the bars at the front and back at the sides – connected at four points. Drivetrain connects to the central bar using Aluset connectors. This concept is lightweight and takes up minimal space within the submarine. **Disadvantages** When operating and transporting the sub, all the loading will be placed through only five beams, which may present a stiffness problem, or place	Hull connects to the Aluset at the top and bottom of the design at several points. Drivetrain connects to the Aluset beams as in the diagram. The hull can connect to the whole top and bottom frame which will provide good support to the hull, but also stiffness when the submarine is lifted out of the water. **Disadvantages** The drivetrain will have to be attached to the vertical bars and this could pose stiffness issues due to the high torsional	Hull connects to the side bars at several points along the length of the submarine, with a central beam down the middle of the submarine. Drivetrain connects to the central bar, which will provide good resistance to the torsional forces generated during cycling. The window-like frame structure will also provide good a good structure for the hull to connect to. **Disadvantages** This concept takes up significant space within

unwanted forces through the hull.	load generated by the pedalling.	the submarine.

The concepts were compared using Finite Element Analysis (FEA) on two load cases designed to test the overall chassis stiffness, in Table 7. These tests produced bending and torsional stiffness values for each concept, and these inform the 'stiffness' parameter of the Pugh Matrix in Table 8. The visual results of this FEA can be found in the appendix, Section 7.2.1.

Table 7 – FEA stiffness comparison

Concept	*Bending Stiffness (N/m)*	*Torsional Stiffness (N/°)*
I-Bar	1580	12.5
Vertical	18200	92.8
Frame	22600	190

2.2.3.2 CONCEPT SELECTION

The next stage of chassis development is the selection of the optimal concept using a Pugh Matrix, for which the criteria justification can be found in the appendix, Section 7.2.4.

Table 8 – Pugh Matrix for chassis concept selection

		Concepts			
Criteria	***Weighting***	***HPS Shakespeare***	***I-Beam***	***Vertical***	***Frame***
Volume / Packaging	8	1	4	3	2
Stiffness	7	4	1	2	3
Durability	6	4	1	2	3
Modularity / Flexibility	5	1	2	3	4
Ease of Manufacture	4	1	4	3	2
Ease of Assembly	3	1	2	2	2

Weight	2	1	4	3	2
Cost	1	1	4	3	2
Total	-	75	89	92	95
Optimum Choice					

2.2.3.3 FURTHER CONCEPT DEVELOPMENT

The output of the Pugh Matrix in Table 8 shows that the Frame chassis is the best concept by a small margin. However, due to the difficulties in modifying the frame design to fit within the new hull, it was decided to create a hybrid chassis design.

This chassis design used the I-beam concept's horizontal front connections to the hull and its central beam design, but strengthened this beam by bolting two Aluset beams together for increased stiffness and durability, whilst maintaining modularity. At the rear of the chassis, the hull connections were taken from the vertical concept, with several connections top and bottom to ensure the stiffness of the chassis and rigid connection to the hull.

2.2.4 DESIGN EVOLUTION AND VALIDATION

2.2.4.1 CHASSIS DESIGN

Through the concept development process, the form of the chassis was evaluated and a final design chosen. This design uses Aluset beams for the majority of the chassis, using the proprietary connectors to bolt together and for component attachment, see Figure 19.

The hull connects to the chassis at five attachment points through the use of custom 'hull-chassis brackets', discussed later. Towards the rear of the chassis, the two beams connect together to improve the stiffness in this key area. The bicycle-drivetrain connects to the rear beam with the custom 'bottom bracket fixture', this was designed to take the standard bicycle 'bottom bracket' component, and is discussed and validated in the next section. At the very rear of the chassis, there is the gearbox and the steering system. The pilot is provided with shoulder braces which hold him in the correct position and provide resistance to pedal against.

Figure 19 – Chassis with components

2.2.4.2 CHASSIS VALIDATION

FEA is a computational technique that allows a model to be analysed with regard to stress, vibration, heat transfer and other physical analyses. It is based on the finite element method, which is a numerical technique for modelling physical effects on a part. This complex method is simplified using a software package such as Abaqus CAE, which was used for the analyses in this report. The purpose of this analysis was to ensure the chassis would function effectively and safety under its operating conditions.

The chassis was given several boundary and loading conditions to simulate its working environment: the hull-chassis brackets were fixed in all directions and rotations, the SCUBA equipment loading was –Y 500N, the gearbox and other components loading was -Y 200N, and 2 cycling load cases. Load Case 1 was the unidirectional loading of the pedals, with both pedals loaded in -Z 500N. Load Case 2 was simulating a torsional loading, with loading of both –Z and +Z 250N on the right and left pedals respectively.

LOAD CASE 1 – STATIC CYCLING WITH CYLINDER AND POWERTRAIN WEIGHT ON CHASSIS

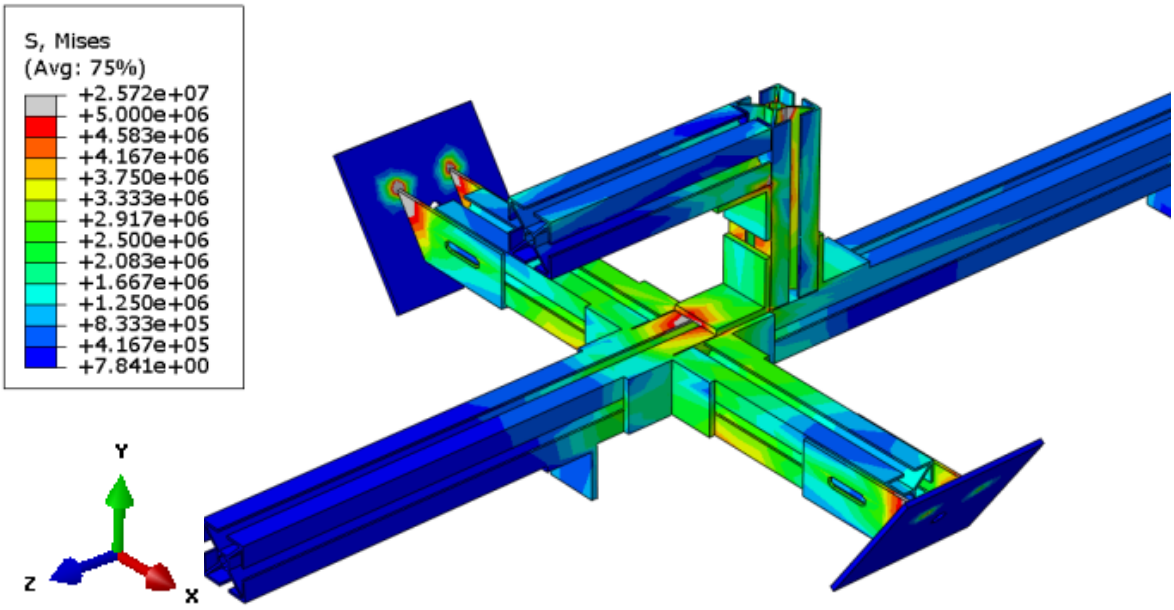

Figure 20 – Load Case 1 frontal focus (front view)

Figure 20 shows the maximum stresses occur at the hull-chassis brackets, specifically at the plate-to-U-channel connection. This stress is a concern as it is approaching 60% of the yield stress of the 6-series aluminium used for this component. To mitigate this, the joint was reinforced by gluing aluminium blocks to the two interfaces, increasing the strength of the adhesive connection. At the intersection of the front two beams, there is a high stress area due to the multiple loading conditions occurring, from the cylinder weight and the shoulder harness loading, which is represented in this simulation by the Aluset right angle assembly on top of the chassis. To design for this loading, substantial angular brackets are used to exceed the structural requirements in this key area; these components are discussed in Section 2.2.4.3.

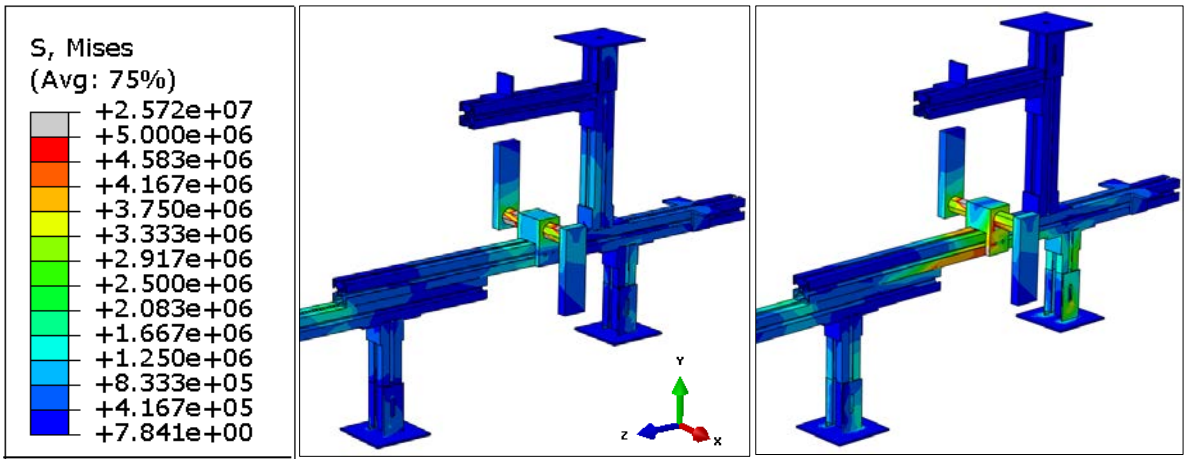

Figure 21 – Load Case 1 rear focus

Figure 22 – Load Case 2 rear focus (front view)

Figure 21 shows the high forces in the bottom bracket block, and the cranks. By designing a large safety factor into the bottom bracket block, choosing high quality machined 7 series aluminium cranks, and using the stiff Rotor chainring, these forces have been considered and designed for. The bottom bracket is further investigated in 2.2.4.3 Component Design.

LOAD CASE 2 – DYNAMIC CYCLING WITH CYLINDER AND DRIVETRAIN WEIGHT ON CHASSIS

The frontal area of the chassis shows little stress difference in this area relative to the previous load case, and thus only the rear is examined, shown in Figure 21. The torsional loading experienced in this load case indicates higher stresses in the upper chassis beam than in the previous simulation, however as the chassis is reinforced through being bolted to the other beam, this should not present any significant problems. At the rear of the chassis, the torsional forces in this load case generate relatively high stresses in the vertical chassis beam and hull-chassis bracket. This should not present a problem as the bracket will be reinforced as mentioned previously.

CHASSIS VALIDATION CONCLUSIONS

To briefly conclude the validation of the chassis; although there are several high stress areas to take into consideration, the stresses observed are significantly lower than the yield strength of the aluminium used in the chassis, in many cases by safety factors greater than 10. Upon addressing the areas of higher stress with the aforementioned design modifications, which are further discussed in the next section, this chassis demonstrates good overall stiffness and will operate safely within its mechanical properties.

2.2.4.3 COMPONENT DESIGN

There are a number of components that interface directly with the chassis. The most structurally key components were designed to ensure their compatibility with the chassis and their optimal performance. In this section, two performance critical components will be analysed and validated, and the selection of the Aluset connectors will also be examined.

BOTTOM BRACKET FIXTURE

The bottom bracket fixture is the static part of the drivetrain, and ensuring the stiffness of this key interface was a key design parameter of this component. It takes the loading of the pedals by the rider and thus must be stiff enough to provide effective power transmission to the gearbox arrangement. Figure 23 shows the Aluset, the fixture (red) and the bicycle component to which the crank arms and pedals attach (blue).

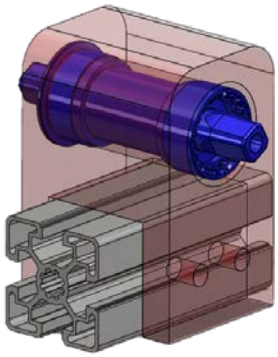

Figure 23 – Bottom bracket fixture

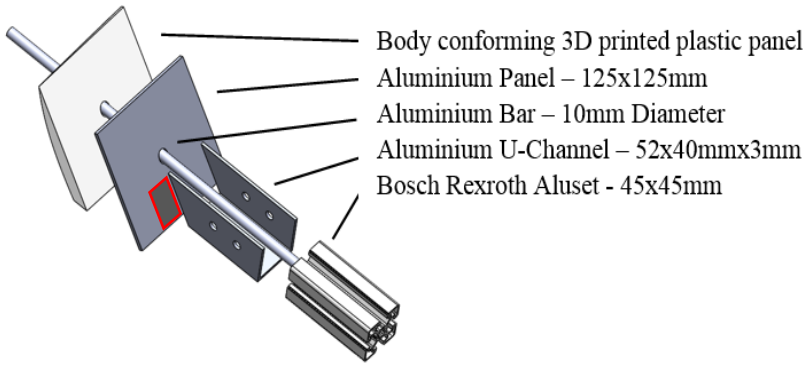

Figure 24 – Hull-chassis side bracket annotated component

CHASSIS-HULL BRACKETS

These brackets are used to connect the chassis to the hull as shown in Figure 24. The 3D printed plastic panels are shaped to fit a certain location on the interior face of the hull such that there is a large surface contact area for the adhesive to secure. The aluminium plate is glued onto the flat side of these panels, and the U-channel is glued to this using a specialist aluminium adhesive. This interface will be reinforced with a glued block to increase the adhesive contact area and thus strength of this connection, see highlighted red. The Aluset chassis can then be bolted into the U-channel, securing the chassis within the hull. The aluminium bar through this assembly is to secure the chassis in a custom cradle. This cradle is discussed briefly later in this section.

ALUSET CONNECTORS

The connection between the bars and the components is key to ensuring the stiffness of the chassis and thus powertrain, and so the proprietary Bosch Rexroth Aluset connectors are used. There are two types of form-fitting nut used in combination with standard galvanised M6/8 bolts: The M8 nut provides a large contact area ensuring a stiff connection and is used on the high load-bearing major components, however it cannot be removed easily. The M6 nut is a

‘turn-to-release’ nut with a lower contact area, and it is used for non-structural systems that may require more regular removal, such as the steering and safety buoy systems.

The other type of connection is the Right Angle connector, this provides comprehensive stiffness between the beams in the chassis, and are specially designed for the 45mm cross section beam. These connectors are heavy duty and will significantly exceed the structural requirements of the chassis.

2.2.4.4 COMPONENT VALIDATION

BOTTOM BRACKET FIXTURE

As with the chassis simulations, this component was tested using two load cases representing the loading conditions in cycling. Load Case 1 is a unidirectional load case, with loads applied away from the theoretical front of the chassis, with a magnitude of 500N. Load Case 2 is a torsional load case, with loads applied forward and backwards, simulating the pulling and pushing of the cyclist on the pedals, with a magnitude of 250N in each direction.

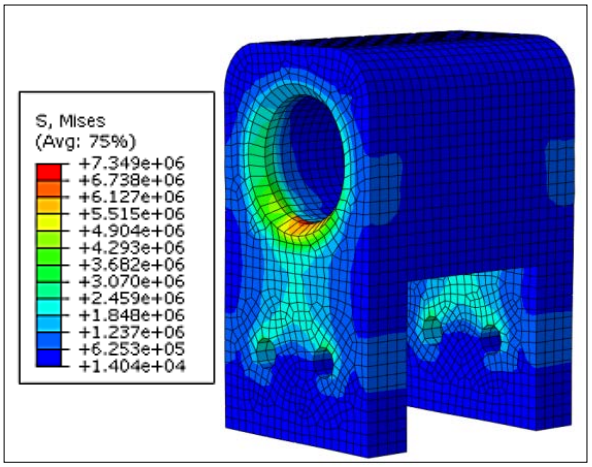

Figure 25 – Fixture Load Case 1 (visual scale factor: 1000)

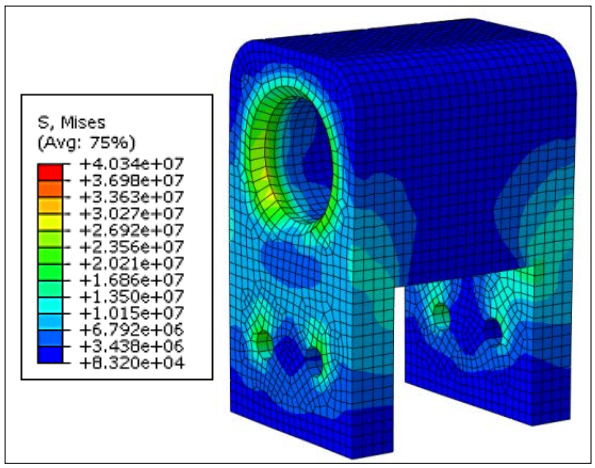

Figure 26 – Fixture Load Case 2 (VSF: 100)

The first iteration of this design was somewhat less substantial, with a lower wall thickness around the central bore. This design showed maximum stresses in excess of the yield stress of the Aluminium 6061 T4, which is 110 MPa, and so consequently this part was modified to increase the wall thickness around the bore, and a chamfer was used to decrease the stress concentration on the edges of the central bore.

The modified design was then simulated to ensure its reliability and safety. The maximum stress observed in Load Case 1 was 7.35MPa, shown in Figure 25, and in Load Case 2 was 40MPa, shown in Figure 26. This gives a safety factor of 15 and 2.5 respectively.

HULL-CHASSIS BRACKETS

The hull-chassis brackets are briefly discussed in the earlier chassis section. The side brackets in Figure 20 show the areas of high stress at the point where the aluminium U-channel meets the plate. This stress is 25 MPa, and whilst it is under the yield stress of the Aluminium 6061, which is 55 MPa, to eliminate any concern, and additional aluminium blocks are glued to the U-channel and the plate along the interface to give a higher area of contact for the adhesive.

SUBMARINE CRADLE

The cradle was designed to support the submarine through the chassis, with front and rear pins connecting to the chassis without directly loading the hull. The cradle fits all competition requirements of negative buoyancy, larger than 4 inch diameter wheels, and a width limitation. The cradle design can be seen in Figure 27.

Figure 27 – Submarine cradle

2.3 PROPULSION

2.3.1 INTRODUCTION

HPS Godiva no longer incorporates the contra-rotating propeller configuration used to propel *HPS Shakespeare*. Instead the effects of torque induced roll mitigated by a contra-rotating design are avoided through the careful positioning of buoyancy aids located through testing [15]. An optimised contra-rotating propeller arrangement requires: the specification of different propeller diameters for each rotating set, careful consideration of spacing to benefit from the effects on flow and a considerably more complex drivetrain. As propellers have not been a core design focus for *HPS Godiva* a new, robust and economical design was favoured.

This section documents the specification of design parameters to generate an optimised propeller geometry using open source software packages (JavaProp and OpenProp) given a set of variable inputs. Having produced a finalised design, a detailed sensitivity analysis was conducted in an attempt to quantify the robustness of the new propulsion system given the inherent input variability of a human power source. This section concludes to emphasise the need for significant design effort on the propeller in future project iterations.

2.3.1.1 SUMMARY OF MAIN DESIGN AIMS

- Use open source software to produce a propeller design based on inputs driven from Section 2.4 Powertrain.
- Assess the degree to which the propeller design is optimised when considering the human engine.

2.3.2 TECHNOLOGY SUMMARY

Open source software packages JavaProp and OpenProp are used to analyse a variety of propeller designs. These tools use configurable algorithms underpinned by blade-element momentum theory to automatically generate propeller geometry from a small series of inputs. As a result, use of these design tools over-simplify the realities of propeller design. To improve confidence in the outputs, the generated geometries have been historically validated against a number of empirical cases. Deviations in numerical output and testing produced errors in the region of 5% for JavaProp and the true values [16]. The propeller design space is constrained by the following software limitations:

- Modelling involves a restriction on blade number. A benchmark of 10 blades was set as the upper limit by the software developers to avoid strong, unrealistic interactions due to thickness of overlapping blades.
- 3D effects must be small, do not incorporate winglets.
- Compressible flow effects are minimal.

2.3.3 DESIGN EVOLUTION AND VALIDATION

2.3.3.1 INPUTS

JavaProp requires a number of inputs to produce propeller shapes. At a temperature of 16.9℃ and salinity of $10\,g/kg$, the kinematic viscosity of the ISR water tank is calculated as $1.10\,x\,10^{-6}m^2s^{-1}$. The speed of sound in water was taken to be $1470.46\,ms^{-1}$. A propeller used in low density, high altitude environments incorporates blades with narrower chord lengths than one used in a high density medium. The final propeller design input parameters are presented in Table 9.

Table 9 – JavaProp design parameters

Parameter	*Blade No.*	*Angular Velocity [RPM]*	*Blade Diameter [m]*	*Hub Diameter [m]*	*Advance Velocity [ms^{-1}]*	*Thrust [N]*
Input	3	250	0.75	0.05	4.5	1000

Four equidistant radial cross sections (r) of the total blade span (R), from root to tip are now defined in Table 10.

Table 10 – Spanwise aerofoil profiles

Spanwise Distance, r/R [-]	*Aerofoil Profile*	*Design Reynolds Number [-]*	*Angle of Attack [°]*
0.00	Clark Y	25,000	7.00
0.33	ARA D 6%	50,000	5.00
0.67	ARA D 6%	50,000	5.00
1.00	ARA D 6%	100,000	3.00

The Reynolds number at the tip was calculated using the Equation below,

$$Re = \frac{\rho V_{tip} l}{\mu} \qquad [2.3.1]$$

Where Re = Reynolds number, $\rho_{water} = 999.97 kgm^{-3}$, $V_{tip} = \left(\left(\frac{250.2\pi}{60} \times 0.375\right) ms^{-1}\right)$, $l = 1x10^{-2}m$ and $\mu = 1.22\,x\,10^{-3} Pa.s$. The Reynolds number at the blade tip is calculated as 80,000. All aerofoil geometry selection is completed according to the closest matching Reynolds number from the available selection within the software.

INPUT JUSTIFICATION

The gearbox is designed to output 250 RPM at the prop shaft. 0.75 metres is set as the upper limit for blade diameter. Theory suggests the use of large, slowly rotating blades for best performance [17]. As the moulds for casting the propeller is being made on a Voxeljet VXC800 3D printer, the machining envelope was not the constraint on maximum diameter. The maximum propeller diameter design constraint was taken as the widest point on the submarine to avoid damaging the propeller if the submarine hit an obstacle. 1000N of thrust is set to give a blade shape of sufficient thickness to provide the mechanical strength and stiffness required.

The previous submarine iteration concluded that increasing the angle of attack increases pitch, but decreases efficiency. Implementing the detailed research undertaken by last year's team into optimising the angle of attack along the length of the blades, this year's design reduced the angle of attack from 7° at the root of the blade to 3° at the tip. These values optimised the trade-off experienced between propeller efficiency and propeller pitch. Using steeper attack angles at the root and shallower angles at the tip facilitate higher fluid velocity at the blade tip, increasing thrust [18].

The final output from JavaProp was optimised for a fixed pitch, angular velocity, advance velocity and thrust. For the inputs mentioned previously in the input section of the report, JavaProp output an efficiency of 77% and a pitch of 1.46 metres.

2.3.4 SENSITIVITY ANALYSIS

The outputs for JavaProp and OpenProp, two open source propeller design programs are compared in this section through a sensitivity analysis (see Appendix, section 7.3.1). Design inputs are changed *ceteris paribus* to compare output geometries and figures. The results conclude that OpenProp and JavaProp produce broadly comparable outputs; however the blade geometry from OpenProp produce results more synonymous of traditional marine propellers. As JavaProp blade geometry has a shorter chord and reduced thickness, the slimmer blades present less surface area and therefore lower resistance. Initiating and sustaining the turning of large blades underwater using human power would be exhausting for the pilot making slimmer blades a more suitable choice.

Furthermore, this section concludes that the variability inherent to a human power source as described in Section 2.4 Powertrain invalidates the optimised blade geometry for the base

case as defined in Table 11 over a realistic uncertainty range. Maximum chord length and span-wise location of maxima are calculated to vary by as much as 200% over the error range of input power, rotation speed and advancing velocity.

2.3.4.1 3-BLADED PROPELLER CONFIGURATION

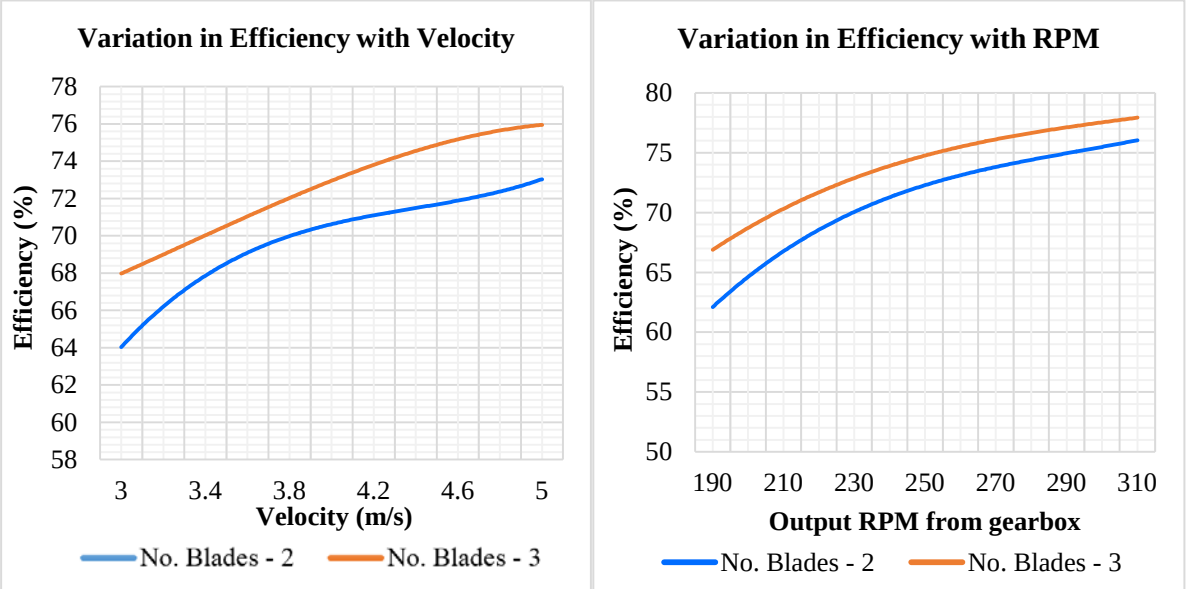

Figure 28 – Variation in efficiency with velocity and RPM

Figure 28 compares the JavaProp simulated efficiency of 2 and 3 bladed propellers generated by input variables declared in Section 2.5.3 over a range of RPMs and advancing velocities. Comparing both configurations, the computed efficiencies for both exhibit an efficiency band ranging between 60 and 70% which is typical of marine propellers [19]. For the considered geometry a 3 bladed configuration performs with higher efficiency in all cases.

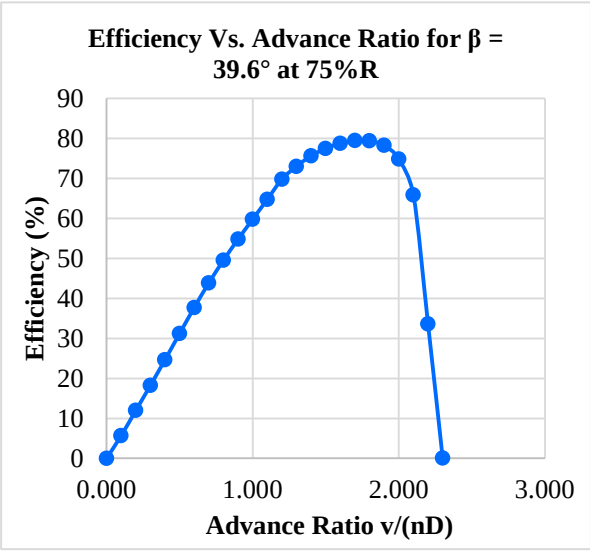

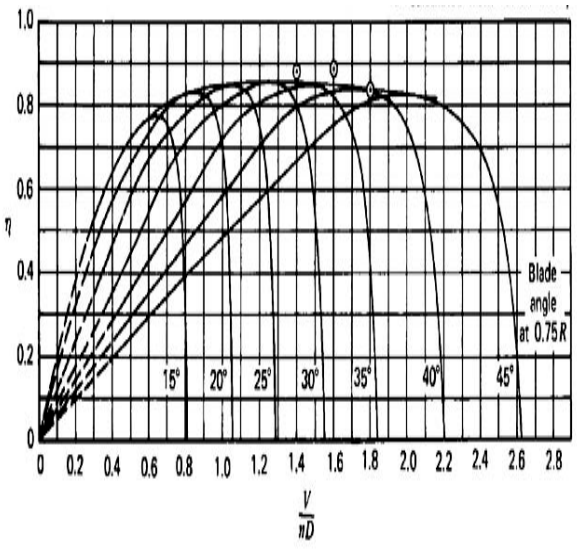

Figure 29 – Efficiency vs advance ratio for design

Figure 30 – Efficiency vs advance ratio from theory

HPS Godiva's final propeller design exhibited an advance ratio ($\frac{V_{ad}}{nD}$) - efficiency (η) relationship seen above in Figure 29. This relationship is not dissimilar to that seen in Figure 29 [20], which illustrates the indicative performance expected for a three bladed propeller with blade angle 40°. This provided further evidence for the validity of JavaProp's output.

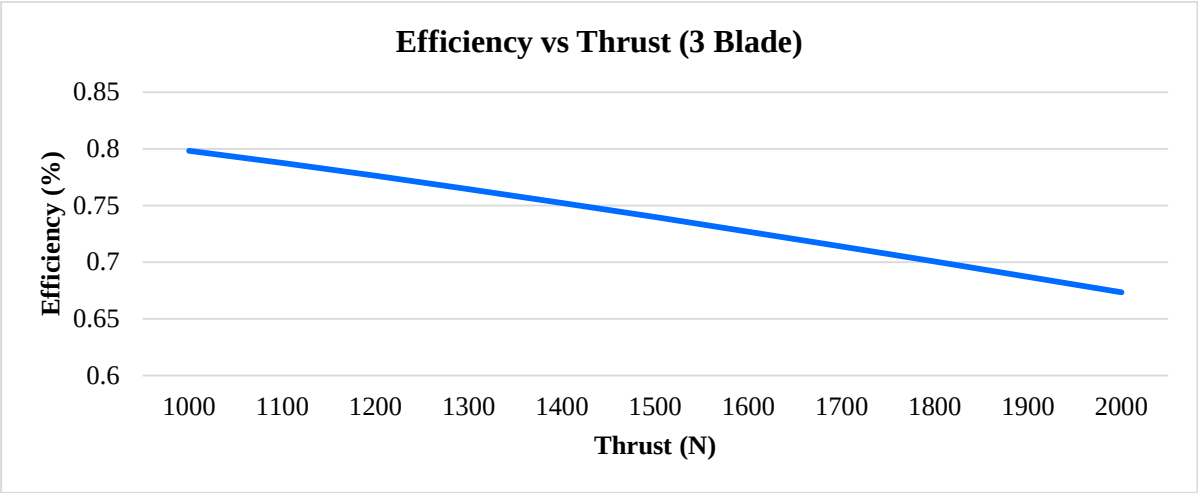

Figure 31 – Variations in efficiency with thrust for design 3 blade arrangement

Figure 31 displays the output from OpenProp software comparing the propeller efficiency over a range of thrusts. The highest efficiency, 80%, is achieved at the design output of 1000N. This input acts as a compromise between maximising propeller efficiency at relatively low thrust while maintaining manufacturable blade geometries.

2.3.4.2 EFFECTS OF UNCERTAINTY ON OPTIMISED PROPELLER GEOMETRY

The uncertainty ranges considered for the software input parameters are given in Table 11.

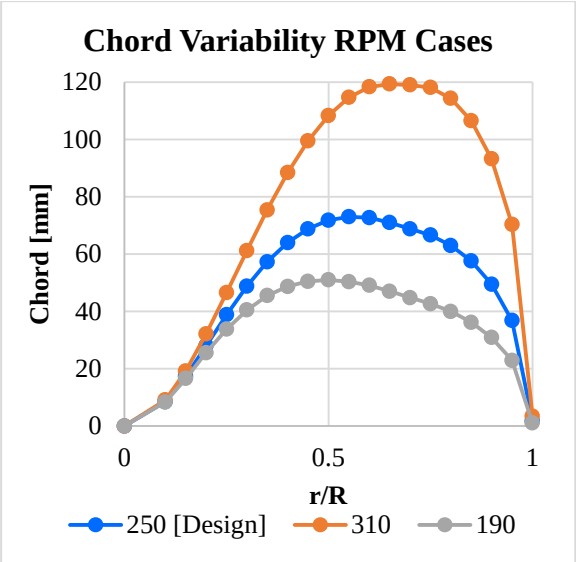

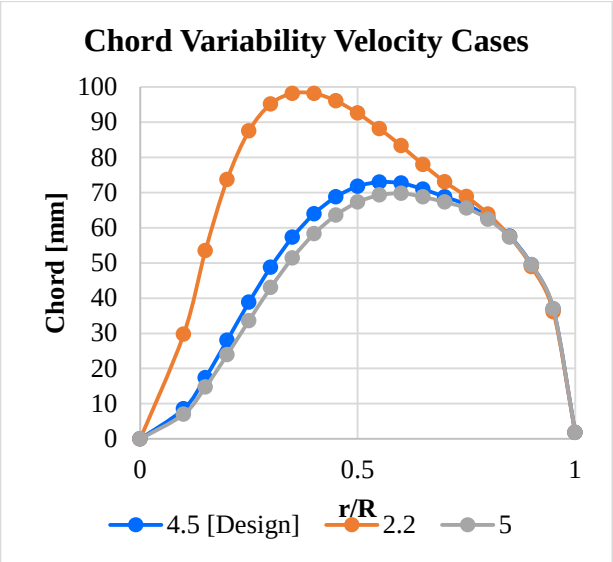

Figure 32a (left), Figure 32b (right) – Variations in optimised propeller blade geometry driven by variations in human power output

Table 11 – Expected uncertainty based on pilot testing

Variable	*Prop shaft Angular Velocity [RPM]*	*Advance Velocity [ms^{-1}]*	*Output Thrust [N]*
Design Input	250	4.5	1000
Uncertainty Range	190-310	2.2-5.0	1000-2000

Figure 32a, Figure 32b display both the variation in maximum chord length and spanwise location of chord length maxima for the range of expected RPM variability at the propeller. This variability is present as a result of the varying input pedal cadence of the human pilot and uncertainty in the advance velocity of the submarine, which is unknown. A summary of these results is presented below in Table 12.

Table 12 – Summary of variation in prop geometry from design case

Variable		*Percentage of Design Case*		
		Design	**Minimum**	**Maximum**
Prop shaft Angular Velocity [RPM]	Maximum chord thickness	100%	68.5%	163%
	Spanwise location of max chord	-	90.9%	118.2%
Advance Velocity [ms^{-1}]	Variation in maximum chord thickness	100%	135%	95.6%
	Spanwise location of max chord	-	63.6%	100%

The results in Table 12 concisely summarise that, for a realistic range of pilot inputs and submarine velocities, the optimised propeller geometry according to the JavaProp algorithm can be expected to vary by a maximum of approaching 100% from the design case. This result significantly reduces confidence in the finalised propeller design being truly optimal

and incentivises future submarine iterations to give considerable thought to a solution which allows the propeller to perform optimally over as large a range of inputs as possible.

Figure 33 – JavaProp outputs from extremes of sensitivity study. Middle prop – design geometry

2.4 POWERTRAIN

2.4.1 INTRODUCTION

The submarine uses a bicycle-based drivetrain to utilise human power input. To create an efficient design for the 'human engine' requires an understanding of cycling, human bio-mechanics and the capabilities of the submarine pilot.

This section discusses the theory behind the cycling drivetrain, including an analysis of the pilot's cycling ability and matching of the pilot input to the required output of the propeller discussed in Section 2.3 Propulsion.

2.4.1.1 SUMMARY OF MAIN DESIGN AIMS

- To design a powertrain that maximises the power output of the submarine from the pilot, based on biomechanics theory and a study of the pilot's capability.
- To design a powertrain that is as simple and robust as possible to ensure durability.

2.4.2 TECHNOLOGY SUMMARY

2.4.2.1 CYCLING DESIGN

From a biomechanical perspective, cycling requires small range of movement from the largest muscle groups in the human body. As the power output of these muscles is delivered over relatively small angle changes, it is important to understand how the body must be placed for maximised output. By using a military grade CAD mannequin in the submarine model, the

design was perfected to ensure the range of movement of the pilot in the key angles from approximately 37° - 111°, from full extension to compression, and angle of 74° total knee motion [21].

2.4.2.2 AN ANALYSIS OF THE PILOT

Using a 'Wattbike' exercise bicycle, an analysis of the pilot's capabilities was conducted providing data on power output, pedalling cadence, and power distribution through the pedalling cycle.

The ISR race takes place over a 100 metre straight-line course known to take most teams between 60-120 seconds to complete. Hence pilot analysis was conducted over these time periods, with the 30 second tests demonstrating the highest power output available, and the 60 second test demonstrating power output at a comfortable pedalling cadence. Comfort of the pilot is attributed exceptional significance in this circumstance as the submersible is free flooding.

Figure 34 shows the pilot's power output relative to the crank angle, reaching a maximum value of 878W, averaging 626W over a 30 second period. When tested for an endurance period of two minutes, a comfortable pedal cadence for consistent power output was obtained to be 95RPM.

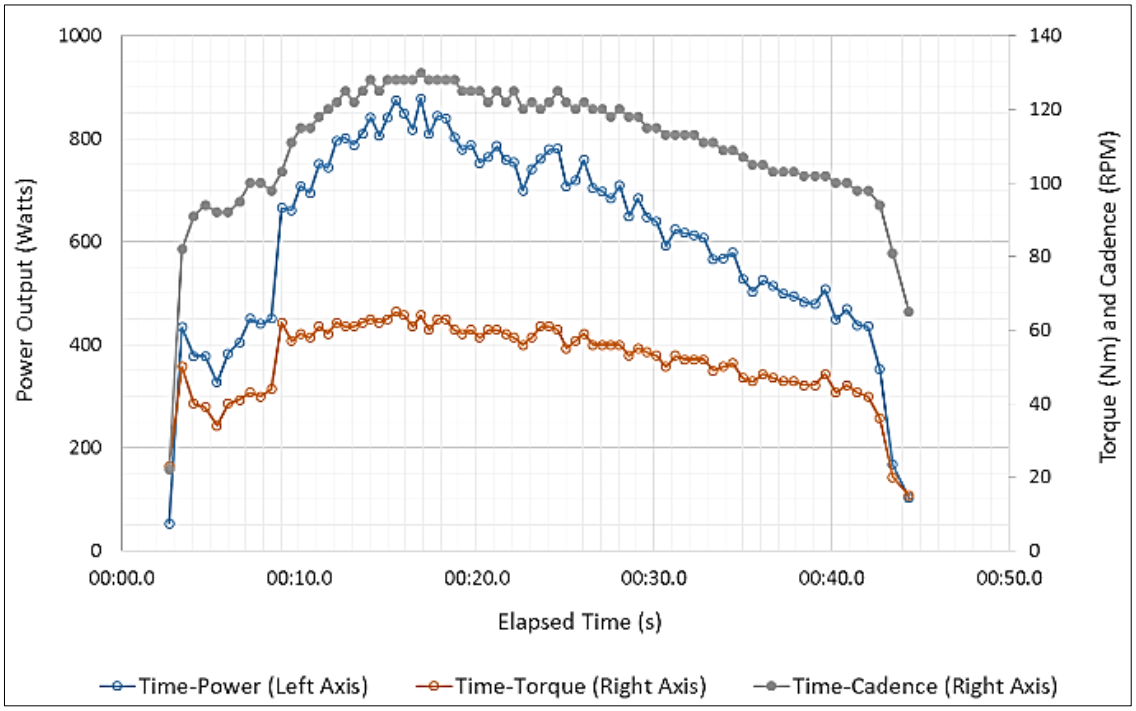

Figure 34 – Pilot's Wattbike data for power, torque and RPM over a sample 30 seconds

For maximum propulsive efficiency, the rotation rate of the propeller should be consistently maintained at the design speed, which should match the pilot's comfortable power cadence. In water, the cadence will decrease due to the water resistance, and so it is essential that the correct gearing ratio for the powertrain is chosen to ensure that at the lower cadence speeds, the powertrain provides sufficient resistance such that the pilot can deliver their maximum power capabilities.

2.4.2.3 ROTOR ASYMETRIC CHAINRINGS

Pedal efficiency is a key area affecting power output of a cycling powertrain; due to the biomechanics of a pedal stroke, there are 'dead spots' and peak power points in every cycle. Pilot analysis found the maximum power delivery to be at 114-6° in the cycle, and minimum at 90° (see appendix, Section 7.4.1).

.

A market survey showed oval chainrings are available which have maximum diameter at power minimum and vice versa, which acts to average the variation over the pilots pedal cadence. The oval Rotor chainring geometry is illustrated in Figure 35 [22].

Figure 35 – Rotor asymmetric chainring [22]

From an independent scientific study in the International Journal of Sports Science and Engineering, on "Effects of Chainring Type (Circular vs. Rotor Q-Ring) on 1km Time Trial Performance…", the Rotor chainrings were found to improve the times and speeds by 1.8%, but critically power by 6.2% (50 watts at maximum input power), and a decrease in heart rate of 2% and a consequent decrease in oxygen consumption, which is key as the pilot is using SCUBA equipment. [23]

2.4.2.4 PILOT AIR CONSUMPTION

As the pilot is using SCUBA equipment, the volume and rate of air are of critical importance when planning a successful run in the submarine. To establish the pilot's air consumption during exercise, a stationary bicycle and standard scuba air cylinder and regulator were used during a 'spinning' style session providing a safe over-estimate of the air used in a run as the exercise is continual, rather than a series of short efforts. In the test, a 12 litre air cylinder pressurised to 210 bar was emptied over a period of 35 minutes, corresponding to a consumption rate of 72 L min^{-1}. At depth the air consumption of a diver is increased [24] according to Boyles Law:

$$P_1 v_1 = P_2 v_2 \qquad [2.4.1]$$

For a planned running depth of 5 metres, the air consumption is increased by a factor of 1.5. In competition, a 300 bar, 7 litre cylinder will be used, which would last for 16 minutes at this air consumption rate, whilst retaining a minimum of 50 bar at the surface. This gives ample air for several attempts, given a projected run time of 30-60 seconds.

Figure 36 – Pilot air consumption trial

2.4.3 MATCHING OF THE HUMAN ENGINE

To achieve the defined propeller rotation output velocity the pilot must be capable of exceeding the torque requirement of the propeller. This section models a simplified version of the propeller and from first principles derives the minimum output shaft torque to ensure the pilot is capable of providing the necessary power. To achieve the desired output rotation rate off-the-shelf bicycle components and a right-angle bevel gearbox have been selected for an input pedal cadence of 70RPM, accounting for underwater operation.

Figure 37 illustrates the overall transmission ratio of the drivetrain.

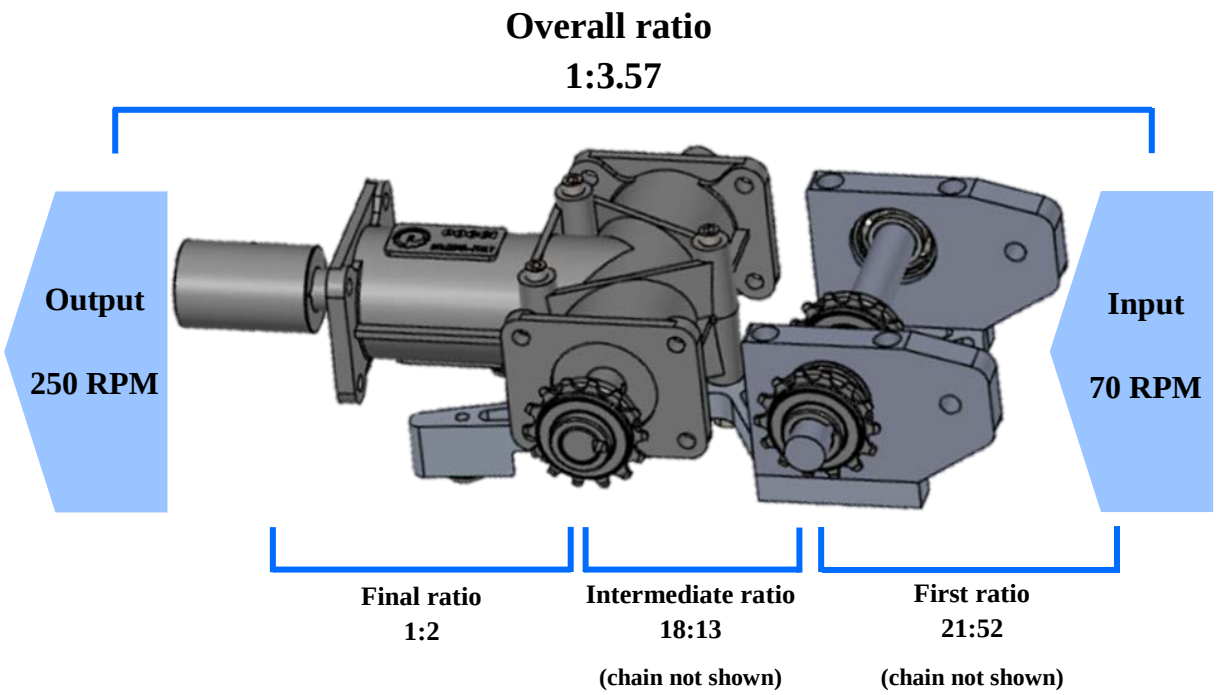

Figure 37 – Drivetrain transmission ratio

The relationship between power and torque, and relation between torque and angular velocity for constant power are given by

$$P = T\omega \qquad [2.4.2] \qquad \frac{T_{in}}{T_{out}} = \frac{\omega_{out}}{\omega_{in}} \qquad [2.4.3]$$

From the transmission ratio, the maximum torque the pilot can deliver at the prop shaft may be calculated. Assuming the pilot can pessimistically output a maximum of 600W at 70RPM while underwater, this gives a torque of 81.9 Nm.

$$\mathrm{T}_{out} = 81.9 \times \frac{70}{250} = 22.9 \qquad [2.4.4]$$

Hence, by Equation 2.4.4, the torque deliverable to the prop shaft is 22.9 Nm, therefore the torque required to turn the propeller must be less than this value.

2.4.3.1 TORQUE REQUIRED TO TURN PROPELLER

Using the ARA-D 6% aerofoil from Section 2.3 at 7° angle of attack as a representative model, the coefficient of lift and drag may be determined. Rearranging Equation 2.1.1 and Equation 2.1.2 to give values for lift and drag:

$$F_{Lift} = \frac{\rho}{2} V^2 C_L A_f \qquad [2.4.5] \qquad F_{Drag} = \frac{\rho}{2} V^2 C_D A_f \qquad [2.4.6]$$

Noting that the blades are rotating, the tangential velocity and hence the drag force varies with span r, by $V = \omega r$. Total drag on the propeller is hence given by the integral of force along the length of the propeller blade, of nominal area given by chord × span:

$$F_{Drag} \approx \frac{\rho}{2} C_D c r \times \omega^2 \int_0^r r^2 dr = \frac{\rho}{2} C_D c \times \omega^2 \frac{r^3}{3} \qquad [2.4.7]$$

As there are three propeller blades, the total drag force will be three times that expressed by Equation 2.3.3.

For an output velocity of 250 RPM the lift and drag forces are given in Table 13.

Table 13 – Summary of simplistic propeller modelling for determination of output torque

Variable	***Value***
$\boldsymbol{Cl}$	1.34
$\boldsymbol{Thrust}$ [N]	1000
$\boldsymbol{Re}$	80000
$\boldsymbol{F_{Drag}}$ [N]	74.6

Note that the modelled propeller thrust matches exactly to 3 significant figures the thrust required from the propeller generated in Section 2.3 Propulsion. Assuming that the distributed lift force may be approximated as a point force acting two-thirds along the propeller span the torque required to overcome drag is found:

$$T \approx \overline{F_{Drag}} \times \frac{2s}{3} \approx 20.0Nm \qquad [2.4.8]$$

Comparing the result of Equation 2.4.4 to the expected torque of the pilot of 22.9 Nm gives confidence that pilot will be able to turn the propeller at design speed, essential to maximise efficiency [19]. The MATLAB script for all fluid dynamics and power calculations is given in the appendix, Section 7.4.2.

2.5 STEERING

2.5.1 INTRODUCTION

The 2014 eISR competition was composed of many events such as a slalom and an obstacle course, requiring high manoeuvrability from the submarine. In contrast, in the 2015 ISR submarine performance is judged purely on a straight-line race. Consequently the role of the steering system is to make small adjustments to the direction of travel if the submarine veers

off course, and the design focus of the steering has shifted to maintaining a straight course whilst incurring as little drag as possible.

The final design provides control for both pitch and yaw, using four steering fins at the aft of the submarine. The fins are arranged in two pairs, perpendicular to one other. The control surfaces are actuated manually by the pilot using a dual-axis control yoke. Steel cables run the length of the submarine and connect the joystick to a cantilevered beam on each dive plane. Pulling on the brake cables produces a moment on the cantilevered beam and provides the torque necessary to rotate the dive planes.

2.5.1.1 SUMMARY OF MAIN DESIGN AIMS

- Provide a steering arrangement with minimum drag penalty to the hull hydrodynamics.
- Provide steering fin arrangement to provide sufficient dynamic response for the pilot given the constraints of the course.
- Ensure the steering solution is compatible with electronics.

2.5.2 TECHNOLOGY SUMMARY

2.5.2.1 DEFINITIONS OF MOTION

A submerged submarine is free to rotate in three dimensions; pitch (rotation about the transverse axis), yaw (rotation about the vertical axis) and roll (rotation about the longitudinal axis) [6]. In the final design, pitch and yaw are controlled directly by the pilot using a control yoke. Roll is general unwanted in a submarine and is mitigated by the shape of the hull and the positioning of the buoyancy aids. Fine tuning in any can be achieved by trimming the control surfaces before the race.

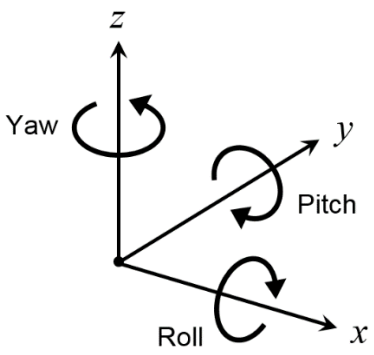

Figure 38 – Freedom of motion

2.5.2.2 DIVE PLANE DESIGN – 2D CONSIDERATIONS

Figure 39 – NACA 0012 aerofoil with pivot point situated at 20%

For *HPS Shakespeare*, control surface design was not a major objective and so the component was made from a simple flat plate which rotated around a pivot. However the cross-sectional shape of a control surface can greatly affect its performance. The surfaces are positioned at an angle of attack to the oncoming fluid flow, creating a pressure difference between the top and bottom of the cross-sectional foil shape. This generates the lift force used to turn. However once a critical angle of attack is reached, stall will occur and the lift force generated begins to decrease. Different aerofoil profiles have different stall angles. A thin flat plate has the smallest stall angle, at approximately $\pm 5°$ from the nominal position [25]. NACA aerofoils provide higher stall angles and have a smaller drag per unit turning force, making them suitable for use as marine control surfaces. Hoerner and Borst suggest using a NACA '00XX' series aerofoil for marine applications due to their symmetric properties [26]. The last two digits of this series refer to the maximum thickness of the foil as a percentage of the chord length. A thinner aerofoil will possess slightly less drag and yield a higher lift coefficient before stall. However thicker aerofoil sections are required to withstand the large bending moments often experienced whilst turning in water. A good compromise is the NACA 0012 aerofoil, shown in Figure 39, which stalls at approximately 15°, as shown in Figure 40.

2.5.2.3 PIVOT POINT OPTIMISATION

The positioning of the pivot point of the rudder along the aerofoil cross-section can make a great difference to the rudder's ease of turn. An unbalanced rudder has the pivot point positioned at the extreme frontal end of the rudder. On a balanced rudder, there will be a certain portion of the blade area forward of the pivot point, which will decrease the force necessary to pivot the rudder. However the portion of the blade forward cannot be too great a percentage of the rudder area as this will make the controls overly sensitive and cause the rudder to turn too easily, requiring the pilot's constant attention. In general a balanced rudder will have an area forward of the pivot point of up to 25% of the total rudder area, as shown Figure 39 [27].

2.5.3 CONCEPT SELECTION PUGH MATRIX

2.5.3.1 HYDROPLANE POSITIONING

The previous year's *HPS Shakespeare* used two large pectoral hydroplanes to control the Pitch. Earlier designs for this year assumed the same system of control would be used, however the pectoral fins could be shrunk to compensate for the smaller size of the submarine. Table 14 analyses this method against steering using hydroplanes positioned at the back (aft) of the submarine. The Pugh matrix criteria weightings are fully explained in Appendix 6.5.

Table 14 – Hydroplane positioning Pugh matrix

		Concepts	
Criteria	***Weighting***	***Pectoral Fins***	***Aft Hydroplanes***
Functionality	10	1	2
Cost	9	1	2
Ease of Manufacture	8	2	1
Simplicity	7	2	1
Modularity	6	2	1
Drag Penalty	5	1	2
Weight	4	1	2
Total	-	70	77
Optimum Choice			

Positioning the bow planes far forwards, like the pectoral fin arrangement on *HPS Shakespeare*, is a simpler design as the angle of the fins can be directly controlled by the pilot by simply twisting the handlebars. Literature also suggests that pectoral fins can provide a more effective movement for low speed control [6].

However, pectoral fins incur a large drag penalty. CFD tests from last year revealed that the hydroplanes contributed up to 50% of the total drag around the submarine. Additionally, by positioning the control surfaces in front of the centre of mass, the force imparted will naturally act to further increase any small perturbations from the water, unless this is corrected by the pilot, i.e. positive feedback. By moving the control system behind the centre of mass, the control surfaces will act to correct any small perturbations from the nominal position, similar to the purpose of feathers on an arrow. However note that by placing the dive planes further back, the pilot no longer has direct control over them so there must be a linkage in between the pilot's actions and the motion of the dive planes. The rudder positioning is justified in the appendix, Section 7.5.1.

2.5.4 DESIGN EVOLUTION AND VALIDATION

2.5.4.1 RUDDER DESIGN EVOLUTION

Table 15 – Summary of steering design evolution

Design description	*CAD mock-up*	*Justification*
Basic concept		The rudder is situated behind the propeller, supported by a square frame which attaches to the submarine via a bearing block on the propeller shaft
Frame shape changes and rudder side profile adapted	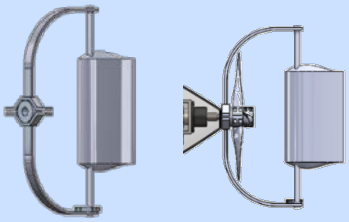	The loop is made smaller to cope with the high forces imparted by the water resistance. The rudder shape side profile was curved to discourage vortex drag
Rudder moved in front of the gearbox	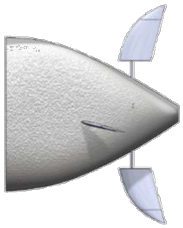	See the Pugh matrix analysis in the appendix, Section 7.5.1
Final design	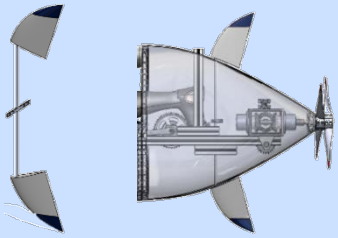	The rudder side profile was adapted such that it followed the shape of the hull. This will reduce induced drag

2.5.4.2 STEERING CONTROL DESIGN EVOLUTION

Table 16 – Summary of control design evolution

Design description	*CAD mock-up*	*Justification*
Joystick	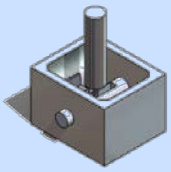	Based on a mechanical 2-axis joystick. A joystick was considered overly complicated for this project.
Pulley design	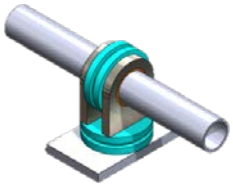	Ergonomic considerations resulted in a two-handed control design at the pilot's preference.
Moment bar design	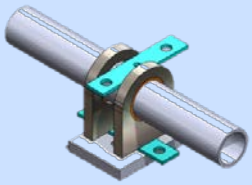	The pulleys were replaced with moment bars as the length of moment bars can be easily adjusted, whereas the diameter of a pulley is fixed.

Yoke style controls	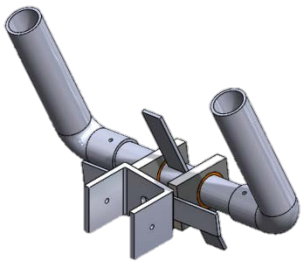	There were fears that the pilot might accidentally twist the handlebars whilst trying to control the rudder. This would cause the dive planes to move and could cause roll. The orientation of the controls was changed so that the controls were more independent of each other. This is very similar to a yoke controller on an airplane
Final design	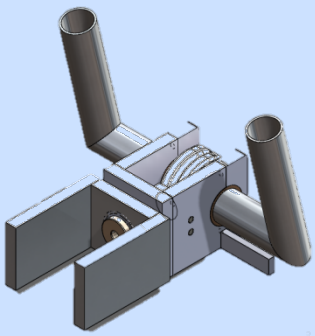	A few design changes were implemented to make the yoke simpler to manufacture. The Lower moment arm, used for controlling yaw, was moved closer to the handles so the pilot could not accidentally hit his wrists against it. The top moment bar, responsible for controlling pitch, was changed back to a pulley design as the cable runs needed for the moment bar design were too sharp.

2.5.4.3 RUDDER AND HYDROPLANE VALIDATION – 3D CONSIDERATIONS

The fin shape has been optimized to be used primarily for direction control, but also to stabilize the submarine. When the submarine is not turning, their function is to keep the submarine moving in a straight line and to prevent roll due to the propeller's torque reaction.

CALCULATING RADIUS OF TURN

Although there is not a requirement for the submarine to turn around within the ISR competition, the size of the rudders and hydroplanes must still be optimised to ensure that they can provide sufficient manoeuvrability. A good way to judge manoeuvrability is by the radius of turn. The lift force imparted by the rudder will in turn cause a lift force on the hull. The lift force imparted by the hull can be equated to the centripetal force to find the radius of turn (R):

$$F_l = \frac{1}{2}\rho V_\infty^2 A_s C_L \qquad [2.5.1]$$

Where ρ is the water density (1000 kg/m^3), V_∞ is the free stream velocity, A_s is the submarine side area, and C_L is the coefficient of lift.

$$F_{cent} = \frac{mV_\infty^2}{R} = \frac{V_\infty^2}{R} \cdot \rho A_s b \qquad [2.5.2]$$

where m is the mass of the submarine, b is the width of the hull. Equating the two yields:

$$\frac{1}{2}\rho V_\infty^2 A_s C_L = \frac{V_\infty^2}{R} \cdot \rho A_s b \qquad [2.5.3]$$

Cancelling out and rearranging to find R:

$$R = \frac{2b}{C_L} \qquad [2.5.4]$$

where w is the width of the submarine (~0.45 m). Assume C_L is 0.3 for the submarine hull, modelled as a cylinder at 5 degrees to the oncoming flow. This yields:

$$R = \frac{2 \times 0.45}{0.3} = 3 \text{ m}$$

And so the submarine should turn with a radius of 3m, or make a complete turn within 6 m. This is smaller than the 25 ft (7.62 m) in between the timing gates at either side of the testing tank and so is sufficient.

CALCULATING SPEED OF TURN

The submarine should be responsive to the pilot controls. For example, the submarine should be able to turn by angle $\alpha = 10°$ (or $\alpha = 0.17$ rad) in time $\tau = 1$ seconds. The angular acceleration of the submarine can be expressed as:

$$\dot{b} = \frac{M}{I} = \frac{F_r \cdot d}{I} \qquad [2.5.5]$$

Where M is the moment caused by the rudder acting at distance d from the centre of pressure/mass, F_r is the lift force imparted by the rudder, I is the moment of inertia of the submarine

$$\alpha = \frac{\dot{b}\tau^2}{2} \rightarrow \dot{b} = \frac{2\alpha}{\tau^2} \qquad [2.5.6]$$

$$F_r = \frac{I}{d} \cdot \frac{2\alpha}{\tau^2} \qquad [2.5.7]$$

The moment of inertia of hull can be approximated as a cylinder, rotated about its central Z axis:

$$I = \frac{1}{2} m \left(\frac{l}{2}\right)^2 \qquad [2.5.8]$$

Where l is the length and m is the mass of the submarine. For calculating the mass, the volume of the submarine (v) has been approximated using a rectangle and a correcting factor (K). The density of the submarine is assumed to be the same as the density of water since it is neutrally buoyant.

$$m = \rho v = \rho \times F_s \times b \times K = 1000 \times 2.6 \times 0.45 \times 0.7 \times 0.65 = 532kg$$

Therefore the lift force required to produce this angular acceleration is:

$$F_r = \frac{(0.5 \times 532 \times 1.3^2) \times (2 \times 0.17)}{0.8 \times 1^2} \approx 191N$$

This can be compared to the steady-state lift force generated by the rudder:

$$L = \frac{1}{2} \rho V_\infty^2 A_s C_L \qquad [2.5.9]$$

Where ρ is the water density (1000 kg/m^3), V_∞ is the free stream velocity, A is the rudder side profile surface area, and C_L is the coefficient of lift.

Figure 40 shows data on the NACA 0012 aerofoil, collated from a variety of experiments. The graph reveals that for small values of α (angle of attack), before stall occurs at approximately $\pm 15°$ degrees, the coefficient of lift is directly proportional to α. Calculating the gradient of the best fit line gives the relationship $C_L = \frac{1}{9}\alpha$, so for maximum α before stall, $C_L = 1.6$.

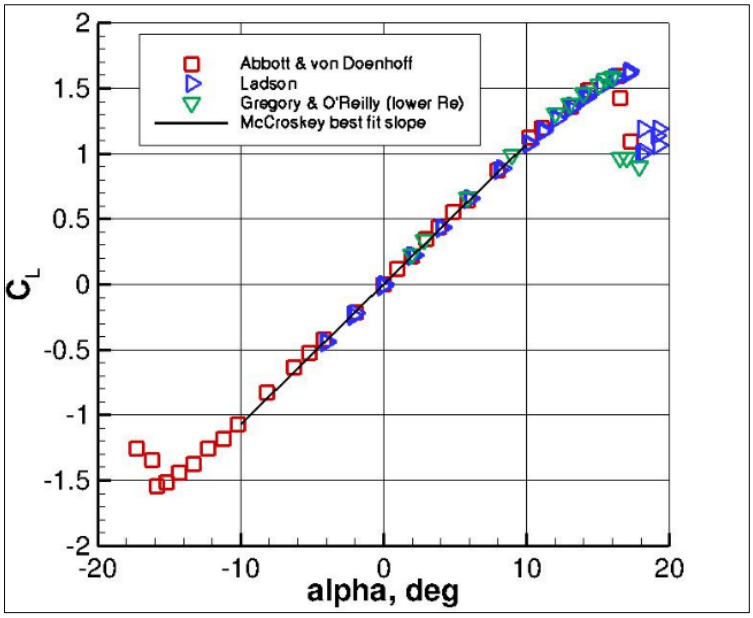

Figure 40 – Graph showing angle of attack vs lift coefficient

The MATLAB code in the appendix, Section 7.5.4 can be used to evaluate the lift force. For the final design of the steering controls, the surface area of each fin was found to be approximately $0.03m^2$. This must be doubled to find the overall lift force, and so $A = 0.06m^2$. For a velocity of $V_\infty = 2ms^{-1}$, the lift force is:

$$L = \frac{1}{2} \times 1000 \times 2^2 \times 0.06 \times 1.667 = 200\ N$$

This lift force is slightly larger than the required force to produce the angular acceleration (191 N). It is calculated using a slower speed than the target speed of 6 knots, and so the force produced by the fins should be more than capable of steering the submarine with sufficient responsiveness.

2.6 ELECTRONICS

2.6.1 INTRODUCTION

Electronics is a new concept for Warwick Submarine, owing to the project being relatively new at the university and previous years' teams focusing on creating a working submarine. However this year's team are in a position to push the design boundaries and build upon *Shakespeare*'s successes. It was agreed that including electronics could add some unique and useful features to the new submarine design.

It was decided that the new system would include: an array of sensors to log data about various aspects of the submarine's operation, a small display for the pilot to provide real-time feedback on his performance, and actuators to move the control surfaces enabling automatic stabilisation of the submarine. The whole system is run by a central microcontroller unit.

2.6.1.1 SUMMARY OF MAIN DESIGN AIMS

- To design a data logging system which provides useful information about submarine performance.
- To allow integration of an electronic control system which reduces pilot workload.
- To produce a reliable electronics package which future years can build upon.

2.6.2 TECHNOLOGY SUMMARY

2.6.2.1 MICROCONTROLLERS

A microcontroller unit (MCU) will be at the heart of the new electronic system. An MCU condenses all the component parts of a typical 'desktop' computer into a millimetre scale integrated circuit (IC). Typically found in 'embedded' applications, the MCU is part of a larger device which requires some kind of computational or interactive ability, but does not need the processing power or flexibility of a standard PC, for example microwave ovens, telephones, and TVs. A focused purpose allows MCUs to be cheaper, more power efficient and generate less heat than a desktop computer, making them particularly appropriate for portable and battery-powered applications.

Figure 41 – The FRDM-K64F Freedom board from Freescale [28]

2.6.2.2 SENSORS

Also key to the system are the various sensors used to gather data about submarine operation. Sensor technology is a fast-moving and heavily-researched area, and modern devices can be extremely sophisticated with integrated MCUs accessed over a digital communications bus. This controller is responsible for: sampling the sensor output, amplification, digital conversion, removing any offset or noise from the signal and often storage. 'Microsensors', which combine all of this functionality and the sensing element itself onto a single silicon chip, are developing rapidly [29]. The submarine system will use several pressure sensors of this kind to measure depth and speed.

2.6.2.3 ELECTROMECHANICAL ACTUATORS

Electromechanical servo motors (servos) can be used to manipulate the control surfaces and steer the submarine. Typically designed for medium sized remote-controlled vehicles, they provide a relatively high-torque output and a simple control interface in a small package. Servos are controlled using a version of pulse-width modulation (PWM) in which the width of the pulse sent determines the position of the servos output arm [30]. This simple protocol is straightforward to implement using a modern MCU like the K64F chosen for this project, and along with the powerful, precise output makes these servos ideal for controlling the submarine.

Figure 42 – Radio control servo disassembled [31]

2.6.3 THE NEW ELECTRONIC SYSTEM

2.6.3.1 MICROCONTROLLER CHOICE

The choice of microcontroller used is very important as it greatly affects how the software is written and the type and number of external devices which can be connected. The Pugh matrix in Table 17 shows why the Freescale FRDM-K64F was chosen over several of its competitors; a combination of its fast, powerful central processing unit (CPU), wide variety of input/output ports and ease of programming.

Table 17 – Microcontroller selection matrix

		Concepts				
Criteria	***Weighting***	***Arduino Uno***	***Arduino Due***	***Teensy 3.1***	***FRDM-KL25Z***	***FRDM-K64F***
Ease of Programming	7	5	3	2	4	4
I/O Pins	6	2	5	4	3	3
Code Space	5	1	4	3	2	5
Cost	4	4	2	4	5	3
Processing Power	3	1	3	4	2	5
Peripherals	2	3	4	4	4	5
Power Consumption	1	5	4	4	4	4
Total	-	82	100	93	94	112
Optimum Choice						

2.6.3.2 SYSTEM OVERVIEW

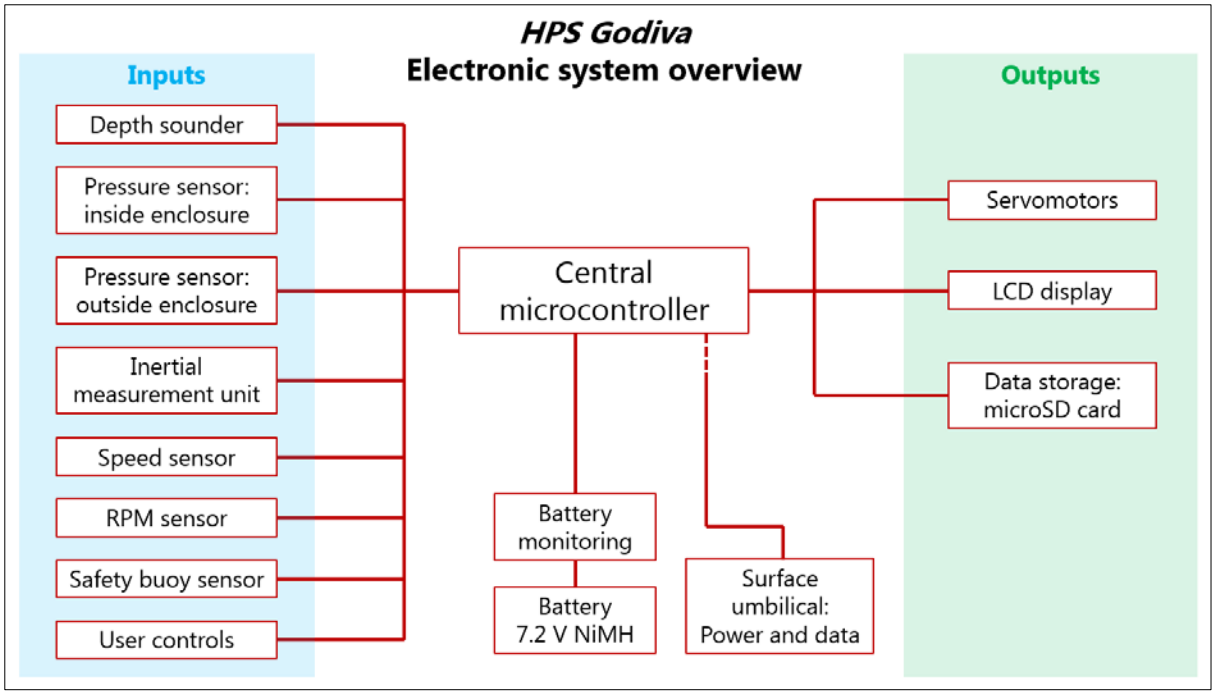

Figure 43 – Electronic system overview

Figure 43 shows a system diagram, indicating the major features of the electronics package. All of the major elements and the general architecture of the system are visible: a variety of sensors feed data to the microcontroller, which both stores the data on a microSD card for later retrieval and displays relevant information in real time on the pilot's 'dashboard'. The electronic 'fly-by-wire' control system monitors the pilot controls and updates the position of the servomotors (and thus, the control surfaces) accordingly. There is also provision for an umbilical cord which can be connected when the submarine is surfaced to charge the battery and download the stored data without having to remove the submarine from the water or open the electronics enclosure.

2.6.3.3 SOFTWARE

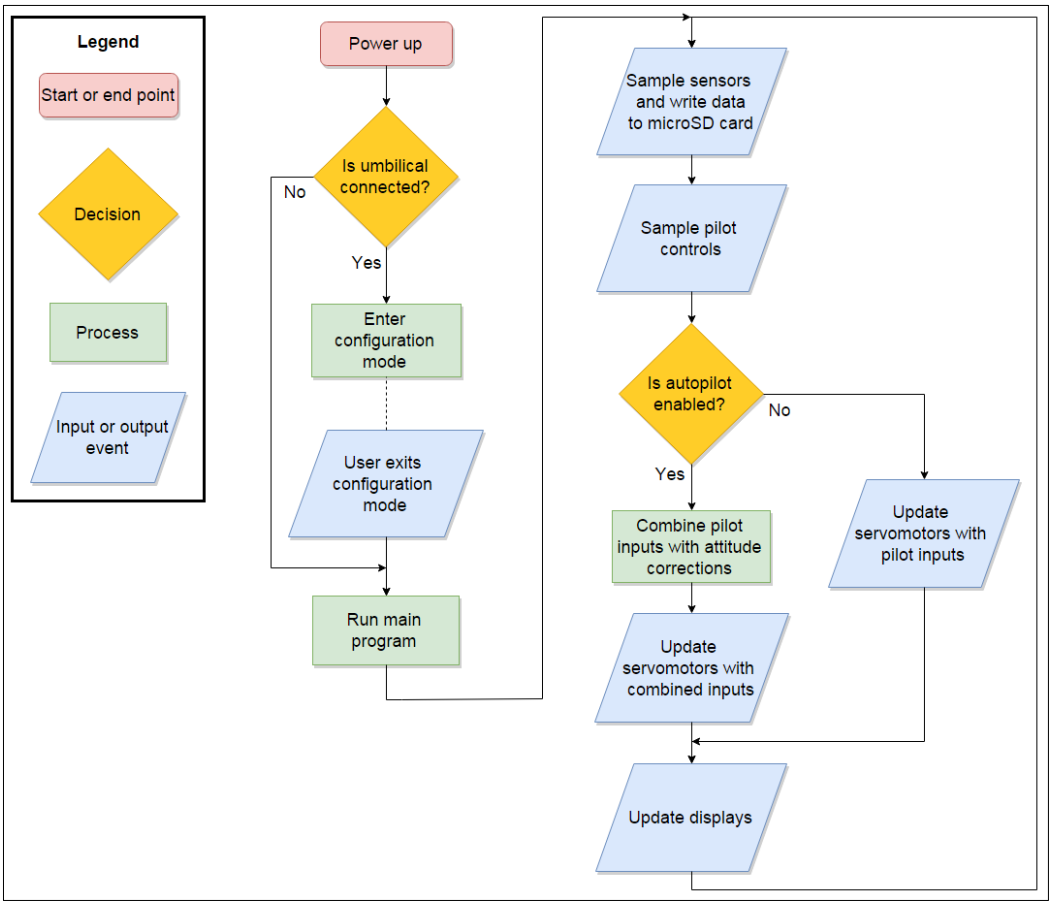

Figure 44 – Flowchart showing the basic operation of the microcontroller software

The code which runs on the microcontroller carries out the various operations required by the submarine is summarised in Figure 44.

In the initial start-up phase, the controller checks if the umbilical cable is connected and if it is, initiates a setup mode allowing the user to reconfigure how the controller operates, including uploading new versions of the software. When the user exits this mode, or if the umbilical cable was not connected on start-up, the software proceeds into its main loop where it provides the various functions of sampling sensors and recording their outputs, displaying those outputs to the pilot where necessary and operating the control surfaces.

2.6.3.4 PILOT INTERFACE

A ‘dashboard’ will be provided for the pilot, which will read out relevant information in real time such as his pedalling RPM, submarine speed, and distance to the bottom of the testing tank (so as not to ground the submarine). The dashboard will also contain controls for turning the whole system on and off, starting and stopping the data logging and enabling the automatic stabilisation feature.

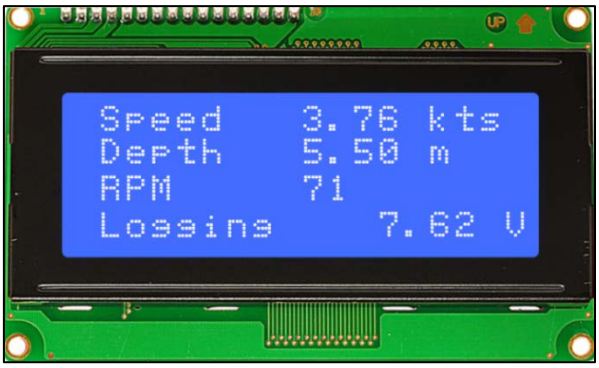

Figure 45 – Mock-up of pilot display

2.6.4 DESIGN EVOLUTION AND VALIDATION CASE STUDY – RPM SENSOR

The detailed design of all sub-circuits and functions is beyond the scope of this report. As a result the design and manufacture of an RPM sensor unit is presented as a technical case study. The drivetrain RPM is an important metric to the pilot because it directly influences the efficiency of the propeller as described in Section 2.3 Propulsion.

2.6.4.1 CIRCUIT DESIGN

The RPM sensor is based on a Hall-effect sensor – a device which responds to the presence of a magnetic field. For a detailed explanation of the Hall Effect and related sensor technology, see Honeywell [32].

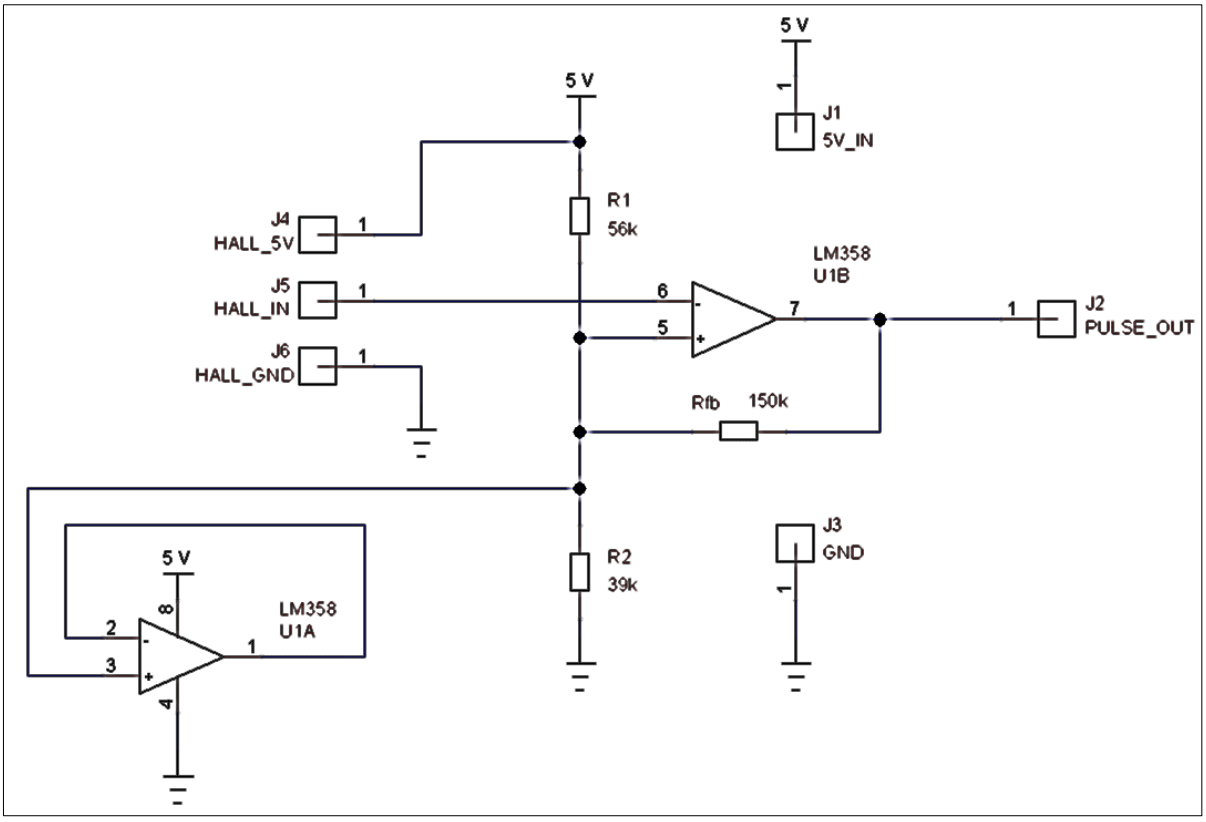

Figure 46 – RPM sensor circuit diagram

Magnets are attached in a regular circular array to a shaft on the drivetrain, with the Hall-effect sensor positioned such that the rotation of shaft causes the magnets to pass by the sensor. This method was chosen because it is non-contact and the sensor chip is solid-state and can be easily sealed to function underwater.

The circuit inside the RPM sensor takes the analogue output from the Hall-effect device [33] and converts it into a series of digital 'on/off' pulses triggered when a magnet passes in front of the sensor. The number of pulses in a fixed period is counted by the microcontroller; this number is directly proportional to the angular velocity of the shaft. Figure 46 shows the circuit used to implement to sensor drawn in TinyCAD. The connections to the Hall-effect device (J4 to J6) can be seen, as well as the Schmitt trigger circuit which converts the analogue output from the Hall-effect device into a digital pulse train. This circuit has a small amount of hysteresis which ensures that each magnet only triggers one pulse, meaning the noisy output of the Hall-effect sensor does not cause spurious pulses which would result in the microcontroller calculating incorrect RPM readings.

2.6.4.2 MANUFACTURE

The prototyped circuit is shown in Figure 47 on a 'breadboard' (electronic prototyping board used to quickly assemble circuits without soldering) in order to emulate operating conditions. A short program to test the circuit was written and uploaded to the microcontroller (the C++ code can be seen in the appendix, Section 7.6.2). It was found that, with the component values shown, passing a magnet across the sensor reliably triggered an output pulse providing the magnet proximity was less than 10 mm.

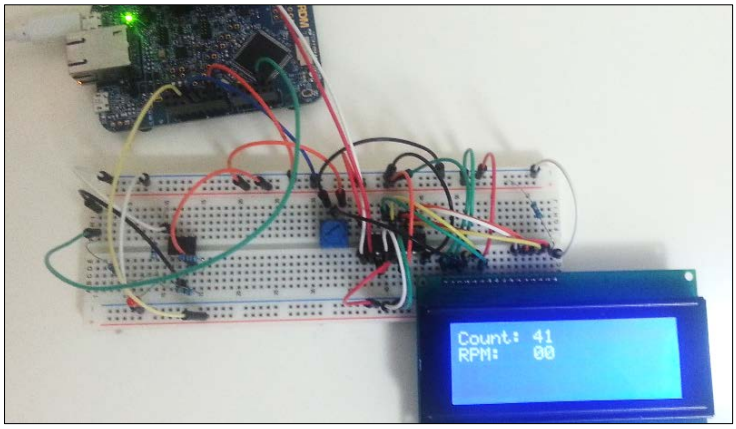

Figure 47 – RPM sensor circuit, assembled on a breadboard

VeeCAD was used to design the physical layout of the circuit board to determine a compact layout and quickly identify circuit errors (Figure 48). This design was then used to quickly assemble the circuit board, which is shown in Figure 49.

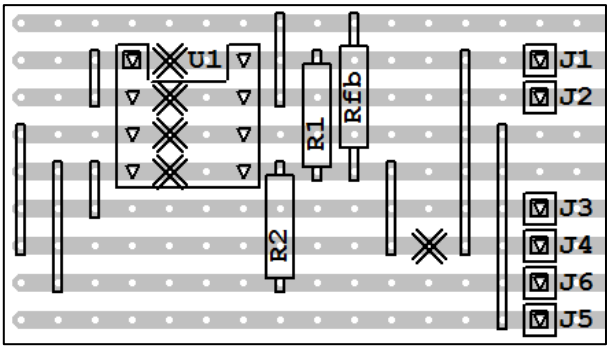

Figure 48 – Physical layout of RPM sensor circuit in VeeCad

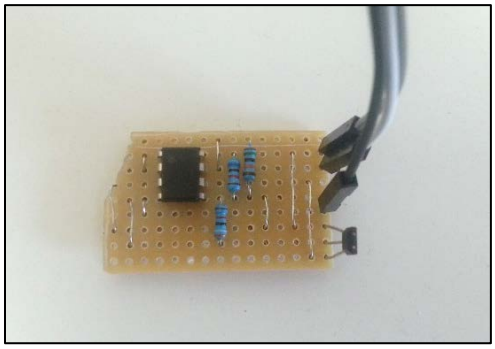

Figure 49 – Finished RPM sensor circuit board

The circuit board was tested by connecting it to the microcontroller and test circuit used during prototyping, and it was found to perform identically to the prototyped circuit. The final step was to design a housing to allow the sensor circuit to be mounted in the submarine. This is shown in Figure 50; visible is the cutout for the circuit board, including the small slot ('A' in Figure 50) where the Hall-effect sensor is situated. Once the board is in place, it will be 'potted' in resin to produce a reliable, waterproof solid-state sensor unit which can be attached to the gearbox using the mounting holes.

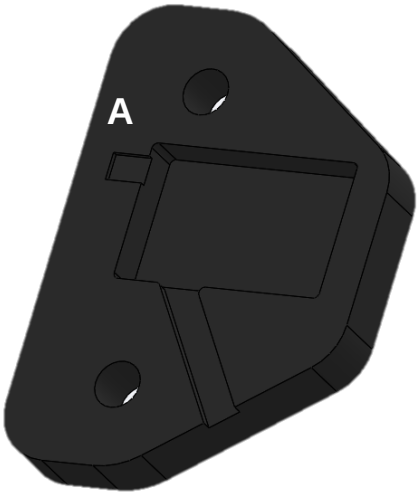

Figure 50 – RPM sensor housing

Figure 51 – RPM sensor rotor, containing 12 neodymium magnets

The rotating part of the sensor which contains the magnets is shown in Figure 51. It mounts onto the unused shaft of the submarine's gearbox, and contains 12 neodymium magnets evenly spaced in a ring. The rotor passes the magnets around 3 mm from the Hall-effect

sensor, ensuring reliable triggering. Several magnets in a regular array are used because, for the more pulses generated at a given rotational speed, the higher the resolution of the RPM sensor. This is particularly important at the relatively low RPMs of the drivetrain. The sensor is attached before the final stage of gearing, meaning the sensor rotates at half the speed of the propeller. At the design speed of 250 rpm at the propeller, the sensor rotor will be turning at 125 rpm. Equation 2.6.1 shows how the number of pulses per second is calculated.

$$\frac{125\ rpm}{60\ sec} \cdot 12\ pulses = 25\ pulses\ sec^{-1} \qquad [2.6.1]$$

With 25 pulses per second being equal to 250 rpm at the propeller, the resolution for a 1-second sampling interval is

$$\frac{250\ rpm}{25\ pulses} = 10\ rpm\ pulse^{-1} \qquad [2.6.2]$$

As seen in Figure 40, the overall transmission ratio is 1:3.57. Therefore, the resolution for the pilot's pedalling RPM is

$$\frac{10\ rpm\ pulse^{-1}}{3.57} = 2.80\ rpm\ pulse^{-1} \qquad [2.6.3]$$

This represents 4 % of the optimum RPM, so with 4 % either side of 70 RPM the pilot has the information required to stay within 10 % of the ideal RPM for the drivetrain.

Both the sensor housing and magnet rotor were designed to be 3D printed for fast turnaround and minimal cost.

2.7 SAFETY

2.7.1 INTRODUCTION

The rules of the ISR competition stipulate the inclusion of deployable safety buoy, attached to the submarine using a high visibility line, to be activated using a 'dead man's switch' configuration. In case of emergency, the pilot will release this safety buoy from the submarine to attract the attention of the rescue divers.

A dead man's switch, in the form of a bicycle brake handle, is attached to each steering handlebar, described in Section 2.5 Steering, with a release mechanism activated using an AND logic system; both handles must be released simultaneously for the buoy to deploy. The

pilot can consequently release their grip on one of the brakes to perform another task without accidentally deploying the buoy and forfeiting a run.

A strobe light for visibility is required for the competition, so a Navisafe Navi light 360° Rescue 2NM strobe was included in the buoy design.

2.7.1.1 SUMMARY OF MAIN DESIGN AIMS

- Design a safety buoy that is easily removable from the main chassis with minimum intrusiveness
- Ensure all safety features are fail-open by design.

2.7.2 SAFETY BUOY DESIGN

The safety buoy must have a quick ascent rate so that the rescue divers can be quickly alerted to an emergency. Equation 2.7.1 below used to calculate the net buoyant force (F_b).

$$F_b = v_b . g \cdot (\rho_{water} - \rho_{buoy}) \qquad [2.7.1]$$

Where v_b is the volume of the buoy (m^3), g is the acceleration due to gravity (ms^{-2}), and ρ is the density (kgm^{-3}). The buoy is made of closed cell polyethylene, density $30 kgm^{-3}$ compared to the liquid density of $999.97 kgm^{-3}$, and has a foam volume of $5.94\ x\ 10^{-4} m^3$ with an additional 3D printed hollow cover. This led to a net buoyant force of 8.85 N; an increase from last year's polyethylene buoy design by 3.7 N. This calculation does not take into the positive buoyant force of the strobe as it is negligible, however it only further increases the margin of safety.

As tight pilot packaging has been a key design goal, the buoy was located at the back of the submarine above the gearbox to prevent interference issues with the pedals. Two mechanical constraints, shown as B in Figure 52, limit the travel in the system. Points D and G (Figure 53) attach the release mechanism to the chassis. When armed, the cables are pulled towards the front of the submarine by a distance of 25 mm. As such, the housing for the stronger spring is designed to be long enough to facilitate the full stroke length of the cables without part interference. Table 18 describes the operation of the mechanism.

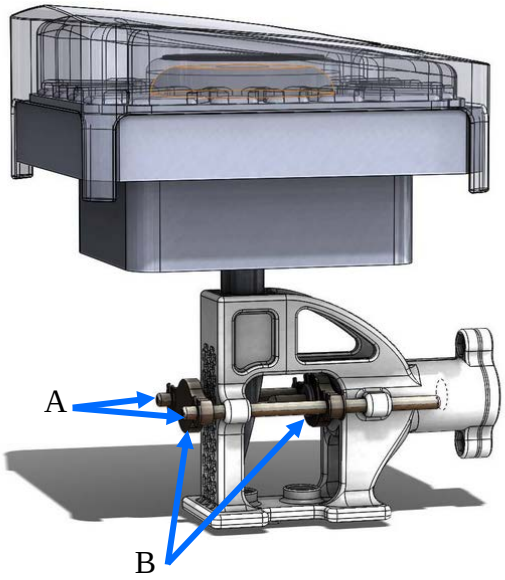

Figure 52 – Buoy release assembly: locked position

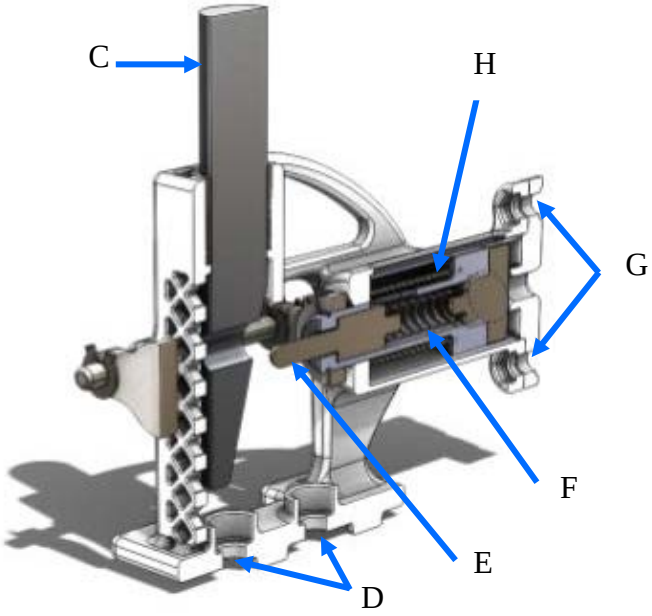

Figure 53 – Safety buoy release mechanism detailed review

Table 18 – Safety buoy arm-release procedure

Action	*Response*
Brake levers depressed	Cables pull on the parallel steel shafts fixed into release mechanism, A. This pulls the pin, E, forwards into the rod, locking the buoy in position. A low stiffness inner spring, F, allows the pin to retract as it meets the slanted surface of the rod, C. The pin retracts until it meets the hole drilled through the rod and locks in place.
Brake levers released	Releasing both brake levers simultaneously releases the tension in the brake cables. The larger, stiffer spring, H, in the outer casing pulls the pin housing back out of the rod. The net buoyant force of the buoy facilitates the release of the rod from the submarine. The 3D printed cover has built-in guide rods to ensure successful deployment of the buoy every time.

The following is an FMEA on a safety critical part that has been designed to fail open. The analysis has been completed to examine the relative consequences of mechanisms not operating as designed. For more details on the FMEA methodology and an explanation of the concept see [34].

2.7.3 SAFETY BUOY FMEA

The following is an FMEA on a safety critical part that has been designed to fail open. The analysis has been completed to examine the relative consequences of mechanisms not operating as designed. For more details on the FMEA methodology and an explanation of the concept see [35].

Table 19 – Safety buoy FMEA

Part	*Part Function*	*Failure type*	*Potential Effect(s) of Failure*	*Severity*	*Potential Cause(s)/ Mechanism (s) of Failure*	*Probability*	*Current Design Controls*	*Detection*	*RPN*	*Response to failure*
Pin	Release Buoy	Dislodged Pin	Buoy release failure	10	Vibrations/knocking	1	Design to fail open	6	60	Rescue Divers
Springs	Forcefully eject buoy from sub-assembly	Buckling	Buoy release failure	10	Vibrations/knocking/ misalignment	1	Design to fail open	6	60	Rescue Divers
Brake Cables	Transmit pilot input	Snapping	Unintentional Release	3	Large applied force	1	Design to fail open	1	3	Rescue Divers
Brake Cables	Transmit pilot input	Stretching	Unintentional Release	3	Repeated use	10	Design to fail open	3	90	Rescue Divers
Brake Cable Sheathing	Guide brake cables	Sticking	Buoy release failure	10	Dirt/repeated use	6	Design to fail open	1	60	Rescue Divers

Hi-Vis Line	Buoy tether to submarine	Tangling	Incomplete Release	5	Incorrect stowage	7	Simple, tested mechanism	6	210	Rescue Divers
Light	Locating device	Magnetic effects	Buoy release failure	10	Steel bolts	1	Avoid proximity to ferromagnetic materials	10	100	Rescue Divers
Light	Locating device	Battery Failure	Reduce visibility	3	Overuse	6	Regularly change batteries	1	18	Rescue Divers
Brake Levers	Prime sub-assembly	Insufficient throw	Unintentional Release	3	Poor Calibration	1	Design to fail open	1	3	Rescue Divers
Line Spool	Contain hi-vis line	Sticking	Buoy release failure	10	Incorrect stowage	7	Simple, tested mechanism	6	420	Rescue Divers
Buoy	Emergency signal	String Snapping	Unintentional Release	3	Poor fixing	1	Design to fail open	1	3	Rescue Divers
Fixing Bolts	Connection to chassis	Loosened bolt	Buoy release failure	10	Poor maintenance	1	Design to fail open	6	60	Rescue Divers
Release Mechanism	Deployment Frame	Broken Back Plate	Buoy release failure	10	Loading direction not-designed	1	Escape hatch break points	6	60	Rescue Divers

The output from the FMEA concludes the safety buoy tether line represents the most potential for failure, and testing will be undertaken to ensure the reliable release of the buoy and line assembly. See the appendix, Section 7.7.1 for a second FMEA on the escape hatch release mechanism.

2.7.4 BUOYANCY

Table 20 – Buoyancy calculations

Part	*Part volume [m^3]*	*Part mass [kg]*	*Equivalent water mass [kg]*	*Net buoyant mass [kg]*
Tail	6.80E-03	8.50	6.80	-1.70
Keel	6.90E-03	8.63	6.90	-1.73
Escape hatch	7.20E-03	9.00	7.20	-1.80
Nose cone	5.70E-04	0.68	0.57	-0.11
Chassis	2.00E-04	1.57	0.20	-1.37
Props	2.12E-04	1.67	0.21	-1.45
Power train	1.40E-03	2.00	1.40	-0.60
Diving equipment	1.00E-02	13.50	10.0	-3.60
Total [kg]				-12.36

Neutral buoyancy describes the operational condition when a body has no net contribution to buoyant lift and is achieved when the mass of a submerged body is equivalent to mass of water displaced.

Neutral buoyancy is critical from the dual perspectives of safety and stability. Uncontrolled rapid ascent from depth is dangerous for the pilot (due to decompression). Furthermore, maintaining depth throughout the race without significant steering effort will allow simple control and minimise the drag contribution of the fins which, in order to compensate for net lift or weight force, will need to permanently operate at non-zero angle of attack.

Table 20 gives an order of magnitude indication as to the net buoyant mass of the submarine, assuming a neutrally buoyant pilot. The output of Table 20 shows a net buoyant mass contribution of the submarine of -12 kg, indicating 12 kg of additional buoyancy is required to achieve the neutral condition. For a representative low density foam such as that used for the Safety Buoy in Section 2.7, this corresponds to a volume of 0.013m^{-3} of foam to achieve neutral buoyancy.

To maximise stability and achieve balanced trim the location of buoyancy should be above the centre of gravity. The exact location of buoyancy will be determined for the craft on an empirical basis.

3.0 MATERIALS AND MANUFACTURE

3.1 DESIGN & MANUFACTURABILITY METHODOLODY

HPS Shakespeare required approximately 306 hours of technician time and 1040 hours of student time to manufacture, with the most time consuming processes being attributable to welding, machining and post-processing operations on what was seemingly a straightforward-to-manufacture design. In order to improve on last year's design, but reduce design and manufacture time by approximately 20% due to shipment constraints, several methods such as advanced CAD, Product Data Management (PDM) and novel manufacturing techniques were employed to cut risk and reduce lead times at every available opportunity. A design ethos was developed early in the project before most of the design work was begun in order to improve the likelihood of project success. The main facets of this ethos are discussed in this section.

3.1.1 PRODUCT DESIGN LIFECYCLE COSTS

It is known that the cost of making changes to a product increases almost exponentially as it progresses through the design stages to completion. Though 'cost incurred/committed' is usually associated in pure financial terms, the graph below also holds true if considering time as the 'cost' (see Figure 54).

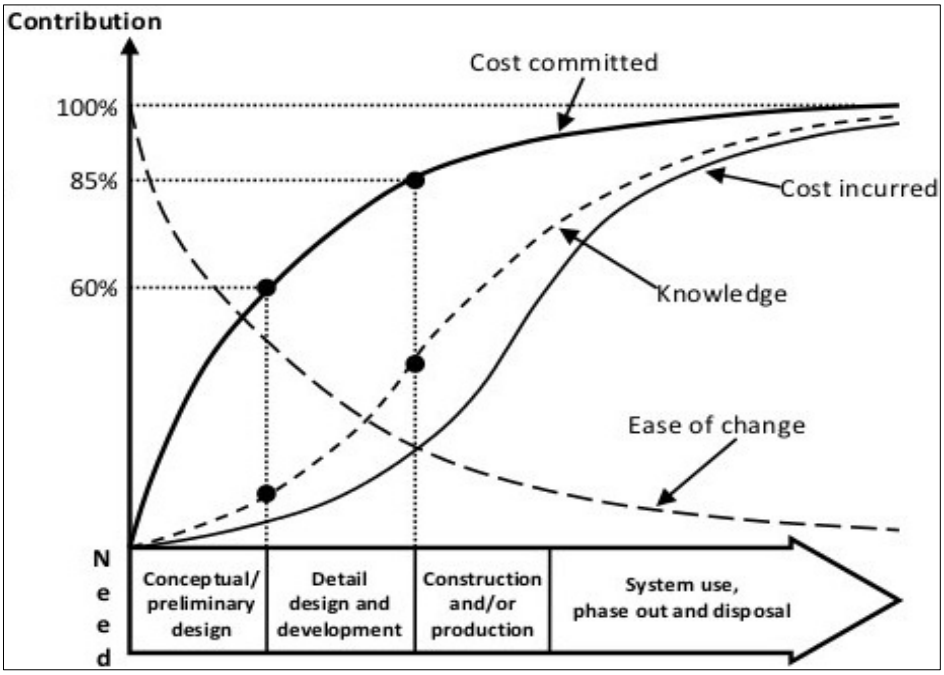

Figure 54 – Cost of changes with time in the product development lifecycle [36]

With this in mind, significantly more time was spent on early stage conceptual design, CAD design, and design verification than would otherwise have been allotted, with considerable care taken to avoid rushing any components into manufacture prematurely.

3.1.2 PRODUCT DATA MANAGEMENT

GrabCAD Workbench, a cloud based Product Data Management (PDM) solution, was implemented to allow seamless sharing of CAD data and efficient collaboration; automated version control and update propagation, eliminating opportunity for data loss or work being based on old parts; and an electronic workflow to formalize, manage, and optimize development; all of which resulted in considerably increased productivity.

The submarine comprises 593 parts, 160 unique parts, and 44 sub-assemblies; more than double *HPS Shakespeare*. Without PDM, a model of this complexity built by eight contributors would have been impossible to achieve in the time available.

3.1.3 PARAMETRIC MODELLING

Parametric modelling CAD techniques, where the geometry of the part is driven primarily by equations and relations rather than explicit dimensions, allows for dimensions to be changed considerably and features to be added or removed without breaking the model.

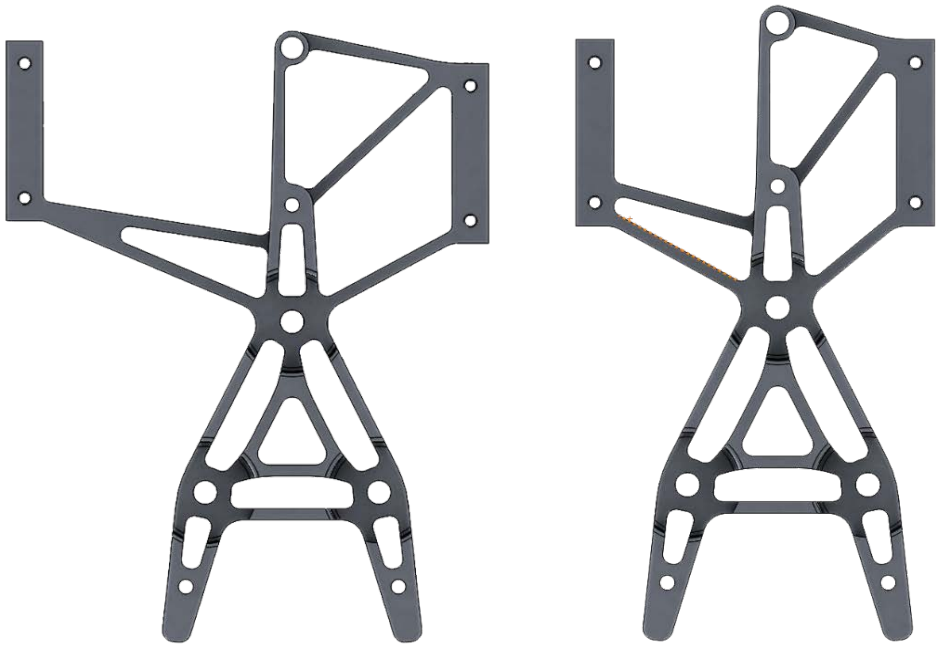

Figure 55 – Parametric design of the gearbox mount allows its geometry to adapt without any geometry maintenance when the locations of mounting points are changed

The use of parametric techniques was essential given the constant changes to requirements, new information and changing ideas as the project progressed. Every component and module was designed to accommodate the greatest possible levels of flexibility to external changes, and to allow basic modifications without requiring any time consuming reconstruction of broken geometry.

3.1.4 CAD VALIDATION

Design verification measures were taken at every stage of the project to ensure the submarine would assemble and function without issue once manufactured. Every part containing dimensions based on other components was modelled using multi-body techniques, including derived parts, equation driven and linked dimensioning. These practices eliminated dozens of errors that could have derailed the project if undetected. A fully articulating and physically representative mannequin was used from the earliest design stages to verify component spacing and ergonomics (see Figure 56).

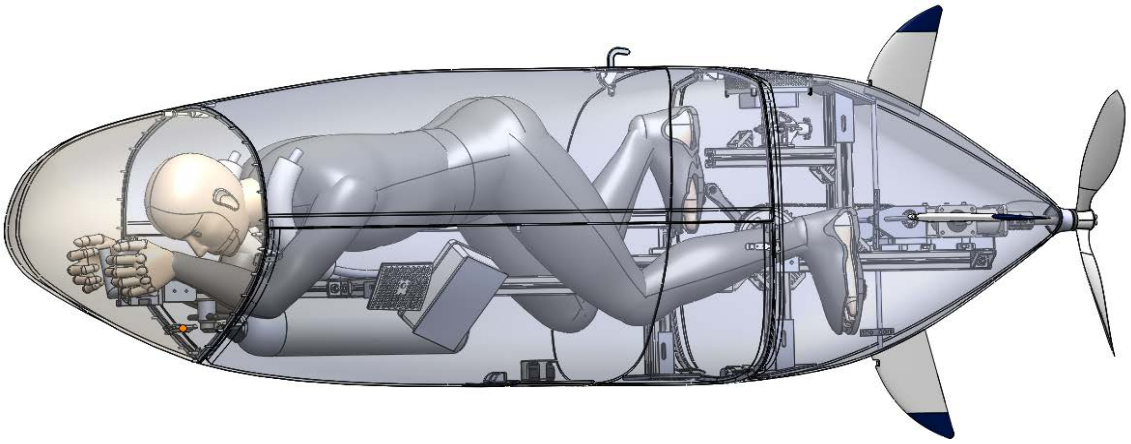

Figure 56 – Fully articulating and physically accurate CAD mannequin used to verify component spacing and ergonomics

3.1.5 MODULARITY

Modular systems were identified as essential from the very beginning, with modules generally being defined by function and envelope (i.e. components from two systems sharing a common dimensional envelope would be grouped together as the same ‘module’). From a design and manufacture standpoint, a lack of design or manufacture progress on any one module would not hold up progress on any other module.

3.1.6 STANDARD JOINING SYSTEMS

Hundreds of man-hours were spent designing and manufacturing the welded aluminium chassis on *HPS Shakespeare*. Components were fixed to this chassis using adhesives and bolts through drilled holes. Besides being intolerably time-consuming, it is also inflexible. Bosch Aluminium Profile was selected for *HPS Godiva*, since it allows freedom to move components along the rails, which also provided some leeway for any inconsistencies between the CAD and reality. Manufacture and assembly of *HPS Godiva*’s chassis took less than five man-hours, and gluing into the hull less than ten.

3.1.7 COTS COMPONENTS

Sub-assemblies were designed to make use of commercial-off-the-shelf (COTS) components wherever possible to cut manufacture and assembly time. CAD for these parts was downloaded from the manufacturer's websites and inserted directly into the assembly for verification purposes. This greatly simplified the design process, allowing components to be analysed for dimensional suitability, and designed into the submarine before even being purchased.

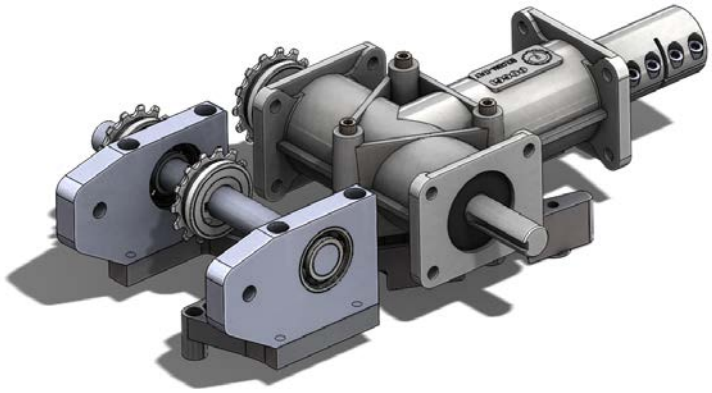

Figure 57 – The bevel gearbox CAD was designed into the assembly and verified before being purchased

3.1.8 DESIGN FOR 3D PRINTING

Components designed specifically to take advantage of the 3D printing process were included throughout the submarine. The lead time for 3D printed components was an average of 48 hours; extremely low compared to an average of two weeks on machined parts. Complexity was deliberately designed into 3D printed components to improve functionality, and simplify the design of any machined components in the same sub-assembly. A prime advantage of 3D printing is that no major penalty is paid for any added intricacy such as undercuts, complex surfaces and internal structures (see Figure 58).

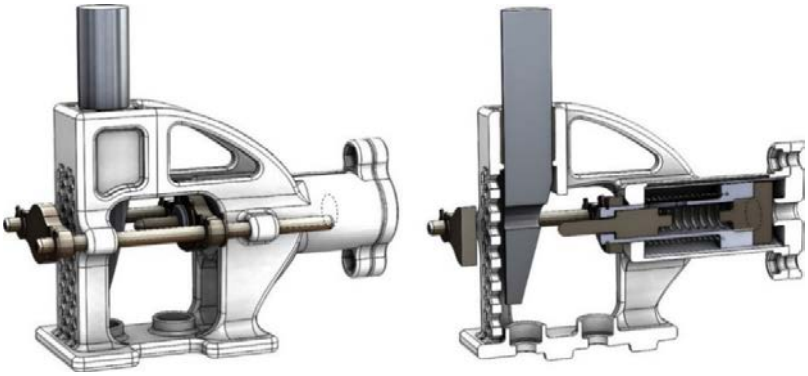

Figure 58 – A complicated 3D printed casing greatly reduced the required number and complexity of machined parts in the safety buoy release system, whilst also improving its functionality and reducing the design time

3.2 HULL MATERIALS

The following section highlights some of the key technical manufacturing highlights of *HPS Godiva* composite hull, summarising both manufacturing methodologies, materials and testing.

3.2.1 INTRODUCTION

As technology advances, evermore frequently the final limitation on performance is attributed to the mechanical, electrical or thermal properties of the material choice. Composites are a group of materials which take considerable steps in the pursuit of an optimally designed material for a given application [37] through the combination of multiple material properties. To be considered a composite, a material must: consist of two or more physically distinct and mechanically separable materials; be manufactured through mixing of the constituents such that optimum properties may be achieved; and that the properties, whether mechanical, thermal or electrical of the result are superior to the parts [38].

This section will iterate the design process through which a composite material is selected, with consideration of the required performance, manufacturing options and cost to justify the choice of composite for *HPS Godiva*.

3.2.1.1 SUMMARY OF MAIN DESIGN AIMS

- Minimise net buoyancy contribution of hull by fibre selection of comparable density to water.
- Ensure the specific properties of the composite selection match or exceed the mechanical properties of the baseline case of glass fibre-reinforced plastic.

3.2.2 TECHNOLOGY SUMMARY

Fibre-reinforced composites are designed such that the resultant material exhibits appropriate mechanical, thermal, electrical, corrosive and aesthetic properties for a given application. By careful consideration of the fibre, polymer matrix and relative volume fraction of each; a material may be tailored to the given application. Fibre-reinforced composites used for applications such as this project are typically made from strong, brittle continuous fibres

encased within a ductile plastic bulk matrix. The relative proportions of fibre to matrix, termed the Volume Fraction, V_f, define the properties of the composite bulk, implying that careful consideration is taken as to the selection of fibre mat weave and relative location and orientation of continuous fibres [39].

3.2.2.1 YOUNG'S MODULUS AND STRENGTH

Consider a load applied to a composite bulk material where all fibres are aligned parallel to the direction of loading. Assuming that the fibres are bonded well to the matrix such that there is no slip, the strain (ε) is common:

$$\varepsilon_c = \varepsilon_m = \varepsilon_f \qquad [3.2.1]$$

Where subscripts c, m and f refer to composite, matrix and fibre respectively. Assuming that the fibre and matrix both behave elastically then the stresses are given by:

$$\sigma_f = E_f \varepsilon_f \text{ [3.2.3]} \qquad \sigma_m = E_m \varepsilon_m \text{ [3.2.3]}$$

The ultimate tensile strength of the composite bulk, σ_{uc} is given by:

$$\sigma_{uc} = \sigma_{uf} V_f + \sigma_{um}(1 - V_f) \quad [3.2.4]$$

For most commercial ductile matrix composites, the stress-strain curve is non-linear due to the decreasing stress contribution of the polymer, however the contribution of matrix tensile strength to the bulk at high stress is typically less than 5% of the fibres, so for most application it is acceptable to assume:

$$\sigma_{uc} \approx \sigma_{uf} V_f \quad [3.2.5] \text{ [39]}$$

3.2.2.2 MATERIAL ANISOTROPY AND THE HYBRID EFFECT

The above analysis is applicable only for loading in the direction of fibres, implying that the mechanical performance of continuous length filaments is dependent on the relative orientation between loading and laminate direction. Anisotropy may therefore be built into the bulk through preferential orientation of fibre laminates aligned with the predicted direction of loading; or perpendicular if designed for preferential failure. Where mechanical isotropy is preferred, fabricating the composite through symmetrical stacking of thin unidirectional fibre in a structured sequence of orientations gives good structural performance. For example, quasi-isotropy can be created through the commonly used arrangement of lamina stacking at 0°/±45°/90°/±45°/0 [39].

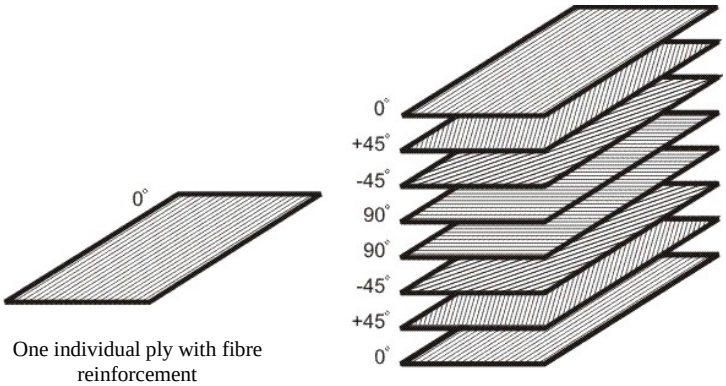

Figure 59 – Symmetrical orientation stacking of fibre laminate [40]

In addition to specifying mechanical performance in predetermined directions, other properties may be optimised for a given application through the synergistic improvement achieved by using a composite made from two or more different fibres [39]. This approach is termed the Hybrid Effect, and allows for the manipulation of various properties between the limits defined by the constituent materials.

3.2.2.3 SUMMARY OF MATRIX PROPERTIES

When cured, epoxy and polyester resins counterpart a myriad of physical and mechanical properties. Thermosetting polymer is applied to a fibre mat as a liquid resin which is converted to a solid through the formation of complex, cross-linked polymer chains where mechanical properties depend on the length and density of the cross links [38].

Entropy Resin Super Sap© CLR/CLF has been selected as an appropriate matrix as the system requires a room temperature cure with relatively short curing times, suitability for simple fabrication methods, proven application in marine environments and good aesthetic and mechanical properties. Additionally this product is derived from 17% bio-base material, acting to compliment the bio-base natural fibre.

3.2.2.4 INTERFACIAL BOND STRENGTH

The difference in elastic properties between a fibre and matrix combination implies that internal stresses must be transmitted via the interface between the constituents. In order to analyse the transfer of stress across the interfacial bond a number of assumption are made, namely:

1. The matrix and fibre both behave elastically under loading.
2. The interface is infinitely thin.

3. No discontinuities exist in material bonding.
4. Matrix close to the fibre has similar properties to the bulk matrix.
5. Fibres are arranged in a perfect array.

Points 2, 3 and 4 are not physically correct and 5 will vary considerably depending on the quality of the fibre. The interfacial bond strength is a dominant factor in the fracture toughness of composite materials and the response to wet environments [38]. A number of direct test methods are established to quantify the interfacial bond strength which are tabulated in the appendix, Section 7.8.1.

3.2.3 FIBRE PROPERTIES & PUGH MATRIX

3.2.3.1 SUMMARY OF FIBRE PROPERTIES

A variety of fibre reinforcement is commercially available in several materials and formats for both structural and non-structural purposes. A summary of mechanical properties for a small range of fibres is presented in Table 21.

Table 21 – Composite fibre material properties [38]; [41]; [42]

Property	***Carbon Fibre***	***E-Glass Fibre***	***Kevlar***	***Flax***
$\boldsymbol{\rho}$	1850	2550	1450	1400
$\boldsymbol{E}$	320	73	125	60-80
$\boldsymbol{\sigma_{UTS}}$	2.5	2.4	2.8-3.6	0.8-1.5
$\boldsymbol{E/\rho}$	170	29	86	26-46
$\boldsymbol{\sigma_{UTS}/\rho}$	$1.4\text{x}10^6$	$0.9\text{x}10^6$	$2.2\text{x}10^6$	$0.9\text{x}10^6$
Elongation at Fracture (%)	0.8%	3%	2..2-2.8%	1.2-1.6%
Price/kg ($)	11	1.3	22-35	1.5
Moisture Absorption (%)	-	-	-	7

WATER ABSORPTION OF NATURAL FIBRES

The drawbacks of natural fibres are due to its poor wettability, high moisture absorption, and incapability with some of the polymeric matrices. Moisture absorption is due to hydrophilic property of natural fibres which adversely affects the mechanical properties such as flexural strength, flexural modulus and fracture toughness [43].

3.2.3.2 FIBRE SELECTION PUGH MATRIX

Table 22 assesses some of these fibres according to a range of criteria to determine the most appropriate for fabrication of *HPS Godiva*'s hull.

Table 22 – Pugh matrix for fibre selection – glass fibre baseline

		Concepts			
Criteria	***Weighting***	***Glass Fibre***	***Carbon Fibre***	***Kevlar***	***Flax***
Cost	8	3	2	1	3
Manufacturability	7	3	1	1	3
Density	6	3	4	5	5
Specific Strength	5	3	4	5	3
Specific Modulus	4	3	5	4	4
Water Absorption	3	3	3	3	4
Risk	2	3	3	3	1
Novel	1	3	3	3	4
Total	-	108	105	104	124
Optimum Choice					

A review of fabrication options is given in the appendix, Section 7.8.2. Note that output from Table 23 concludes that flax is the optimum choice for fibre reinforcement, including the consideration of 'risk', i.e. accounting for the low maturity of natural fibre in marine applications and the negative impacts of water absorption.

To reduce the effects of moisture on mechanical performance, *HPS Godiva* employs the Hybrid Effect through the use of a flax-glass sandwich structure. By sandwiching the flax between glass, the mechanical properties of the composite will be maintained while the resistance to water absorption improved by a physical barrier to the water as shown in Figure 60.

Figure 60 – Illustration of hybrid flax-glass composite

3.2.3.3 3-POINT BEND TESTING OF HYBRID FLAX COMPOSITE AFTER EXTENDED EXPOSURE TO MOISTURE

A 3-point bend test in accordance with BS EN 2746-1998: Glass fibre reinforced plastics – Flexural test – Three Point Bend Method was conducted on an Instron 5980 to assess the impact of moisture absorption on the mechanical performance of the composite material.

Multi-objective optimisation of the composite has been achieved using the hybrid effect, with fibre orientations positioned perpendicular between layers sandwiched between two layers of low-weight fiberglass to best prevent the absorption of moisture. Samples were tested in both the original manufactured state and also after a 15 hour immersion period which represents a worst case scenario of moisture exposure time.

Table 23 – Summary of immersion composite testing

	Flexural Modulus [GPa]	***UTS [MPa]***
Dry Flax	7.29	131.0
Wet Flax	4.68	137.0
Variation (%)	35.8%	4.68%

The results shown in Table 23 show that the immersed samples lose stiffness with immersion time, however variation in ultimate tensile stress of the material remains is within experimental error. As the applied loading to the submarine hull is principally hydrodynamic, by design, this result shows the application of a hybrid flax fibre composite is appropriate. Stress-strain data in Figure 62 exhibits nonlinear deformation typical of composites.

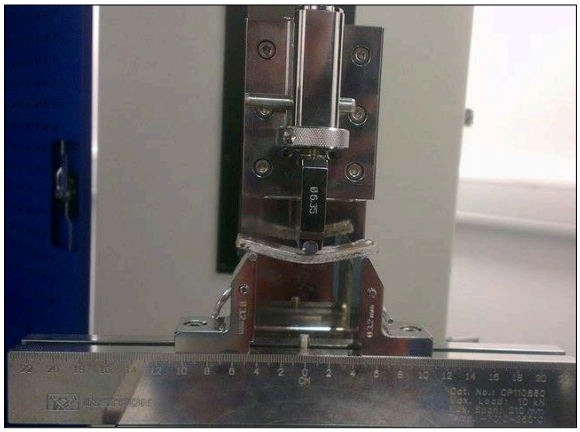

Figure 61 – 3-point composite bend test of hybrid flax fibre composite

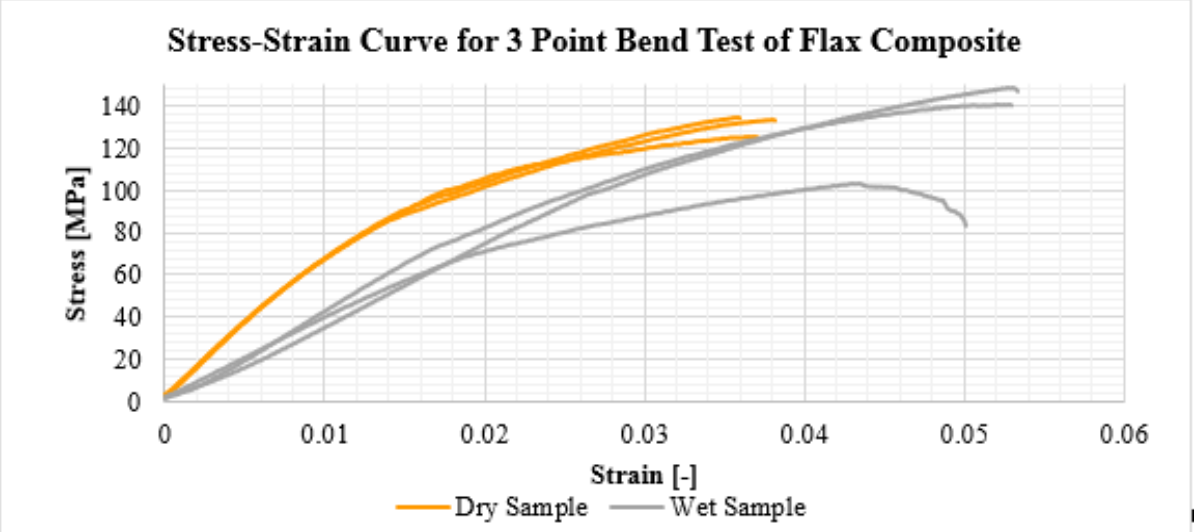

Figure 62 – Stress-strain curve for flax composite samples

4.0 CONCLUSION

This project concludes, through the application of a Systems Approach Framework and the Fozberg and Mooz's Vee model, with the design of a new and fully modular submarine *HPS Godiva* to be raced at the ISR in June 2015.

With reference to the project Aims and Objectives, the principle design goal to improve hydrodynamic efficiency compared to *HPS Shakespeare* has been achieved through aggressive volume reduction and comprehensive CFD modelling. The finalised hull design has brought about a reduction in frontal area of 32% and a simulated 72% decrease in drag coefficient on the previous year, corresponding to a total reduction in drag of approximately 80%.

In addition the use of a hybrid natural fibre composite, novel to marine applications, has permitted manufacture of complex three-dimensional streamlined profiles and led to a significant buoyancy advantage due to its specific strength. Furthermore the *design-for-packaging* objective has been satisfied through a unique *fold-away* hull and chassis, which permits the attachment of all submodules whilst minimising the additional cost constraint of shipping the submarine internationally.

As a result of the aforementioned innovative approaches to the design brief and novel solution to the challenges when competing overseas, the team are optimistic *HPS Godiva* will be a strong contender for the 'Best Use of Composites' and 'Best Design' categories at the competition.

While beyond the scope of this report, the Outreach activities and unprecedented sponsorship success have allowed the team to exhibit and promote the project at nationwide events, satisfying the final project aim to increase the exposure of Warwick Human Powered Submarine.

Through the commitment and consistent engagement of the team throughout the project horizon, *HPS Godiva* brings about a step-change in performance from the perspective of multi-objective optimisation, manufacturing technologies and sponsorship legacy. As a result the team are in a strong position to build upon the successes of the previous year and represent internationally both the academic and vocational excellence of the University of Warwick.

5.0 RECOMMENDATIONS

With modularity being a core design focus for the submarine, the legacy impact of *HPS Godiva* allows future teams to focus their efforts on the improvement of individual modules. In critical review of the design and manufacture of the submarine, the majority of the design effort was expended in the areas that would bring about the greatest level of benefit to the total assembly, namely the hull and chassis. The emphasis in future years should remain focused on areas where the most benefit can be derived; particularly the propulsion, steering and electronics submodules.

5.1 PROPULSION

The propeller design for *HPS Godiva* is detailed in Section 2.3, which discusses not only the propeller geometry but also evaluates the design robustness when considering the human 'engine'. The sensitivity analysis summarises that a fixed bladed propeller does not represent an optimal design over the expected range of uncertainty for the pilot input. A more complicated and costly variable-pitch propeller will allow for a flatter efficiency curve with respect to power output and bring about performance benefits, particularly on race courses where acceleration is a key consideration.

When assessing competitor designs a range of active and passive systems may be designed with various degrees of complexity and expense requiring both mechanical and electronic expertise.

5.2 STEERING

The ISR race course discussed in Section 1.2 is a straight line, hence steering is optimised from a stabilisation, rather than manoeuvrability perspective. Partner courses such as the European ISR historically have a more complicated layout, therefore additional attention to designing an effective steering system will result in overall performance gains.

5.3 ELECTRONICS

HPS Godiva's electronic system, shown in Section 2.6, provides a plethora of valuable functions which can be further enhanced. For example, measuring the overall transmission efficiency will allow the effectiveness of submodule improvement to be readily quantified and will play a crucial role in defining future project directions.

6.0 WORKS CITED

[1] International Submarine Races, “International Submarine Races Contestant's Manual,” Foundation for Underwater Research, Washington DC, 2014.

[2] F. P. Brooks, The Mythical Man-month: Essays on Software Engineering, Reading: Addison Wesley, 1995.

[3] J. M. Nicholas and H. Steyn, Project Management for Engineering, Business and Technology, Abingdon: Routledge, 2012.

[4] International Submarine Races (ISR) & the Foundation for Underwater Research and Education (FURE), “5. Submarine Design Guidelines,” in *International Submarine Races Contestants' Manual Version 1.0*, 17, ISR/FURE, 2014, p. 10.

[5] P. P. Joubert, “Some Aspects of Submarine Design Part 1. Hydrodynamics, Pg16,” DSTO Platforms Sciences Laboratory, Victoria, 2004.

[6] R. Burcher and L. Rydill, Concepts in Submarine Design, New York: Cambridge University Press, 1994.

[7] F. M. White, Fluid Mechanics, 3rd Ed. ed., McGraw-Hill)., 1994.

[8] J. Hervey, Submarines, London: Brasseys, 1994.

[9] Breaking Muscle, “TOP 10 MOBILITY ARTICLES OF 2013,” 2015. [Online]. Available: http://www.elixirpilates.co.nz/wp-content/uploads/2015/01/shutterstock111578147copy.jpg. [Accessed 14 03 2015].

[10] F. R. Goldschmied, “Integrated Hull Design, Boundary-Layer Control, and Propulsion of Submerged Bodies,” *Hydronautics,* vol. 1, no. 1, pp. 2-11, 1967.

[11] McKeion Research Group, “Flow Separation,” 2015. [Online]. Available:

https://www.its.caltech.edu/~bmckeon/group_documents/mckeon%20flow%20separation.html. [Accessed 26 03 2015].

[12] InitialDave.com, “Chassis Basics 1 - Chassis & Bodyshells,” [Online]. Available: http://www.initialdave.com/cars/tech/chassisbasics01.htm. [Accessed 22 03 2015].

[13] Formula 1 Dictionary, “Chassis,” [Online]. Available: http://www.formula1-dictionary.net/chassis.html. [Accessed 22 03 2015].

[14] RS Components, “Bosch Rexroth Aluminium Strut Profile,” [Online]. Available: http://uk.rs-online.com/web/p/tubing-struts/3900032/. [Accessed 25 03 2015].

[15] J. S. Carlton, Marine Propellers and Propulsion, Oxford: Butterworth-Heinemann, 2007.

[16] M. Hepperle, “JavaProp - Users Guide,” JavaProp, 2009. [Online]. Available: http://www.mh-aerotools.de/airfoils/java/JavaProp%20Users%20Guide.pdf. [Accessed March 16 2015].

[17] M. Hepperle, “Design of a Propeller,” MH Aerotools, 8 September 2003. [Online]. Available: http://www.mh-aerotools.de/airfoils/jp_propeller_design.htm. [Accessed 27 April 2015].

[18] Soutter, Cole and et al., “Warwick Submarine: First stage design and development of a human-powered submarine entry for the European International Submarine Races in July 2014,” University of Warwick, School of Engineering, Coventry, 2013.

[19] A. F. Molland, S. R. Turnock and D. A. Hudson, Ship Resistance and Propulsion, Cambridge: Cambridge University Press, 2011.

[20] B. McCormick, Aerodynamics, Aeronatutics, and Flight Mechanics, New York: John Wiley and Sons, 1979.

[21] W. Timmer, “Cycling Biomechanics: A Literature Review,” *Journal of Orthopaedic &*

Sports Physical Therapy, 1991.

[22] Rotor Bike Components, “Rotor Bike Components,” [Online]. Available: http://www.rotorbike.com/products/road/q-rings-130-bcd_20. [Accessed 29 03 2015].

[23] O’Hara, Clark, Hagobian and McGaughey, “Effects of Chainring Type (Circular vs. Rotor Q-Ring) on 1km Time Trial Performance Over Six Weeks in Competitive Cyclists and Triathletes,” *International Journal of Sports Science and Engineering*, vol. 06, pp. 025-040, 2012.

[24] D. Ellerby, The Diving Manual: An Introduction to Scuba Diving, Southen-On-Sea: AquaPress Ltd, 2009.

[25] C. O'Donnell, “Foil Chart for NACA Section Profiles,” Boat links, 13 January 1997. [Online]. Available: http://www.boat-links.com/foilfaq.html. [Accessed 10 January 2015].

[26] S. Hoerner and H. Borst, Fluid Dynamic Lift, 1st ed., New Jersey: Hoerner Fluid Dynamics, 1975.

[27] Glen L., “Inboard Hardware: Rudders,” Glen L., [Online]. Available: https://www.glen-l.com/weblettr/webletters-4/wl38-rudders.html. [Accessed 6 November 2014].

[28] KG, Conrad Electronic Internation GmbH & Co., “Freescale Semiconductor FRDM-K64F from Conrad.com,” 2015. [Online]. Available: http://www.conrad.com/ce/en/product/1271993/Freescale-Semiconductor-FRDM-K64F. [Accessed 20 April 2015].

[29] J. Gardner, “ES434: Microsensors & Smart Devices Lecture 3,” 2014. [Online]. Available: http://www2.warwick.ac.uk/fac/sci/eng/eso/modules/year4/es434/resources/es434_2014_l3_microsensors__smart_devices.pdf. [Accessed 20 April 2015].

[30] G. Lazaridis, “How RC Servos Works,” 19 June 2009. [Online]. Available: http://pcbheaven.com/wikipages/How_RC_Servos_Works/. [Accessed 20 April 2015].

[31] oomlaut, “File:Exploded Servo.jpg,” 2015. [Online]. Available: https://commons.wikimedia.org/wiki/File:Exploded_Servo.jpg. [Accessed 20 April 2015].

[32] Honeywell, “Hall Effect Sensing and Application,” 2015. [Online]. Available: http://sensing.honeywell.com/index.php?ci_id=47847. [Accessed 20 April 2015].

[33] Allegro MicroSystems, Inc., “Continuous-Time Ratiometric Linear Hall Effect Sensor ICs,” 2010. [Online]. Available: http://www.farnell.com/datasheets/715798.pdf. [Accessed 20 April 2015].

[34] N. R. Tague, “Failure Mode Effects Analysis (FMEA),” American Society for Quality, 2004. [Online]. Available: http://asq.org/learn-about-quality/process-analysis-tools/overview/fmea.html. [Accessed 28 April 2015].

[35] ASQ, “Failure Mode Effects Analysis (FMEA),” ASQ, 2015. [Online]. Available: http://asq.org/learn-about-quality/process-analysis-tools/overview/fmea.html. [Accessed 10 April 2015].

[36] N. Raffish, “ES178,” *Management Accounting USA*, pp. 36-39, 1991.

[37] K. K. Chawla, Composite Materials: Science and Engineering, New York: Springer, 2012.

[38] D. Hull, An introduction to composite materials - Cambridge Solid State Science Series, Cambridge: Cambridge University Press, 1993.

[39] F. R. Jones, Handbook of Polymer Fibre Composites, Harlow: Longman Scientific and Technical, 1994.

[40] Home Made Composites, “What are composites?,” 2014. [Online]. Available:

http://www.composites.ugent.be/home_made_composites/what_are_composites.html. [Accessed 22 December 2014].

[41] W. D. Brouwer, “Natural Fibre Composites in Structural Components: Alternative Applications for Sisal?,” 2014. [Online]. Available: http://www.fao.org/docrep/004/Y1873E/y1873e0a.htm. [Accessed 22 December 2014].

[42] Materials Systems Laboratory, “Composite / Steel Cost Comparison: Utility,” 2014. [Online]. Available: http://msl1.mit.edu/MIB/3.57/LectNotes/gm_tech_composites.pdf. [Accessed 22 December 2014].

[43] C. W. Nguong, S. N. B. Lee and D. Sujan, “A Review on Natural FIbre Reinforced Polymer Composites,” *International Journal of Chemical, Nuclear, Metallurgical and Materials Engineering*, vol. 7, no. 1, 2013.

[44] T. A. Shiparo, “The effect of surface roughness on hydrodynamic drag,” US Naval Academy, Maryland, 2004.

[45] S. V. Hoa, Principles of the Manufacturing of Composites Materials, 1st ed., Pennsylvania: DEStech Publications, 2009.

[46] e. -. SuperSap, “Entropy Resins Plant-Based Bioresins,” 2014. [Online]. Available: http://www.elmira.co.uk/content/documents/FD_RESIN_BROCH14_ENTROPY_ELMIRA-2.pdf. [Accessed 28 December 2014].

[47] D. Cripps and GURIT, “Guide to Composites,” 2014. [Online]. Available: http://www.netcomposites.com/guide/spray-lay-up/51. [Accessed 28 December 2014].

[48] Aerospace Web, “NACA 0012 Lift Characteristics,” Aerospace Web, [Online]. Available: http://www.aerospaceweb.org/question/airfoils/q0259c.shtml. [Accessed 29 January 2015].

[49] Rovers North, “Land Rover Parts,” [Online]. Available: http://www.roversnorth.com/Land-Rover-Parts/170. [Accessed 25 03 2015].

[50] Euro Car News, “Volkswagen XL1 Concept Car,” [Online]. Available: http://www.eurocarnews.com/19/0/2651/16995/volkswagen-xl1-bodyshell-frame-cfrp-monocoque/gallery-detail.html. [Accessed 25 03 2015].

[51] Human Power Team Delft & Amsterdam 2010-2014, “Home,” [Online]. Available: http://www.hptdelft.nl/en/. [Accessed 25 03 2015].

[52] G. Obree, “Home,” [Online]. Available: http://obree.com/. [Accessed 25 03 2015].

[53] NASA, “Shape Effects on Drag,” NASA, 12 June 2014. [Online]. Available: http://www.grc.nasa.gov/WWW/k-12/airplane/shaped.html. [Accessed 10 November 2014].

[54] Cranfield University, “The effect of ERP on the product development lifecycle,” 01 12 2011. [Online]. Available: http://www.slideshare.net/mateecgolob/es-the-effect-of-erp-on-product-development-lifecycle.

7.0 APPENDICES

7.1 HULL APPENDIX

7.1.1 COMPETITION REQUIREMENTS OF HULL DESIGN

In order to be a reduce risk and satisfy scrutineers at the ISR, there are a number of design rules that must be adhered to. Each has an impact on the design of the hull which is recorded below:

Table 24 – ISR design constraints

ISR Ruling	*Effect on Design*
5.1. Definition: "a submarine shall be defined as a free flooding (liquid-filled) vehicle that **fully encapsulates the occupant**(s), and operates entirely beneath the surface of the water.**"**	The hull fully encapsulates the pilot, by use of a split hull structure. Entry is by a large hatch, while visibility is provided by a transparent nose-cone. The design allows for the draining while being lifted by use of a removable panel in the keel.
5.2 Propulsion Systems: "SCUBA exhaust air from the crew may be eliminated by any method at the discretion of the team, but may not be used to produce a propulsive force. You are encouraged to give this considerable thought; any exhaust air trapped in the hull will cause major changes in trim and buoyancy.**"**	To prevent the entrapment of exhaust air, holes are incorporated into each section of the hull. A larger slot is placed in the top of the escape hatch to allow air to escape from the top of the submarine and also allows external operation of the escape hatch release mechanism.
5.5.4 Rescue egress: "Any and all exits that are to be used by a submarine crew for emergency egress shall be clearly marked at the location of the handle or release mechanism by a 4" square orange patch bearing the word "Rescue." If this is not possible, the handle or release mechanism must be clearly marked with at least fluorescent tape. The handle or release mechanism shall be easily accessible from both inside and outside the submarine."	To maximise the chance of a safe and fast emergency escape, the escape hatch has been made as large as possible. It is held by a simple sprung pin mechanism which can be opened from both the inside and outside of the submarine. The escape hatch itself is sprung loaded and so will automatically detach once the release has been pulled. To prevent it from sinking, the hatch will be tethered to the hull.
5.5.4 Crew visibility: "Viewports, windows, canopies, etc., shall be located on the submarine so that the crew has as unrestricted a view as possible, especially forward in the case of the navigator. The crew's face and head areas shall also be visible to the support and safety divers at all times.**"**	The entire nose-cone of the submarine is formed of a single Vacuum formed piece of Poly-carbonate, giving the required shape, whilst allowing the pilot maximised visibility.

5.6.1. Submarine Width Limitations: "The only method of entry of submarines into the water is via the basin's elevator. The maximum width permitted of a submarine is 84 inches (2.13 meters) to allow it to be launched via the basin's elevator. It is acceptable to remove parts of the submarine or have folding components to meet this width limitation**"**	As part of the modularisation ethos and need for aggressive packaging to facilitate international shipping means that the overall width of the submarine (950mm) is well within the maximum.
5.6.6. Drag Reduction Materials and Submarine Fluids: "Beyond the use of waxes on the submarines hulls and fins, the use of drag-reduction material is prohibited. The submarine shall not release any type of fluid into the basin's waters.**"**	As the use of drag reduction materials is prohibited, the quality of hull finish is paramount and so the use of high quality tooling is required.

7.1.2 *HPS SHAKESPEARE* & COMPETITOR ANALYSIS OF HULL

A critical appraisal of *HPS Shakespeare's* hull from a hydrodynamics perspective highlights a number of noteworthy points, shown in Figure 63.

From the appraisal of *HPS Shakespeare* and ISR competitors, a more detailed specification is outlined:

- Minimised Internal Volume fully encapsulating shell.
- Hydrodynamic packaging to be achieved by volumes studies with the pilot in a prone cycling position.
- Use of bespoke female tooling to achieve an A-class exterior surface.
- Integration of nose-cone into the hull shape for improved point visibility.
- Design of a symmetric hull along at least one plane of symmetry.
- Optimisation of the hull shape through computational methods, with experimental validation.
- Allowance for fast access to both the pilot and powertrain through the use of hatches.
- Use of established aerofoil profiles to drive hull design.
- Using a split hull design to facilitate a knocked-down transport state.
- Where appropriate employ Bio-mimicry to develop naturally optimised designs.
- To ensure the safety of pilot, focusing on ingress/egress, visibility and dynamic stability.

- Absolute compliance with design rules for both the ISR and eISR to ensure legacy value of the design.
- Resilience to cope with the demands of use, testing, transportation and competition.
- Stability of motion through the minimisation of Coefficient of Drag, Coefficient of lift, yaw moments and rolling moments.
- Allow manufacture to be completed in a timely manner given the correct tooling.

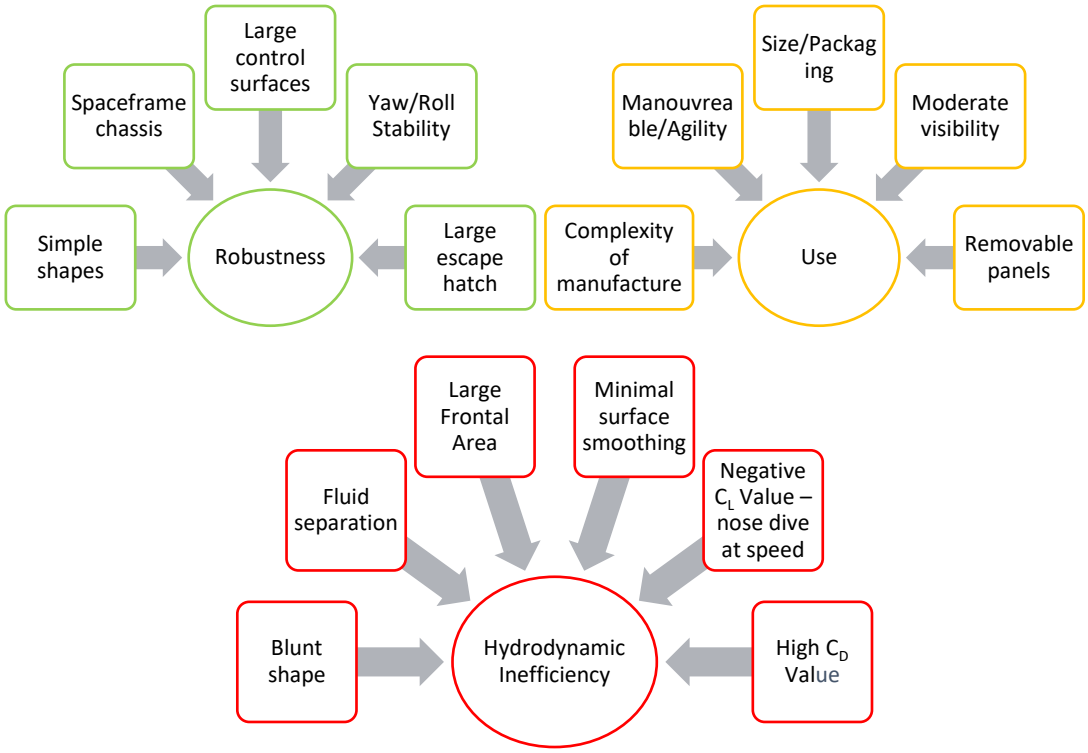

Figure 63 – *HPS Shakespeare* high level appraisal

A high level appraisal of submarines competing in the 12th ISR (2013) to ascertain the current state-of-the-art has also been conducted, in order to drive design. Table 25 shows the main hull design and manufacturing themes along with their popularity.

Table 25 – High level competitor analysis

Submarine Technology	*Arcangello IV*	*Archimede*	*FAU Boat 2*	*IL Calamaro*	*Jesse III*	*Laurie Bell*	*Legasea*	*Leviathan*	*Menrva*	*Omer 8*	*Phantom 6*	*SS Rowdy*	*Sublime*	*Subzero*	*Sultanah II*	*Talon 1*	*Umptysquatc*	*WASUB 3*	Total
Minimised Volume	1	1	1	1	1		1	1	1	1		1	1	1	1			1	14
Prone Pilot	1	1	1	1	1			1	1	1	1	1	1	1				1	13
Male Plug	1	1	1	1	1			1	1		1	1	1	1				1	12
Pilot Volumes	1			1						1		1	1	1	1	1	1	1	10
Female Tooling	1		1	1	1		1		1		1		1	1				1	10
Deep Draw Nose-cone		1	1							1		1	1	1	1	1		1	9
Multiple Hatches			1					1	1	1			1	1		1	1		8
Symmetric Hull	1				1			1	1	1			1	1					7
CFD Optimisation		1								1					1	1	1		5
Flat Windows			1	1				1						1		1			5
NACA 6 series										1			1	1	1			1	5
Split Hull							1					1				1			3
Bio-mimetic	1																		1
Scale Model Testing	1																		1
Metal Band Reinforcement			1																1
Wood Frame Fabric Skin				1															1
NACA 16									1										1

7.1.3 CONCEPT HULL SHAPES

Each of the concepts were modelled to a standard design envelope (2500 mm x 550 mm x 750 mm - L x W x H) and without escape hatch details. Propellers and control surfaces were also omitted unless explicitly part of the design.

Table 26 – General hull shape concepts

Concept	*Details*
1 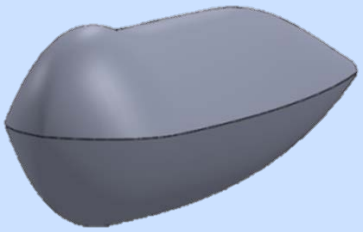	Split mould design with port/starboard symmetry Traditional submarine shape Larger depth than width to accommodate pedalling motion Full visibility nosecone Tapered tail
2 	Developing the idea of underwater cycling further, the concept was shaped to place the pilot in a time trial position. Bow mounted hydroplanes and rudder Rear stability strake to oppose roll. Body conforming packaging
3 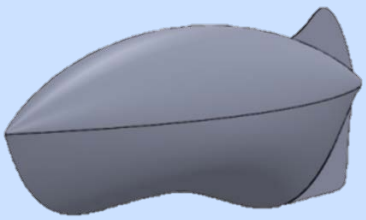	Sharp bow with following aerofoil shape in plan view Split mould design with port/starboard symmetry Rear stability strakes to oppose roll with integrated rudders. Body conforming packaging Tapered tail
4 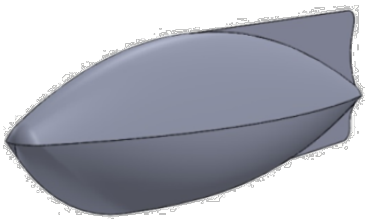	Sharp bow with following aerofoil shape in plan view Split mould design with port/starboard symmetry Rear stability strakes to oppose roll with integrated rudders. Body conforming packaging Tapered tail

7.1.4 PUGH MATRIX WEIGHTING JUSTIFICATIONS

Table 27 – Justification of selection criteria

Selection Criteria	*Weighting*	*Justification*
Robustness	13	As safety is intrinsically linked to the design functioning as it should, robustness of design is key
Minimised CD x A	12	To allow comparison of hydrodynamic efficiency between concepts the product of frontal area and drag coefficient is considered. Defined by comparative CFD investigations
Neutral CL	11	Neutral buoyancy is attainable whilst stationary, however dynamic neutral buoyancy can only be achieved with a neutral coefficient of lift. Otherwise hydroplanes must be used to correct depth, resulting in increased drag. Defined by comparative CFD investigations
Simplicity	10	Safety and ease of manufacture are also linked to the simplicity of design and so a simple design is preferred
Minimised CD	9	Minimised drag coefficient is required for hydrodynamic efficiency. Defined by comparative CFD investigations
Minimised internal volume	8	Minimised internal volume leads to reduced submarine inertia to be overcome. Defined by comparative CFD investigations
Innovative shape/design	7	To reflect the innovative design philosophy of Warwick Sub, the hull design must show a degree of innovation.
Conformance with best design practice	6	In order to ensure that the hull will be competitive, conformance with best design practice is necessary
Cost	5	As the project has no approved budget, cost implications of a design must be considered
Minimised frontal area	4	Minimised frontal area leads to reduced form drag to be overcome. Defined by comparative CFD investigations
Engineering judgement	3	As with all decisions, a certain amount of the decision is based on previous experience. However in a new application of previous experience, it should not be an overriding factor, hence the relatively low weighting
Ease of manufacture	2	Though manufacture should be considered at the concept stage, manufacturability issues can be overcome in the detail design stage such that at this point ease of manufacture has a low weighting
Ease of assembly	1	Assembly should also be considered at the concept stage, however assembly issues can be overcome in the detailed design stage such that at this point ease of

assembly has a low weighting

7.1.5 DETAILED DEFINITION OF THE HULL SHAPE

The side elevation of the design was based on the Griffith aerofoil for flow retention. To optimise for the pilot package an asymmetric shape was developed for both volume and wetted surface area minimisation. Symmetry of the tail was included to minimize lift on the hull; however it was acknowledged that the asymmetric nose may also be a cause of lift. In the plan elevation, an elliptic leading edge and tapering parabolic rear section was used in conjunction with a bulbous bow to enable space for the pilot's shoulder width. The form featured a continuously changing diameter in order to promote flow retention, and a symmetrical profile was used to minimize yaw from flow turning at the trailing edge.

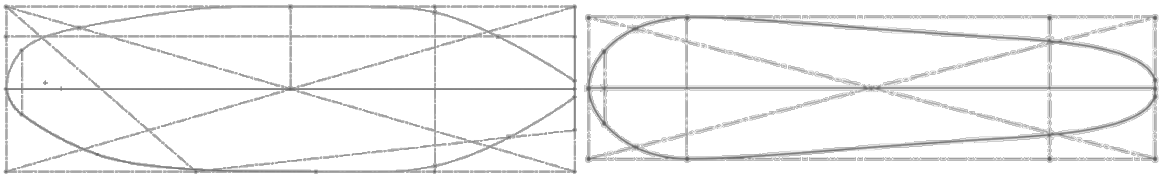

Figure 64 – (left) Side elevation of the hull (right) plan elevation of the hull

The profiles in the front elevation gave the hull its shape as they were used to drive the 3D shape formation. The nose profile (Figure 65 (left)) defines the shape at the submarines widest point, and is responsible for the formation of the forward keel strake. As the nose is asymmetric, this keel serves to deflect flow from the underside of the submarine with the aim of reducing lift forces on the hull while also providing resistance to roll. This is in favour of an additional fin appendage which could add an additional 30% drag and would be susceptible to damage. The second profile (Figure 65 (centre)) sits at the central point of the submarine, and provides a transformation profile from the keeled section of the hull to powertrain housing area. The final profile (Figure 65 (right)) sits at the beginning of the tail section in order to provide the pedal volume within the hull.

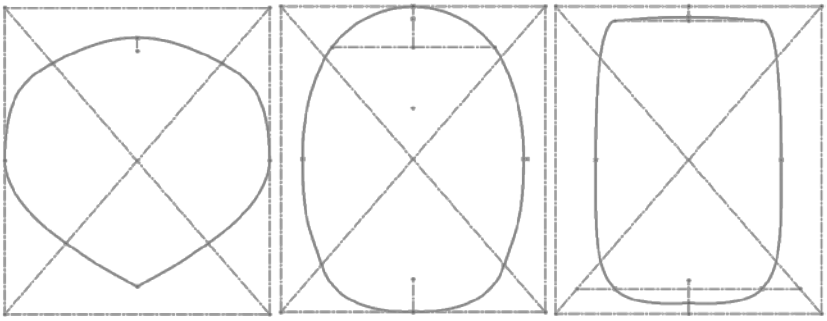

Figure 65 – Front elevation hull (left) nose profile, (centre) central profile and (right) tail profile

7.1.6 CFD CASE MESH REFINEMENT AND VALIDATION RESULTS

CFD CASE VALIDATION

Milestone	CFD VALIDATION	Target C_D =	Range: 0.2-0.08

Geometric setup			Hydro-measurables	Status	Target
Max Length	3000	mm	Frontal Area (m^2)	VARIOUS	MINIMISED
Max Width	1500	mm	C_D	0.06	MINIMISED
Max Height	1500	mm	C_L		
Propeller	NO	Y/N	C_{MY}		
Prop Nacelle	NO	Y/N	C_{MZ}		
Strake	NO	Y/N	C_DxA		
Pectoral Fin	NO	Y/N	Date of Aero Status	29/10/2014	
Dorsal Fin	NO	Y/N			
Attitude Planes	NO	Angle	mm		
Rudder	NO	Angle	mm		

Image

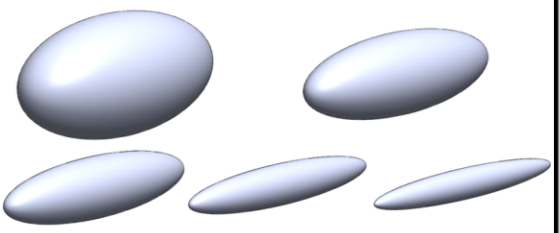

GRID INDEPENDENCE - Ellipsoid L:B=4 where byWhite Cd=0.1

Mesh	Base Size	Prism Layers	%Thickness	Medium Size %	No. PL	%Thickness	Fine Size %	No. PL	% Thickness	Cell No.	Cd Value	CL Value	Time Taken (Hrs)
4	0.20	5	33	50	5	50	25	10	25	953112	0.053670528	-0.000158552	4.8
1	0.20	5	33	50	5	50	15	10	15	1700000	0.053947601	-0.000716706	8.7
5	0.15	5	33	50	5	50	25	10	25	2110000	0.049920334	0.000229852	11.1
2	0.15	5	33	50	5	50	15	10	15	3960000	0.050022318	0.000186458	20.8
6	0.10	5	33	50	5	50	25	10	25	7077861	0.04693243	-6.87411E-05	38.2
3	0.10	5	33	50	5	50	15	10	15	12678293	0.053370114	-0.000150604	>48hrs

GRID INDEPENDENCE - Results

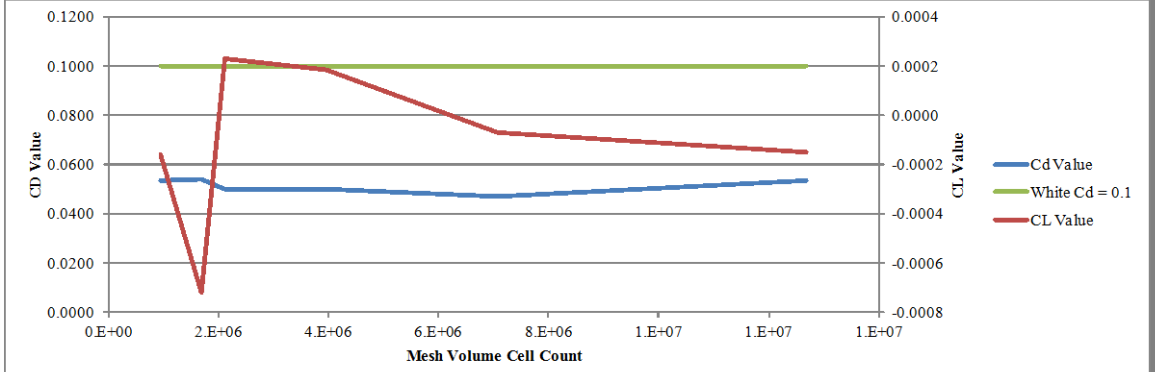

CFD Validation of Ellipsoid Shape

Case	Length (m)	Beam (m)	L:B	Volume (m^3)	Mesh Cell count	Cd Value	White Cd Value.	CL Value
1	3000	1.5	2	3.53	1867075	0.044022	0.130000	-0.000028
2	3000	1	3	1.57	1978472	0.042320		0.000026
3	3000	0.75	4	0.88	2110000	0.049920	0.100000	0.000230
4	3000	0.5	6	0.39	2044938	0.067065		-0.000027
5	3000	0.375	8	0.22	2043352	0.090340	0.080000	0.000217

CFD Validation of Ellipsoid Shape - Results

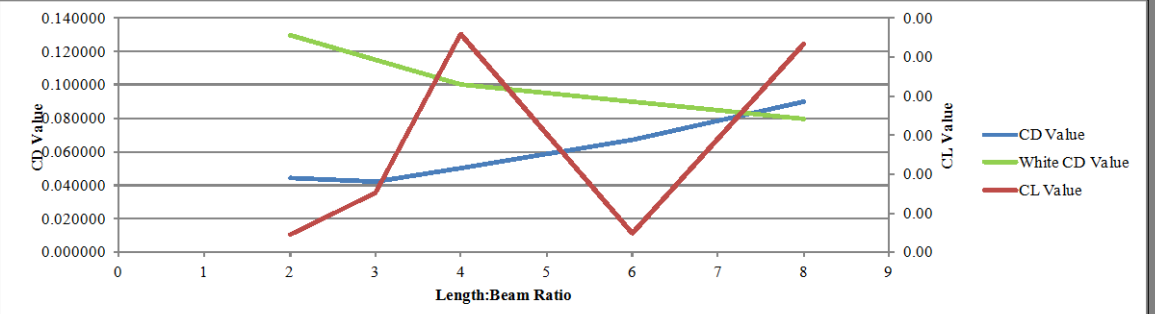

7.1.7 CFD OPTIMISATION DATA

Table 28 – Summary of CFD results

Iteration	ΔC_d *Potential*	C_D	C_L
Shakespeare	N/A	0.2440	-0.0060
Concept 1	0.1770	0.0670	0.0010
Concept 2	0.0080	0.0520	-0.0044
Concept 3	0.0060	0.0610	-0.0001
Concept 4	0.0010	0.0600	-0.0011
HS2_0024	-0.0035	0.0555	-0.0001
HS2_0036	-0.0009	0.0564	0.0002
HS2_0045	0.0012	0.0552	0.0002
Final Hull	-0.0132	0.06839	0.0039

The reduction in flow disturbances around the front of the hull can be attributed to the optimisation of the nose cone plan profile. Figure 66 (left) shows the initial '36' profile, with a sharp profile change in the second half of the nose cone. This sharp gradient can be seen in Figure 11 (c) and (e) to cause a low pressure band and high vorticity. Such a combination is indicative of highly turbulent flow, and as such was the largest opportunity to improve the flow field around the submarine. By employing an elliptical nose profile as per conventional submarine practice, the '45' profile shown in Figure 66 (right), the flow around the nose cone was able to be better controlled. Figure 11 (c) shows how the profile change led to a 12 drag count (2.2%) reduction as the low pressure band around the rear of the nose was reduced in both size and severity. As a result the vorticity in that region was seen in Figure 11 (e) to reduce in magnitude, confirming that turbulence in that area had been reduced. This optimisation study according to accepted practice on naval submarines validated the assumption that for Godiva's hull design, the application of full size design guidelines still applied.

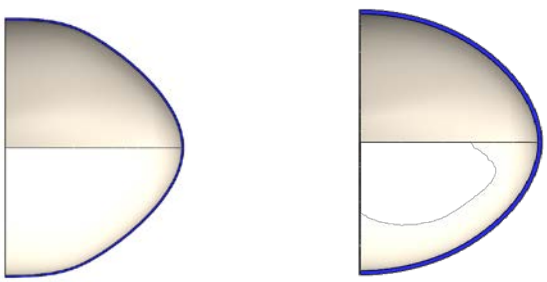

Figure 66 – Nose cone plan profile: (left) HS2_0036 (right) HS2_0045

7.2 CHASSIS APPENDIX

7.2.1 COMPETITION RULES AND THEIR EFFECT ON CHASSIS DESIGN

The competition rules specify guidelines which must be adhered to in the design of the submarine. The relevant rules that affect the chassis design are outlined in Table 29.

Table 29 – Competition requirements and their effect on design

ISR Ruling	*Effect on Submarine Design*
5.2 Propulsions Systems **5.2.1 Propeller System** "Submarine propulsion systems shall be directly coupled to a human being"	The submarine must be able to withstand the forces of a human providing the mechanical force into the drivetrain.
5.4 Life support systems **5.4.2 Submarine Primary Air Supply** "The primary air supply shall be carried onboard the submarine, and have the calculated capacity…"	This has an effect on cylinder selection and thus on chassis weight bearing capability. This load and space must be designed for on chassis.
5.5 Submarine Safety Requirements **5.5.6 Emergency Pop-Up Buoy** "All submarines shall carry a high visibility buoy that will release from the hull and float to the surface when an emergency occurs."	This component must be securely attached to the chassis.
5.6 Other Requirements **5.6.1 Submarine Width Limitations** "The maximum width permitted of a submarine is 84 inches (2.13 meters) to allow it to be launched via the basin's elevator." **5.6.3 Launch Cradle** "…it is recommended that your submarine have a cradle with wheels or some sort of cart to move it around on. … must be negatively buoyant… cradles should have a minimum of 4" diameter wheels for easy movement over the elevator grates."	This places a specific design envelope for the hull and consequently chassis of the submarine. This must be taken into account when design the mounting points for the chassis, and the related design of the launch cradle or trolley.

7.2.2 COMPETITOR ANALYSIS

From the ISR 2013 competition, the top three teams' technical reports have been scrutinized with regards to their submarine structure including load bearing capability and attachment methods. Table 30 shows the observations made from the respective reports.

Table 30 – ISR 2013 top 3 teams – one person propeller driven – design observations

Omer - Ecole de Technologie Supérieure, Canada	**WASUB - TU Delft, Netherlands**	**Talon 1 - Florida Atlantic University, USA**
Carbon fibre and epoxy resin moulded in an infusion process to make monocoque structure	Fibreglass - vacuum moulded symmetrical monocoque structure	A combination of fiberglass with aluminium reinforcement
Fixtures are bolted directly to hull body in a monocoque design	Fixtures are bolted directly to hull body in a monocoque design	Fixtures are bolted directly to the hull in a monocoque design
Direct-to-gearbox configuration used, thus no chain. This gearbox area is reinforced to provide enough strength and the gearbox is attached directly to the hull	Direct-to-gearbox configuration used to remove need for chain and keep packaging to a minimum and localised attachment. All forces placed through reinforced crank and gearbox area for strength	Drivetrain is bolted in its component parts to the hull of the submarine. All forces are distributed through the hull body. Composite trolley shaped to fit hull used to transport vehicle

7.2.3 CONCEPT DEVELOPMENT – FINITE ELEMENT ANALYSIS

To understand the ability of each concept to bear significant loading, the concepts were tested with simple bending and torsional loading conditions. The figures below show each concept under each loading condition, the results of these simulations were summarised in Section 2.2.4.2 Chassis Validation of the main report.

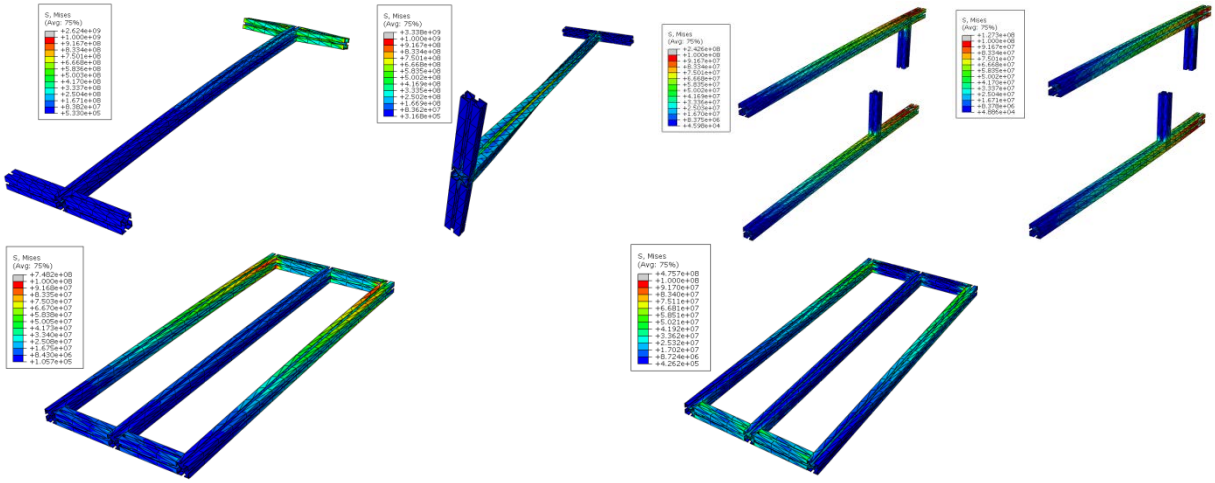

Figures illustrating the 2 load cases, bending and torsional, for the 3 concepts discussed.

7.2.4 JUSTIFICATION OF PUGH MATRIX CRITERIA

Table 31 – Justification of Pugh matrix criteria

Criteria	*Justification*
Volume / Packaging	As one of the key design goals for this project was to minimise the packaging and optimise hydrodynamics as much as possible, this was the highest weighted of the Pugh Matrix criteria
Stiffness	The primary goal for the chassis was to transmit the loading from the pedals to the powertrain and through to the propeller as effectively as possible
Durability	Ensuring the submarine was safe was also a primary design goal, and so the durability of the chassis fits directly into this goal, hence its high weighting
Modularity / Flexibility	One of the most important design goals for the submarine was the consistency of the modularity ethos. This was an undercurrent of the whole project. The reason for this criteria being relatively low-weighted in the Pugh matrix, was there was little difference between all of the concepts in terms of modularity and flexibility and so it would be a misrepresentation of each concept to give this a high weighting
Ease of Manufacture	Due to the limited time constraints, it was important for the submarine to be easy to manufacture, and thus this criteria, although not a high priority, must be included in the Pugh matrix
Ease of Assembly	Along with the Ease of Manufacture, the submarine must be simple to assemble when it is delivered to the competition
Weight	This criteria is more with regards to the transportation and assembly of the submarine, as the minimal difference in weight between these concepts is not important from a performance standpoint
Cost	The cost difference between these designs was relatively minimal and thus is was the lowest weighted of the Pugh Matrix Criteria

7.3 PROPULSION APPENDIX

7.3.1 PROPELLER SENSITIVITY STUDY

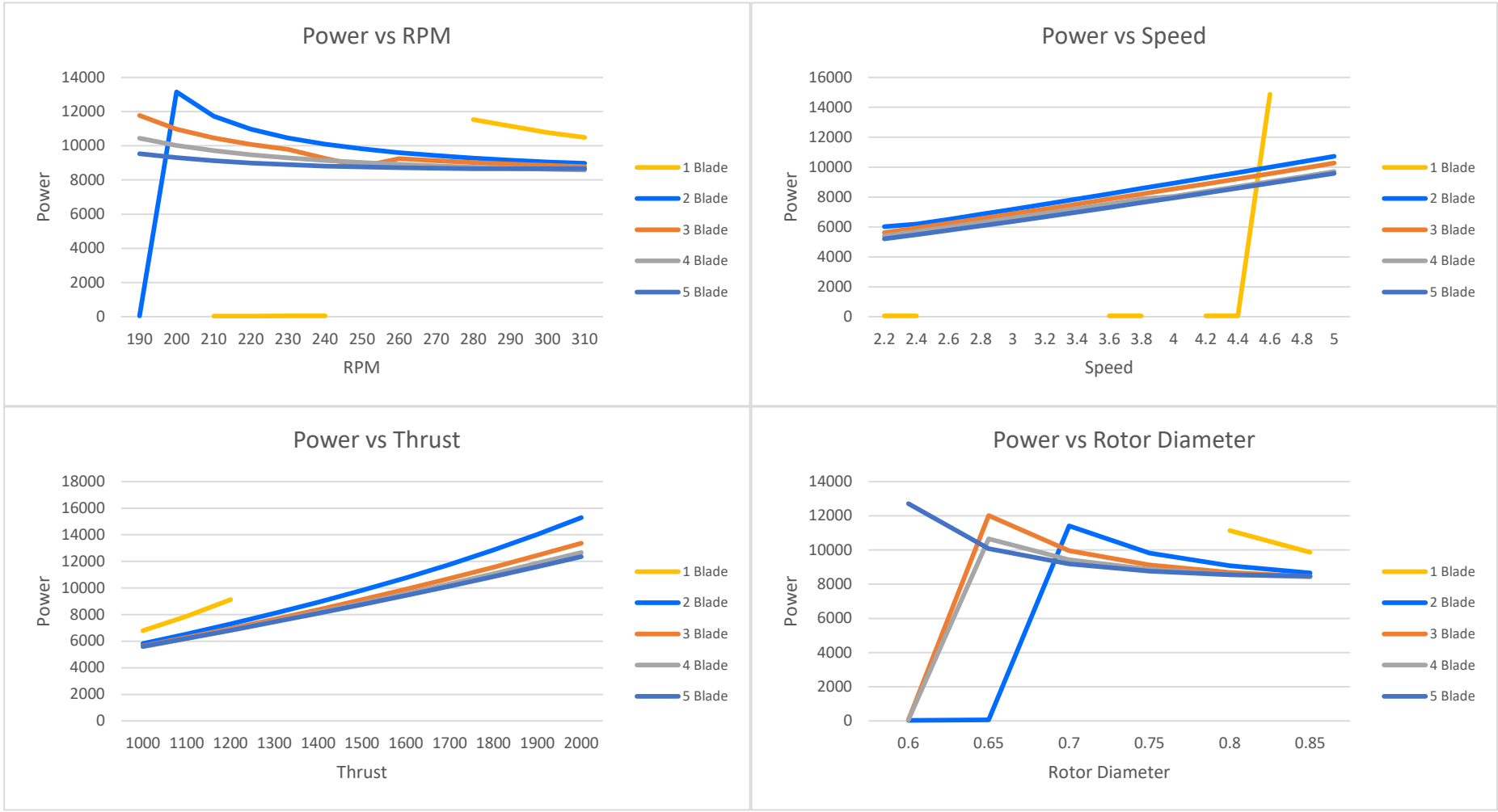

Figure 67 – Propeller sensitivity study results, effects on power output

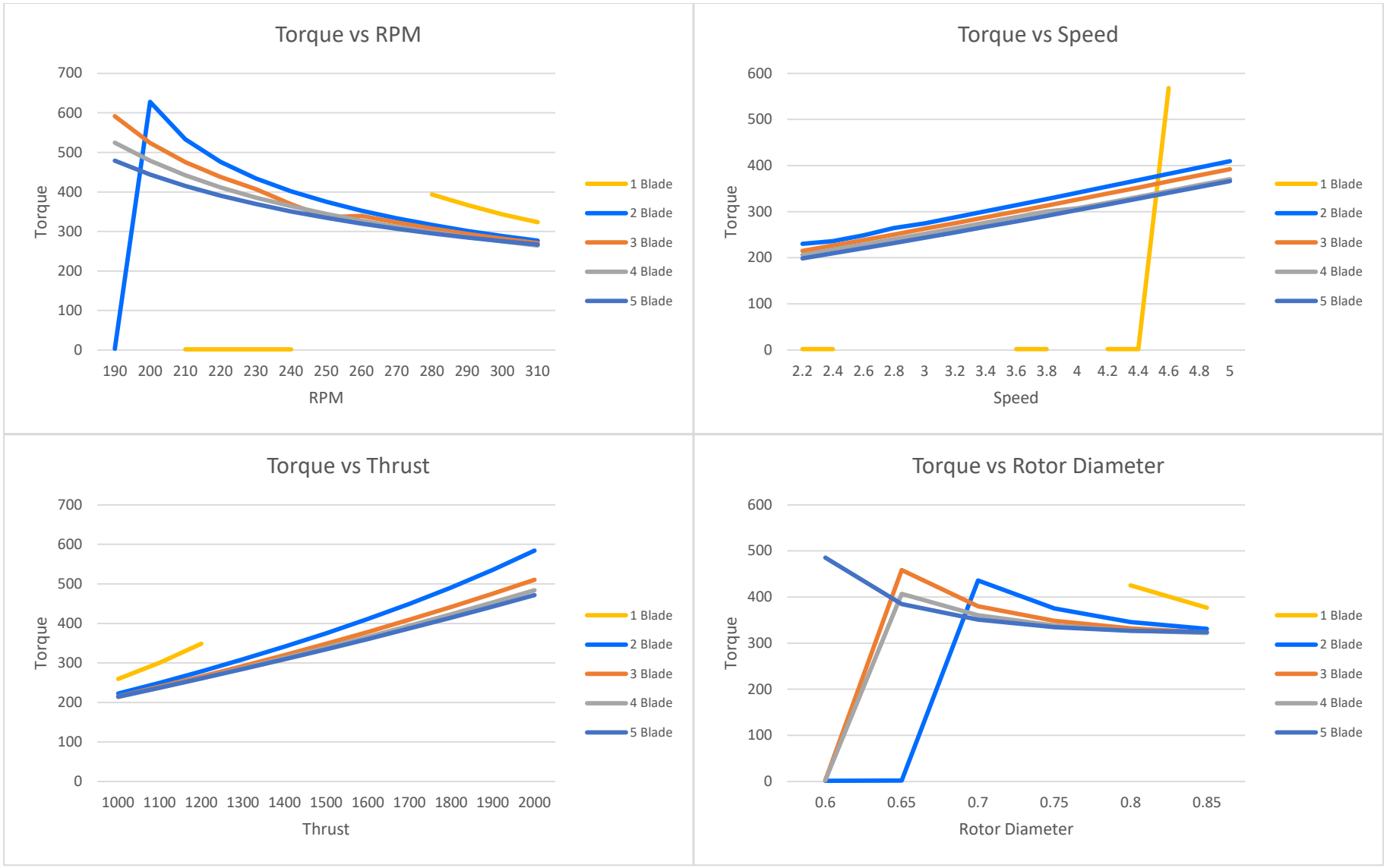

Figure 68 – Propeller sensitivity study results, effects on torque required

The graphs displayed above display the output comparison from the OpenProp sensitivity study. As is clearly evident, OpenProp is not suited to modelling single bladed propellers. The chosen propeller operates with three blades, 750 mm single rotor diameter at 1500 N of thrust, at approximately 4.5ms^{-1}. The propeller was chosen to maximise efficient power output from the pilot.

7.4 POWERTRAIN APPENDIX

7.4.1 WATTBIKE PILOT ANALYSIS EXTENSION

Average angle to force peak in whole session, Right Leg: 114°

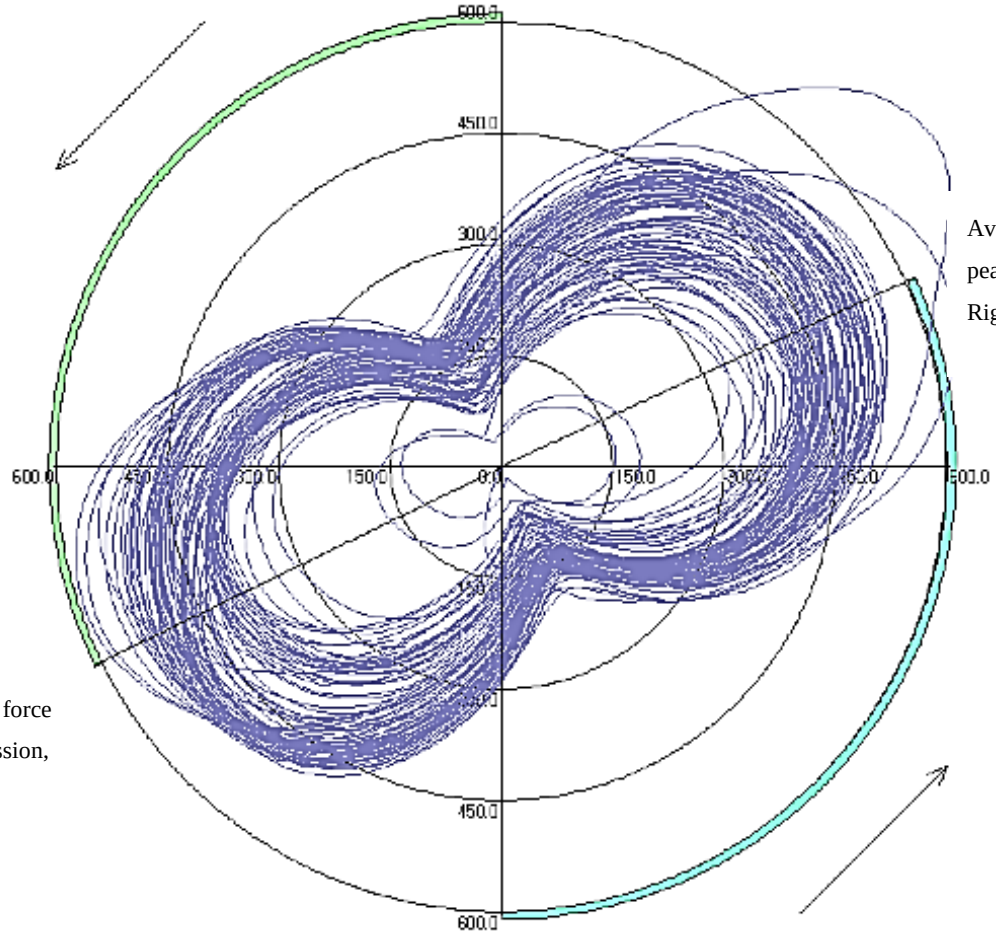

Average angle to force peak in whole session, Left Leg: 116°

Figure 69 – Detailed analysis of pilot pedalling motion

7.4.2 MATLAB SCRIPT FOR CALCULATION OF HUMAN ENGINE MATCHING

```
clear
hold off
c=0.035; %prop chord length
omega=250*2*pi/60; %prop rotation speed
aoadeg=7; %representative AoA for the blade in deg
aoarad=aoadeg*pi/180; %convert to rad
rho=1000; %water density
s=0.4;


%%plot airfoil profile - this is roguhly the same as the one
for the prop
cent= [0,c;0,0;];
xtop=[0;0.003;0.01;0.02;0.04;0.07;0.1;0.15;0.2;0.25;0.3;0.35;0
.4;0.45;0.5;;0.55;0.6;0.65;0.7;0.75;0.8;0.85;0.9;0.95;0.975;1]
*c;
xbot=xtop;
ybot=[0;0.009099;0.017152;0.024678;0.035135;0.045809;0.053377;
0.062118;0.068235;0.07275;0.076067;0.078178;0.079022;0.078668;
0.077173;0.074566;0.070912;0.06626;0.060628;0.054022;0.046416;
0.037752;0.028002;0.017193;0.011484;0.0055]*c;
ytop=[0;-0.004658;-0.007411;-0.008934;-0.009318;-0.007339;-
0.004076;0.002198;0.007996;0.01275;0.016295;0.018834;0.020553;
0.021539;0.021827;0.021435;0.020401;0.01875;0.016501;0.013723;
0.010504;0.00694;0.003084;-0.001015;-0.003184;-0.0055]*c;
cline=((ytop+ybot)/2);
hold


figure (1)
title('Profile')
axis([0,(c+0.0005),-0.01,0.01])
plot(xtop,ytop)
plot(xbot,ybot)
plot(xbot,cline,'r')
plot(cent(1,:), cent(:,1), 'g');
bestfit = fit( xbot, cline, 'poly2')
coeffs=coeffvalues(bestfit);
x0=coeffs(1,2)/((coeffs(1,1)*-2));
y0=(coeffs(1,1)*x0^2)+(coeffs(1,2)*x0);
```

```
plot(bestfit, 'bl'); %plot camber line
xlabel('c')
ylabel('Thickness')
legend('Top Surface','Bottom Surface', 'Camber Line', 'Centre
Line');
Cl=(pi*4*y0*(1/c))+(2*pi*aoarad) %coefficient of lift
mu=0.00000122; %viscosity
Re=((omega*(s)*c)/mu); %Re
%BLT= 0.048*(c/Re^(1/5));
Csf= 1.3/(Re^(1/2)); %coeff skin friction
Cf=0.045; %coeff form drag
Cvd= (Cl^2*c)/(pi*s); %coeff vortex drag
Fsf= ((rho/2)*c*Csf*(s^3/3)*omega^2); %skin friction
Ff=(rho/2)*c*Cf*(s^3/3)*omega^2; %Form drag
Fvd=(rho/2)*c*Cvd*(s^3/3)*omega^2; %vortex drag
TotDrag=3*(Fsf+Ff+Fvd); %Tot Drag
L=(rho/2)*c*Cl*(s^3/3)*omega^2*3; %prop lift force
DragMoment= TotDrag*s/2; %Torque to turn prop, must be less
than the output of the pilot
P=TotDrag*omega*s/2
%%
pilotpower= 150;
inputrotation=100*2*pi/60;
inputtorque = pilotpower/inputrotation;
```

7.5 STEERING APPENDIX

7.5.1 RUDDER POSITIONING

The initial concept for this year was to design the rudder to sit behind the propeller, at the very back of the submarine. The alternative design was to implement a system similar to last year and mount the rudder in front of the gearbox. The Pugh matrix below analyses these systems.

Table 32 – Rudder positioning Pugh matrix

		Concepts	
Criteria	***Weighting***	***Rudder behind propeller***	***Rudder in front of gearbox***
Functionality	10	2	1
Cost	9	1	2
Ease of Manufacture	8	1	2
Simplicity	7	1	2
Modularity	6	1	2
Drag Penalty	5	2	1
Weight	4	1	2
Total	-	65	83
Optimum Choice			

By placing the rudder behind the propeller, it is as far away as possible from the centre of mass. Therefore a larger turning force can be produced. It also means that maximum thrust from the propeller can be diverted. Consequently it scored highly for functionality. The design is also modular, and can easily be unattached from the main chassis at a bearing block by the propeller shaft. However the design ran into complications; namely how to attach the rudder to the submarine, whilst contending with huge forces. Having the rudder as a separate body also results in a larger drag penalty. Although the initial concept appeared simple, more design holes slowly appeared and in the end it became clear that this would be an uneconomical, unfeasible system to implement.

7.5.2 PUGH MATRIX WEIGHTING JUSTIFICATION

FUNCTIONALITY

The most important characteristic of any component is that it performs its design role.

COST

With limited project funds, cost efficiency is key.

MANUFACTURABILITY

Any design produced must be simple to manufacture in the engineering workshops.

SIMPLICITY

As this year's competition is a drag race, steering has been chosen as a secondary focus; a simple design will be easier to implement, thence allowing more time must be spent on high priority areas such as the hydrodynamics of the hull.

MODULARITY

A key design focus has been to create modular subsystems which can be dismantled from the main submarine.

DRAG PENALTY

Although attaching any appendages to the streamlined hull is likely to cause more drag, this must be kept to a minimum to allow the submarine to travel as fast as possible.

MASS

A steering system of higher mass will be harder to move through the water, creating more work for the pilot.

7.5.3 CONTROL SURFACES VS DUCTED PROPELLER PUGH MATRIX

There are two main ways in which the direction of travel of a submarine can be changed. The first is by using a vectored thrust. Either the propeller shaft, or the duct surrounding the propeller, is rotated to change the direction of thrust. The second method is to use control surfaces, or dive planes. These can be rotated to redirect the flow of the water across them. This produces a force which causes the submarine to turn. The Pugh matrix below analyses each system.

Table 33 – Steering method selection method Pugh matrix

		Concepts	
Criteria	***Weighting***	***Control Surfaces***	***Thrust Vectoring***
Functionality	10	1	2
Cost	9	2	1
Ease of Manufacture	8	2	1
Simplicity	7	2	1
Modularity	6	2	1
Drag Penalty	5	1	2
Weight	4	1	2
Total	-	73	68
Optimum Choice			

Thrust vectoring is an extremely effective method of changing direction and consequently scores highly for functionality. However rotating the propeller shaft is mechanically complicated – both in design and manufacture, and costly to implement, requiring the purchase of a universal joint. The steering would be difficult to keep as a separate component; it would have to be permanently connected to the propulsion system, going against this project's modular design ethos. If instead thrust vectoring is implemented by rotating a duct surrounding the propeller (vectoring nozzle), this leads to large inefficiencies. The duct must rotate without impeding the rotation of the propeller, and so must have a diameter far greater than that of the propeller. A duct of this size is inefficient at redirecting the thrust and can greatly increase the total drag force. It is also ineffective for our design envelope. In contrast, steering the submarine by rotating four control surfaces is easy to implement, as illustrated by last year's team. Although they can be slightly less efficient than thrust vectoring, this high level of efficiency is not required for this year's drag race.

7.5.4 MATLAB SCRIPT TO ANALYSE RUDDER LIFT AND DRAG

```
%INPUT DESIGN PARAMETERS
%L= FIN LENGTH (M)
%C1= BASE CHORD LEGNTH (M)
%C2 TIP CHORD LEGNTH (M)
%NEED ALPHA TO BE BETWEEN +/- 16 DEGREES
V=input('insert velocity')
legnth = input('insert legnth')
A= input ('insert surface area')
alpha= input('insert angle of attack of foil +/1 16 deg')
rho=1000; %density of water
mu=1.3*(10^(-6)) %kinematic viscosity
cL=1.2*alpha/16; %lift coeff
cD=0.004; %drag coeff
R=(V*A)/mu;
lift=0.5*rho*V^2*A*cL;
drag=0.5*rho*V^2*A*cD;
```

7.6 ELECTRONICS APPENDIX

7.6.1 JUSTIFICATION OF MICROCONTROLLER SELECTION CRITERIA WEIGHTINGS

PROCESSING POWER

This rates the raw arithmetic and data-moving capability of the central processor core of each microcontroller. This is of moderate importance as the submarine MCU will have to carry out some processing on the data gathered by the sensors, as well as calculate the outputs for the steering system in real time. Updating a display takes a lot of CPU cycles, so the unit chosen has to be fast enough to update the pilot's screen at a useful rate.

EASE OF PROGRAMMING

With so many different functions to implement, it is vital that the MCU chosen is easy to program and develop code for. This includes the quality of the development software and how many software libraries are available.

COST

MCUs vary in cost, which roughly correlates to how powerful the unit is. None of the MCUs under consideration are very expensive but some are better value for money than others, and cost is still a powerful factor in deciding which components to buy.

POWER CONSUMPTION

Low power consumption is important to minimise downtime spent charging batteries. However, all modern microcontrollers have very low power usage, especially when the various 'sleep' modes are used intelligently, making this less of a differentiating factor.

CODE SPACE

Microcontrollers have a limited amount of onboard memory where the program is stored, and this cannot be expanded. It is essential therefore to pick a microcontroller that has lots of space for the user code. It also gives future teams room to expand without replacing the MCU. Using existing libraries to implement functionality makes writing the code easier, but can fill code space rapidly so having plenty gives peace of mind.

PERIPHERALS

One thing that makes MCUs so useful is their built-in communication peripherals which make interfacing to other hardware simple. Common interfaces like USB, I^2C and SPI as well as PWM modules, analogue-to-digital converters (ADCs) and digital-to-analogue converters (DACs) all factor into this rating.

I/O

This rating is simply how many input and output pins the microcontroller features, and is relevant because the aforementioned hardware peripherals cannot be used simultaneously if they all share the same pins on the microcontroller. The submarine system also requires many general purpose digital input and output pins, so having a large number is beneficial.

7.6.2 TEST CODE FOR RPM SENSOR

```
#include "mbed.h"
#include "TextLCD.h"
#include "SPI_TFT_ILI9341.h"
#include "Arial12x12.h"
#include "Arial24x23.h"
#include "Arial28x28.h"

InterruptIn RPM_sensor(PTB20);

I2C i2c_lcd(PTE25,PTE24); // SDA, SCL

//I2C Portexpander MCP23008
TextLCD_I2C lcd(&i2c_lcd, MCP23008_SA0, TextLCD::LCD20x4,
TextLCD::HD44780); // I2C bus, MCP23008 Slaveaddress, LCD
Type, LCDTCtrl=HD44780 (default)

SPI_TFT_ILI9341 TFT(PTD2,PTD3,PTD1,PTB2,PTB3,PTB10,"TFT"); //
mosi, miso, sclk, cs, reset, dc

int count = 0;

void rpm_isr(){
    count++;
}
```

```
int main(){

    int count_curr = 0, count_prev = 0, rpm = 0;

    RPM_sensor.rise(&rpm_isr);

    lcd.cls();

    TFT.set_orientation(1);
    TFT.background(Black);                          // set
background to black
    TFT.foreground(White);                          // set
characters to white
    TFT.set_font((unsigned char*) Arial28x28);      // set font
to large Arial
    TFT.cls();                                      // clear
the screen

    TFT.locate(0,12);
    TFT.printf("RPM");

    while(1){

        count_curr = count;
        rpm = (count_curr - count_prev)*5;
        //lcd.locate(0,0);
        //lcd.printf("Count: %i",count);
        //lcd.locate(0,1);
        //lcd.printf("RPM:   %i",rpm);
        TFT.locate(0,48);
        TFT.printf("%i",rpm);
        count_prev = count_curr;

        wait(1);
    }
}
```

7.7 SAFETY APPENDIX

7.7.1 FAILURE MODES AND EFFECTS ANALYSIS – ESCAPE HATCH

Part	*Part Function*	*Failure type*	*Potential Effect(s) of Failure*	*Severity*	*Potential Cause(s)/ Mechanism(s) of Failure*	*Prob*	*Current Design Controls*	*Det*	*RPN*
Release Cable	Releases pins	Break / Stretches	Pins do not release	7	Repeated use	3	Pins are designed to shear	3	63
Pins	Hold Escape Hatch	Do not release	Escape hatch does not release	7	Release cable / mechanism failure	7	Designed to shear	3	147
Pins	Hold Escape Hatch	Do not shear	Worst Case Scenario	10	Shear force not achieved / Pin too strong	2	No design control	3	60
Spring	Hold pins in *out* position	Buckle / Dislodges	Pins do not release	7	Knock / Vibration / Cracked Casing	4	Concentric constraints to inner and outer / pins are	3	84

							designed to shear		
3D Print Casing	Supports mechanism	Cracking failure	Pins do not release	7	Impact / Knock / Vibration	3	Pins are designed to shear	3	63
Lever Release Arm	Actuates pin release	Shear failure	Pins do not release	7	Impact / Knock / Vibration	3	Pins are designed to shear	3	63
Lever Pivot Bolt	Pivots to release cables	Shear failure	Improper Pin Release	6	Impact / Knock / Vibration	3	Pins are designed to shear	3	54

7.7.2 KEY TO FMEA

7.7.2.1 SEVERITY

Table 34 – Key to FMEA severity ratings

Effect	*Severity of Effect*	*Ranking*
Hazardous without warning	Very high severity, catastrophic failure can occur without warning	**10**
Hazardous with warning	Very high severity, catastrophic failure can occur with warning	**9**
Very high	System inoperable with destructive failure, safety not compromised	**8**
High	System inoperable with equipment damage	**7**
Moderate	System inoperable with some damage	**6**
Low	System inoperable without damage	**5**
Very low	System operable with significant degradation of performance	**4**
Minor	System operable with some degradation of performance	**3**
Very Minor	System operable with minimal interference	**2**
None	No effect	**1**

7.7.2.2 PROBABILITY

Table 35 – Key to FMEA probability ratings

Probability of Failure	*Approximate Numerical Probability*	*Ranking*
Very high: failure is almost inevitable	> 1 in 2	**10**
	1 in 3	**9**
High: repeated failures	1 in 8	**8**
	1 in 20	**7**
Moderate: occasional failures	1 in 80	**6**
	1 in 200	**5**
	1 in 400	**4**
Low: relatively few failures	1 in 1,000	**3**
	1 in 5,000	**2**
Remote: failure is unlikely	< 1 in 5,000	**1**

7.7.2.3 DETECTION

Table 36 – Key to FMEA detection likelihood ratings

Detection	*Likelihood of Detection by Design Control*	*Ranking*
Absolute uncertainty	Design control *cannot* detect potential cause of problem and the subsequent failure	**10**
Very remote	*Very remote* chance the design control will detect potential cause of problem and the subsequent failure	**9**
Remote	*Remote* chance the design control will detect potential cause of problem and the subsequent failure	**8**
Very low	*Very low* chance the design control will detect potential cause of problem and the subsequent failure	**7**
Low	*Low* chance the design control will detect potential cause of problem and the subsequent failure	**6**
Moderate	*Moderate* chance the design control will detect potential cause of problem and the subsequent failure	**5**
Moderately high	*Moderately high* chance the design control will detect potential cause of problem and the subsequent failure	**4**
High	*High* chance the design control will detect potential cause of problem and the subsequent failure	**3**
Very high	*Very high* chance the design control will detect potential cause of problem and the subsequent failure	**2**
Almost certain	Design control *will always* detect potential cause of problem and the subsequent failure	**1**

7.8 COMPOSITES APPENDIX

7.8.1 INTERFACTIAL BOND STRENGTH TESTING METHODS

A number of direct test methods are established to quantify the interfacial bond strength which is tabulated below.

Test Method	*Description*	*Issues*
Fragmentation Test **(a)**	Tension load applied to a single fibre embedded in a resin specimen. The fibre fragment length after fracture is related to the interface shear properties	In the simplest form this method does not account for non-idealities such as presence of matrix cracks, residual stresses and statistical nature of fibre strength
Pull-Out Test **(b)**	Pull a single fibre from a bubble of resin. Pull out shear stress may be calculated from a known embedded fibre length	Difficult to calculate critical stress condition for micron fibre diameters and experimentally complex
Micro-indentation Test **(c)**	Apply compressive load to a single fibre until the interface fails under shear	Experimentally complex and time consuming

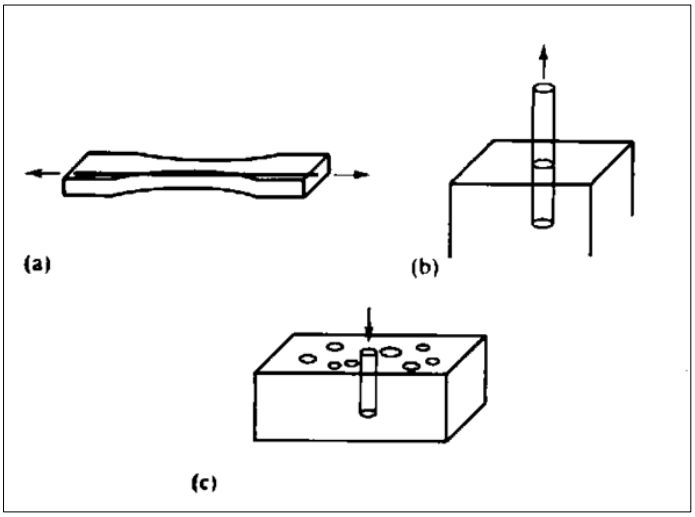

Figure 70 – Schematic of interfacial bond strength testing methods [39]

7.8.2 COMPOSITE FABRICATION – OPEN MOULD PROCESSES

Manufacturing Route	*Process Outline*	*Advantages*	*Disadvantages*	*Applications*
Hand Lay Up	Fibre matt placed on mould surface and impregnated with resin. Consolidation is achieved by painting and rolling. Layers are built up until design thickness is achieved.	Moulding cures without heat or pressure. Low tool cost High Fibre content achievable	Quality is dependent on skill of laminators Only surface incident with mould is properly defined Voids common	Boat hulls Wind turbine Blades
Spray Up	Discontinuous chopped fibres and resin are sprayed into a prepared mould and rolled smooth before resin cures.	Low cost Established method	Glass Fibre only Short fibres limit mechanical properties Specialist equipment	Bath tubs Caravan Bodies
Vacuum Bagging	Layers of fibre matt, commonly pre-impregnated with resin, are placed on a mould within a vacuum bag. Application of vacuum or pressure eliminates voids	Remove voids in finished component Better uniformity in fibre wet-out Improved Health and Safety as cure contained	Additional cost High operator skill Specialist equipment	Race car components One-off cruising boats

7.8.3 JUSTIFICATION OF FIBRE WEIGHTING CRITERIA

The following is a summary of the weighting score in order of significance, noting that all the materials are fundamentality capable of fulfilling the basic operating requirement.

COST

Consideration of the budgetary constraint imposed upon a project is commonly the principal limitation imposed on the mechanical performance of the ideal design. As a result, with the specific project requirements in mind, cost performance is presented as the most significant target.

MANUFACTURABILITY

Certain fibres require specialised manufacturing techniques which may require specialised machinery and specific processing requirements e.g. autoclave curing; hence this criterion is rated highly as it impinges constraints as to the realisation of an idealised design.

DENSITY

Neutral buoyancy of the submarine is a core design goal, which is more easily realisable if the densities of the materials used are closely matched to the surrounding fluid. Assuming the density of water is 1000 kgm^{-3} weightings are based according to the minimum density disparity of the materials.

SPECIFIC STRENGTH ($^{\sigma_{UTS}}/_{\rho}$)

As mentioned, all of the considered fibres are sufficiently strong for the given application; hence the optimum material for multi-objective optimisation will offer the best ratio between strength and density.

SPECIFIC MODULUS ($^{E}/_{\rho}$)

Similarly to the above, stiffness is an important criteria to ensure the hull form does not deform from the optimised geometry or impinge upon the freedom of the pilot.

MOISTURE ABSORPTION

Absorption of water is known to detrimentally effect the mechanical properties of natural fibre composites [43]. As a consequence the use and expertise of natural fibres in wet applications is currently not established beyond experimental projects.

RISK

The risk of using a relatively a fibre in a relatively new application is an important consideration; however risks can be mitigated through testing to ensure performance is maintained in a wet environment.

NOVEL

This project aims to push the boundaries of current composite application in accordance with ISR award guidelines, and as a result testing material in a novel application should be rewarded.

7.8.4 JUSTIFICATION OF FABRICATION WEIGHTING CRITERIA

The following is a summary of the weighting score in order of significance, noting that all the materials are fundamentality capable of fulfilling the basic operating requirement:

FIBRE COMPATIBILITY

A chosen fabrication method must be compatible with the selected fibre. The fibre selection process has already considered manufacturability as explained in Section 7.8.3 and therefore this criterion is of fundamental importance.

COST

As discussed in Section 3.2.3.1 Fibre Properties & Pugh Matrix consideration of cost is a principle limitation.

FABRICATION QUALITY

The presence of voids in the composite act as inclusions which act as stress raisers and crack initiation sites adversely affecting the resultant mechanical properties of the fabricated part. Additionally the voids, created at ambient pressure, will act as isolated pressure pockets which may collapse when the submarine is at operating water pressure.

GEOMETRICAL ACCURACY

Deviation of the hull geometry from design will adversely affect the validity of conclusions from numerical method analysis. Furthermore as the submarine is designed to be assembled from multiple sections, stacking of tolerances implies dimensional inaccuracies should be minimised.

SURFACE QUALITY

Skin friction is sensitive to surface roughness incentivising producing surface roughness below the thickness of the boundary layer [44].

OPERATOR SKILL

Fabrication is to be completed by the authors whom have low expertise and experience in fabricating composite parts, therefore low operator skill is preferable.

7.8.5 FABRICATION ROUTES FOR FIBRE-REINFORCED COMPOSITES

The final consideration for composite selection is an appropriate method for fabrication. Significant effort has been expended in the design of a hydrodynamically optimised hull form which, for the efficiency gains to be realised in practice, must be manufactured with good dimensional accuracy. A wide array of techniques are available to produce a final form from the constituent fibres and resin matrix which may be grouped in two categories: open mould and closed mould processes. See [45] for a more detailed overview of composite manufacturing techniques. Note that all methods consider require the manufacture of a mould which incurs significant cost.

7.8.6 FABRICATION SELECTION CRITERIA & PUGH MATRIX

Fabrication technique selection is based on the information presented in Table 37 with the significance of attributes weighted according to desirability.

Table 37 – Pugh Matrix for fabrication technique selection – hand lay up

		Concept		
Criteria	***Weighting***	***Hand Lay-Up***	***Spray Up***	***Vacuum Bag***
Fibre Compatibility	6	3	1	3
Cost	5	3	1	2
Fabrication Quality	4	3	2	5
Geometrical Accuracy	3	3	1	4
Surface Quality	2	3	1	4
Operator Skill	1	3	3	1
Total	-	63	27	69
Optimum Choice				

The output from Table 37 shows that the preferable fabrication technique is Vacuum bagging, as the requirement of increased operator skill and cost compared to the baseline Hand Lay-Up is outweighed by the significant advantages of improved geometrical accuracy and surface quality making it the optimum choice. However the budget constraints impinged on the project must be allocated according to the potential significance design improvements will have on the iterative design improvement process. As a result Hand Lay-Up has been selected for part fabrication as the cost savings made may be distributed with greater effect to other design priorities.

2015

WARWICK SUB

Cost Benefit Analysis

Team Members

Verity Armstrong

Rupert Barnard

Sam Clifton

Jack Fairweather

Richard Freeman

Theo Saville

Matt Shanahan

Stuart Snow

TABLE OF CONTENTS

LIST OF FIGURES

LIST OF TABLES

SUMMARY

This work assesses the costs and benefits of the third iteration of the Warwick Human Powered Submarine project from the perspective of the School of Engineering and University of Warwick strategic objectives. Costs associated with the design and build of the new submersible, HPS Godiva, have been separated according to: design time of the project team, material and manufacturing costs incurred to build the submersible, and other project related costs which have allowed the University to enter the 2015 13th International Submarine Races (ISR) in Washington DC. The analysis goes on to decompose and discuss the broad range of benefits in both the micro-context of valuable experience for future professional engineers, to the macro-scale impact on the University and wider community over a long term investment horizon.

This Cost Benefit Analysis concludes that the project has been a worthwhile endeavour, and Warwick Sub represents an exceptional example of an innovative undertaking which will benefit the student community in terms of diversity and practical experience.

1.0 INTRODUCTION

This report assesses and critically reviews the costs and benefits realised by the Warwick Human Powered Submarine project in the design, manufacture, test and race of new submersible HPS Godiva. The project continues from the unprecedented success of previous project iteration, HPS Shakespeare, with a vision to compete at the 13th International Submarine Races, Washington, USA in June 2015.

2.0 AIMS AND OBJECTIVES

The University of Warwick Human Powered Submarine project consists of the following high level aims, which have been condensed into a number of concise objectives:

- To compete at the 13th International Submarine Races in Washington DC:
    - Finish manufacture and testing by 21st May 2015 for timely shipment
    - Achieve a speed target of 6 knots
    - Design for packaging to reduce transportation costs
- To design with three key themes:
    - Efficiency – optimise the design using computer simulation packages
    - Practicality – modular design ethos for ease of assembly
    - Innovation – use of novel technology to enhance performance
- To raise the profile of Warwick Sub
- Promote STEM disciplines in schools and the wider community

3.0 SPONSORSHIP ACTIVITIES

In order to achieve our primary aim of competing at the 13th ISR, the team have committed a significant amount of effort toward establishing a strong sponsorship position. Without the autonomy of team members and the support of industrial partners established during this project, the noteworthy progress made would not have been possible. For example, presence of the Warwick Sub team at the 2014 Advanced Engineering Show, held at the NEC Birmingham, prompted substantial interest from a number of firms whose products are relevant to the submarine challenges. Additionally three team members organised and attended the Subsea Expo in Aberdeen at which they were a central exhibitor. This event was an unprecedented success and established a wealth of personal contacts which will contribute positively to the legacy success of the project. A summary of the sponsorship position for this year, totalling in excess of £50,000, is given in Table A1 (Appendix A).

To accompany our sponsorship search the team have produced a professional "Sponsorship Prospectus" document which is included in Appendix B. In securing sponsorship, mutual benefit has been derived for the team and sponsors by providing exposure to employers who are looking to recruit University of Warwick students. Where appropriate, PDR events may be organised where a firm presents the technical challenges their organisation specialises in and may advertise positions for internships and graduate positions simultaneously. Furthermore creating industry links through sponsorship will attract new employers and expose students to industry in an ever more competitive job market. This will bring about long term benefit to the students, School of Engineering and the University.

Figure 71 – Warwick Sub sponsorship business card

4.0 PROJECT COSTS PER FUNCTION

This section summarises and compares the value of project sponsorship to the costs incurred over the duration of the HPS Godiva project iteration. The following tariffs have been used to value the time of students, technicians and academic staff:

Table 1 – Project Time Tariffs

	Tariff (hr-1)
Students	£15
Technician	£30
Academic	£75

Note that the cost of student time has been attributed to the function in which each student's design effort was focused. This enables better representation of the true cost for each engineering sub-function.

Table 2 – Warwick Human Powered Submarine Costs Summary

	Breakdown	Value
Sponsorship	**Industry**	**£ 41,445.00**
	WMG CATAPULT	**£ 9,500.00**
	School of Engineering & WMG	**£ 2,427.00**
Total		**£ 53,372.00**
Costs per Function	**Hull**	**£ 9,880.00**
	Chassis	**£ 5,129.00**
	Propeller	**£ 6,135.00**
	Composites	**£ 5,430.00**
	Drivetrain	**£ 6,169.00**
	Steering	**£ 4,875.00**
	Safety	**£ 5,544.00**
	Electronics	**£ 4,436.00**
	Project Related Costs	**£ 9,808.00**
Total		**£ 57,406.00**
Net		**-£ 4,034.00**

The conclusion drawn from Table 39 is that when comparing the total value of all sponsorship awarded to the project this year to the total costs of all activities, the result is a net cost to the School of Engineering of £4,036.16. This value takes in to consideration the value of all in-kind and monetary sponsorship obtained by the team which has enabled the manufacture of the submarine to take place, which is supplementary to the academic deliverable of the project.

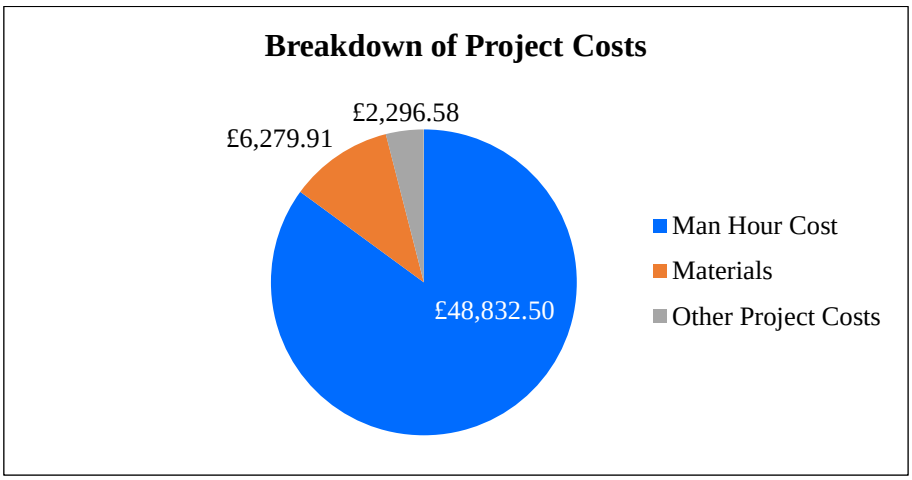

Figure 72 – Project cost breakdown

Figure 72 presents a cost breakdown which indicates where most of the cost has been allocated across the project. The chart shows that a considerable majority of the total cost

distribution is attributed to man-hours, billed according to the tariffs detailed in Table 38. Project related costs include all costs to enter the ISR and Outreach activities to which Warwick Sub contributed.

4.1 OPPORTUNITY COST – A CASE STUDY

Inherent to projects which require the multi-objective optimisation of a fiscally constrained design is the opportunity cost of any and all decisions made to arrive at the end goal. Defining opportunity cost as "*the loss of other alternatives when one alternative is chosen*" [1], the project offers a plethora of examples where the decision has been made to preferentially distribute funds to certain design functions which will bring about the greatest overall benefit. The following is an example of where a decision was made with care taken to consider the opportunity cost of the allocated resources.

4.1.1 BEVEL GEARBOX – BUY VS. MAKE

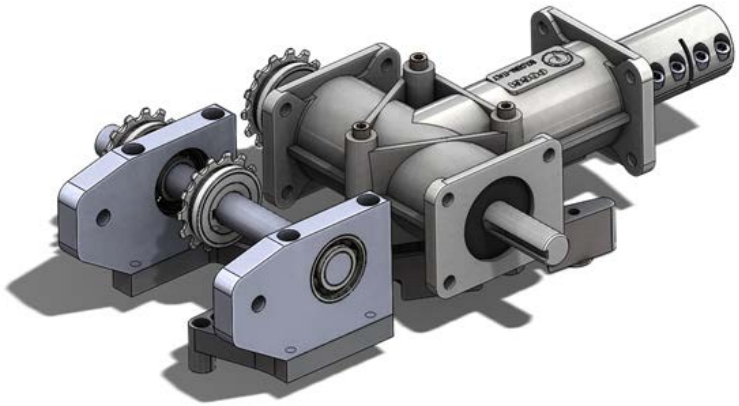

Figure 73 – HPS Godiva bevel gearbox CAD

Inherent to the design of HPS Godiva is a bicycle drive train to a single three-bladed propeller, which involves transmission of input power through a 90° angle. Noting that the gearbox is a critical component in the propulsion of the submarine, a robust gearbox design is critical to the performance of the vehicle. Design, manufacture and test of a bevel gearbox is considerably time and resource intensive, with a severe efficiency penalty for gear misalignment. As a result of the above considerations, the decision was made to allocate more monetary budget to the purchase of an off the shelf right-angle gearbox compared to the likely cheaper base case of design and build of a bespoke unit. Purchase of the gearbox brought about a significant reliability advantage for a performance critical component, as well as saving time which would have been spent on designing this part from scratch. Fair consideration of the next best alternative hence brought about a time and performance

advantage which, while difficult to monetise, brought about additional benefits which exceeded the costs given the time constraints of the project.

5.0 BENEFITS

5.1 BENEFITS TO TEAM

The benefits to the team are principally attributed to the experience of working as part of an interdisciplinary group where communication, coordination and knowledge sharing are imperative to realising the project deliverables in the declared timeframe. The following have been extracted as key skills and experiential benefits realisable in the long term:

- Application of structured project management and decision making
- Negotiation with suppliers and accounting for material lead times
- Operating in a wide design space to a complicated specification
- Plan, design, manufacture and test to a long term deadline

5.2 BENEFITS TO SCHOOL OF ENGINEERING

The benefits to the School of Engineering are predominantly in the form of a strong legacy for the project which continues to generate significant interest both internally and externally. The opportunity to represent the school externally has stimulated activity and engagement of undergraduate students who can meaningfully participate in an exciting and novel project. This will act to raise the profile of both the project and the school, and is an exceptional showcase of Warwick Engineering student potential aligned to the third and fourth project aims; see Figure 74 as an illustrative example of increased awareness of the project. The following are identified as key benefits to the school:

- Medium through which to apply research technologies
- Self-contained technical challenges inspire third-year projects and feed talent pipeline
- Showcase of talent and potential to attract future students
- Industry interest through press releases and presence at exhibitions attracting employers

5.3 BENEFITS TO THE UNIVERSITY OF WARWICK

The benefits to the academic community may be broadly linked to the University Vision 2015 strategy [2]. In relation to the key goals of the strategy, the project works to promote innovation, make the university resources accessible, and permit the championing and nurture of interdisciplinary activity. The following have been identified as key benefits to the University as an institution seeking to raise its international profile:

- STEM promotion through Outreach activities at local schools
- Potential to compete against other academic institutions internationally
- Presence at academic and industry exhibitions across the UK
- Showcase of talent to attract future students

An appraisal of the benefits against the University strategic objectives will be further discussed in Section 6.2.

5.4 BENEFITS TO THE WIDER COMMUNITY

The benefits to the wider community arise from an increased awareness of the marine engineering sector and applications of novel technologies of interest to industry bodies internationally. The following have been identified as impacting upon the wider community:

- Using materials novel to the marine industry, sparking significant interest
- Establish industry relations through sponsorship for potential mutual benefit in the medium-long term
- Contributing to the success of the International Submarine Races as an organisation
- Inspiring pupils to engage in STEM and Engineering as a career or hobby

6.0 COST-BENEFIT APPRAISAL

The costs and benefits are appraised from the separate perspectives of the project aims and both the School of Engineering and University of Warwick Strategic Plans. By doing so it is possible to directly justify the activities of the project according to what was intended at the outset, and match the intangible benefits to the long term interests of the academic community.

6.1 PROJECT AIMS AND OBJECTIVES

In the broadest context the project aimed to build upon the success and knowledge of the previous year's HPS Shakespeare, and design, manufacture, test and race an improved submarine at the 13th ISR with three core design aspects: efficiency, practicality and innovation. Compared to HPS Shakespeare, HPS Godiva applies significantly more advanced technology employing the extensive manufacturing capability of the Engineering department and WMG. As summarised in Section 4, material costs may have been reduced by prioritising minimum manufacture cost at the expense of performance or packaging in early design decisions, however with reference to the project objectives, greater benefits are brought about by prioritisation of the declared design goals. The use of novel technologies has afforded an exceptional opportunity for the team to utilise the equipment and expertise available within the department and allowed for the manufacture of a competitive submarine for the race.

The ambitious project aims demanded the application of a concurrent engineering approach to design and manufacture which is of increasing relevance to industry. The nature of the project permits the shared contribution of engineers from a variety of backgrounds who can take ownership of a key design task which will meaningfully impact on performance, which is relatively unique among the available Masters projects. The experience of working and communicating within an interdisciplinary team is of paramount importance to a professional engineer and directly affects the desirability of students to future employers. In addition the project sources a large amount of its materials externally bringing the benefit of increased interaction with industry and experience of managing budgets and dealing with suppliers. Finally the potential to access additional funding through WMG by a process of pitching the project aspirations to a panel closely emulates industry practice and is a valuable learning experience for the team. The submarine is an outstanding means to practically demonstrate these skills giving intangible benefits realisable in both the short and long term to the University and team members.

6.2 SCHOOL OF ENGINEERING AND UNIVERSITY OF WARWICK STRATEGIC PLAN

The School of Engineering 2014 Strategy document states a number of strategic goals against which the costs of the project are now appraised. The department aim to *"play an active role … [to] promote the practice of engineering, public understanding of our work and attract talented people to the profession"*. The project has demonstrated that it represents an excellent medium through which to achieve this target by being engaged in STEM Outreach and improving understanding of marine technology. For example the team exhibited HPS Shakespeare at the Midlands Imagineering Fair at the Ricoh Arena, and conducted a number of water-based educational activities, which attracted considerable interest among all age groups. Moreover, the continuous engagement of the Warwick Sub team with other Outreach events and industry has brought about numerous opportunities to raise awareness of the project and enhancing the institutional reputation. The new submersible will offer the department a showcase of Warwick student potential and attendance at external events aids in creating a legacy for the project in terms of both profile and sponsorship.

The project has also offered a means for the School of Engineering to publicise research through the University Communications office. Warwick Sub has featured on numerous occasions as a topic of interest and featured article in press releases, and the University is well positioned to act as a central hub for all UK entrants to the ISR, from which the shipment to the US can depart. This fosters synergetic relationships with other universities, presents PR opportunities and raises the University's profile as a centre for engineering excellence and innovation.

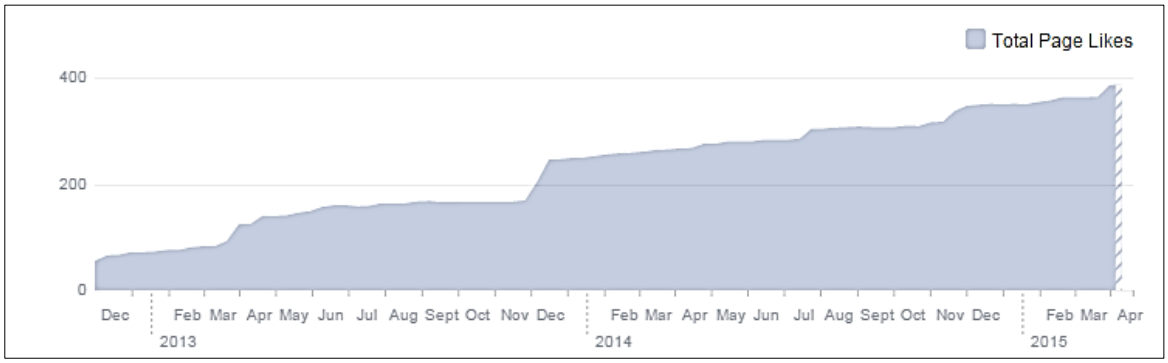

Figure 74 – Total 'Likes' on social media, quantifying project awareness

The University of Warwick also define a number of broad strategic goals against which the project may be appraised. Firstly, the University declares that it wishes to embed an outstanding student experience through learning and facilities. While the project has incurred

additional costs through the ambition of competing internationally at the ISR, the realisation of this objective provides a number of rich opportunities for students, which satisfy the University's goals in this area. These include the opportunity to represent the university at variety of public events, broaden the student experience through SCUBA diving training associated with the project, and competing at the 13th ISR in Washington DC. Enhancing the student experience in this way will encourage a talent pipeline through the lower years to engage in the project and the benefits can be reaped in the long term.

Warwick Sub has also been able to contribute to 'The Global Research Priorities' through the use of innovative materials and manufacturing, specifically on the global stage. As an extension of this, the University aims to secure a strong global position, enhance international standing, improve our reputation and increase our scale in Engineering. By competing internationally and encouraging Warwick to act as a central hub for Human Powered Submarine projects at university across the UK, the project brings about significant tangible benefits in moving toward those goals. It is clear in this case that the project costs incurred have brought about a plethora of benefits to both the individual and department according to

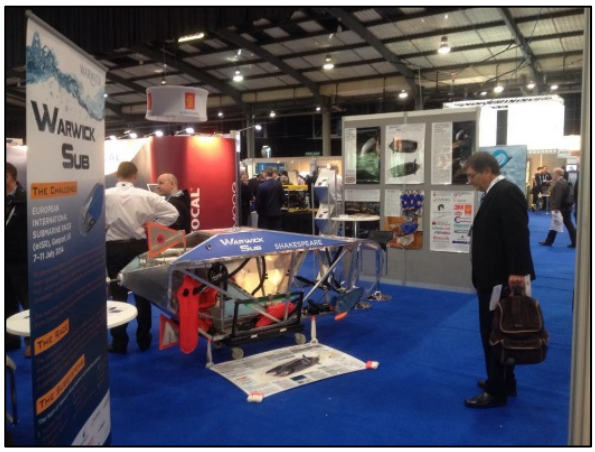

the project aims and the strategic goals of the department and University.

Figu

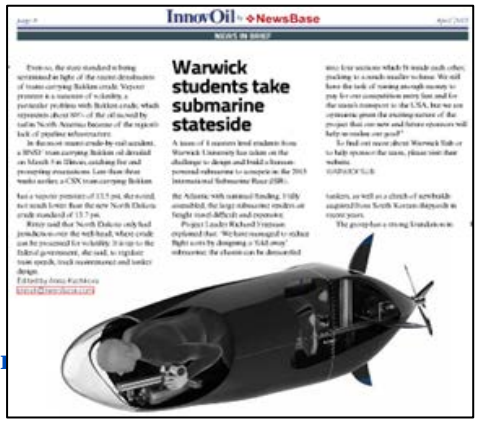
InnovOil NewsBase

Warwick students take submarine stateside

Figure 7 – Feature in InnovOil magazine

Figure 8 – Herbert Gallery, Coventry

7.0 CONCLUSION

This Cost Benefit Analysis concludes that the third iteration of Warwick Human Powered Submarine has been a worthwhile endeavour and has contributed positively to a broad range of project stakeholders. The nature of the project implies that a large portion of the described benefits are intangible and as a result, an attempt to monetise these for the purposes of direct comparison to the project costs is inappropriate in this context. The benefits of the Warwick Human Powered Submarine project are realisable by team members in the current and successive iteration. A long term benefit investment horizon such as this delivers over a time period which is particularly appropriate given the University's commitment to an exceptional student experience in the 50th anniversary celebrations.

Therefore, while a direct monetary comparison of the costs and benefits is not possible, the alignment of the School of Engineering and University strategic objectives with the experiential, technical and employability benefits embodied by the project makes it a valuable undertaking that should continue in the future.

Figure 9 - HPS Godiva

8.0 WORKS CITED

[1] Regulation, Australian Government: Office of Best Practice, "Cost-Benefit Analysis," Australian Government, 2014.

[2] University of Warwick, "Our Strategy," 2012. [Online]. Available: http://www2.warwick.ac.uk/about/vision2015/. [Accessed 28 February 2015].

APPENDIX A – SPONSOR BREAKDOWN

Table A1 – Breakdown of project sponsorship

Sponsor	Sponsor Value	Sponsor Medium	Application
BCOMP	£442.83	In-Kind Sponsorship	Composite Fibre Reinforcement
Entropy Resins	£150.00	In-Kind Sponsorship	Composite Fibre Matrix
CGI	£28,000.00	In-Kind Sponsorship	Hull Tooling
WMG GRP	£5,000.00	Cash	ISR Support
WMG Catapult	£4,500.00	Cash	Lightweight Structures
Davall	£1,000.00	In-Kind Sponsorship	Gearbox Transmission
SELEX ES	£250.00	Cash	Electronics
Wartsila	£1,500.00	Cash	Materials
Societe Generale	£1,000.00	Cash	Materials
Bosch Rexroth	£500.00	Cash	Materials
Outreach	£500.00	Cash	Materials
Stoney Cove	£1,750.00	In-Kind Sponsorship	Diving
Navisafe	£710.00	In-Kind Sponsorship	Safety Lights
Ergo-Link	£500.00	In-Kind Sponsorship	Mannequin CAD
Big Bear Plastic Products	£2,300.00	In-Kind Sponsorship	Nose Cone
Subsea UK	£1,890.00	In-Kind Sponsorship	Legacy Sponsorship
Indespension	£150.00	In-Kind Sponsorship	Trolley
School of Engineering	£1,600.00	Cash	Sponsorship
Rotor	£130.00	In-Kind	Powertrain

		Sponsorship	
Stratasys	£1,500.00	In-Kind Sponsorship	3D Print Material

APPENDIX B – WARWICK SUB SPONSORSHIP SUITE

WARWICK HUMAN POWERED SUBMARINE

2015 SPONSORSHIP PROSPECTUS

WMG Innovative Solutions

THE UNIVERSITY OF WARWICK

WARWICK SUB is a team of eight engineering finalists at the University of Warwick. We are designing and building a human-powered racing submarine to compete at the 2015 International Submarine Races in Washington DC.

We have access to cutting edge engineering research from both Warwick Manufacturing Group and the Warwick School of Engineering.

PAGE 2

THE ISR or International Submarine Races, is a week-long biennial competition held at the Naval Surface Warfare Centre at Caderock in the USA. The event challenges teams from around the world to design and build the world's best human powered submarine with the aim of developing the next generation of naval engineers. The overall winner is determined on the basis of quality of design, manufacture and performance.

The competition has seen more than 230 submarines since 1989, with 21 competitors in 2013. **The world record for speed stands at 4.13 metres per second** and is held by Omer of the Ecole de Technologie Superieure.

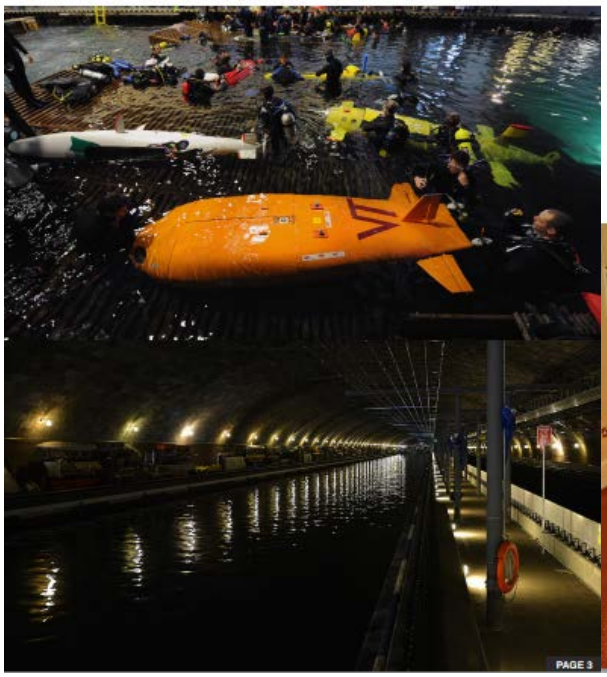

PAGE 3

OUR TEAM is formed of eight engineering masters students from a variety of disciplines, including mechanical, manufacturing, robotics and electronic engineering. It is supported by the Warwick University School of Engineering, Warwick Manufacturing Group, and a host of sponsors.

The team is supervised by Dr. Ian Tuersley, Dr. Neil Davis and Professor John Flower of WMG.

The 2014 team placed 4th in the world at the European ISR with their sub Shakespeare (below). We have their experience to build on and hope to place highly in the face of fierce competition at the 2015 ISR.

PAGE 4

WARWICK SUB IS FUNDED ENTIRELY THROUGH SPONSORSHIP

Unlike most other teams, we have to raise all of the cash to build the sub and get to the competition ourselves. As of January, we're two thirds of the way towards our target of £34,000.

We would greatly appreciate any support that your company is willing to provide. This might include direct financial support or in-kind contributions, including expertise, materials, use of manufacturing facilities or testing.

In return, we will place your logo on our submarine, on our event posters, in our workcell and on our website and social media platforms.

We are able to provide direct access to some of the best and most highly regarded graduates in Europe. We are happy to arrange events for you to speak directly to students, to leave promotional materials, and consider other activities that you may find beneficial for recruitment.

Use of the submarine for your own marketing and events is also possible.

The 2014 submarine is shown off daily to groups of executives, engineers, apprentices and students taking tours of WMG. It is also taken to engineering shows and events across the UK by WMG and CATAPULT.

We can guarantee significant and targeted exposure for your firm should you help us get to the competition.

Figure B1 – Sponsorship prospectus

WARWICK SUB

HUMAN POWERED SUBMARINE

WARWICK SUB is a team of 8 engineering finalists at the University of Warwick. We are designing and building a human-powered submarine to compete at the 2015 ISR (International Submarine Races) held in Washington DC. The event aims to develop the next generation of naval engineers. The 2014 Warwick team placed 4th in the world. We hope to build on their experience and place highly this year.

PROJECT FUNDING is entirely from sponsorship. We would greatly appreciate any support your company can provide. In return, we can:

1) Place your logo on our submarine, posters, website and social media platforms.
2) Provide access to some of the best graduates in Europe. We are happy to arrange events for you to speak directly to students, to leave promotional materials, and consider other activities that you may find beneficial for recruitment.

MORE INFO: www2.warwick.ac.uk/fac/sci/eng/meng/submarine

warwicksub@eng.warwick.ac.uk www.facebook.com/WarwickSub

Figure B2 – Sponsorship Flyer